UNIVERSIDADE FEDERAL DE VIÇOSA

FERNANDA SALES DE ARAÚJO

ANÁLISE DA EXPRESSÃO GÊNICA E PERFIL METABÓLICO DE CARRAPATOS *Amblyomma sculptum* INFECTADOS COM *Rickettsia amblyommatis*

VIÇOSA – MINAS GERAIS
2021

FERNANDA SALES DE ARAÚJO

ANÁLISE DA EXPRESSÃO GÊNICA E PERFIL METABÓLICO DE CARRAPATOS *Amblyomma sculptum* INFECTADOS COM *Rickettsia amblyommatis*

Tese apresentada à Universidade Federal de Viçosa, como parte das exigências do Programa de Pós-Graduação em Bioquímica Aplicada, para obtenção do título de *Doctor Scientiae*.

Orientador: Cláudio Lísias Mafra de Siqueira

Coorientadores: Edvaldo Barros
Humberto Josué de O. Ramos
Tiago Antônio de O. Mendes

VIÇOSA – MINAS GERAIS
2021

Ficha catalográfica elaborada pela Biblioteca Central da Universidade Federal de Viçosa - Campus Viçosa

T
A663a
2021

Araújo, Fernanda Sales de, 1990-
Análise da expressão gênica e perfil metabólico de carrapatos *Amblyomma sculptum* infectados com *Rickettsia amblyommatis* / Fernanda Sales de Araújo. – Viçosa, MG, 2021.
134 f. : il. (algumas color.) ; 29 cm.

Inclui anexos.
Orientador: Cláudio Lísias Mafra de Siqueira.
Tese (doutorado) - Universidade Federal de Viçosa.
Inclui bibliografia.

1. *Amblyomma sculptum*. 2. *Rickettsia amblyommatis. 3.* Metabolismo. I. Universidade Federal de Viçosa. Departamento de Bioquímica e Biologia Molecular. Programa de Pós-Graduação em Bioquímica Agrícola. II. Título.

CDD 22. ed. 595.429

Bibliotecário(a) responsável: Bruna Silva CRB6/2552

FERNANDA SALES DE ARAÚJO

ANÁLISE DA EXPRESSÃO GÊNICA E PERFIL METABÓLICO DE CARRAPATOS *Amblyomma sculptum* INFECTADOS COM *Rickettsia amblyommatis*

Tese apresentada à Universidade Federal de Viçosa, como parte das exigências do Programa de Pós-Graduação em Bioquímica Aplicada, para obtenção do título de *Doctor Scientiae*.

APROVADA: 25 de maio de 2021.

Assentimento:

Fernanda Sales de Araújo
Autora

Cláudio Lísias Mafra de Siqueira
Orientador

AGRADECIMENTOS

Para a execução deste trabalho, gostaria de agradecer:

- A Deus, por ter me concedido sabedoria, saúde e discernimento durante toda a minha trajetória;

- À minha família, pelo suporte e apoio durante toda a vida, amparando-me nos momentos difíceis e nas tomadas de decisão;

- Ao professor Cláudio Mafra, por me receber no Laboratório de Parasitologia e Epidemiologia Molecular (LAPEM) como estagiária na época, auxiliando no meu crescimento profissional e pessoal. Pelas dicas e conversas extrovertidas sobre música e trabalho. Foram vários anos de parceria que vou carregar para sempre. Obrigada por ser um dos responsáveis pela profissional que sou hoje;

- Aos companheiros de laboratório, dentre tantos que passaram pelo LAPEM e Núcleo de Biomoléculas (Nubiomol): Bruno Milagres, Higo, Rafael, Carlos, Gabriel, Natasha, Raquel, Cínthia, Ananda, Carlos, Paulo, Edvaldo, Nívea, Cláudia, Pedro, Thaís e Maria José;

- Aos estagiários João Pedro, Lucas, Larissa, Carol e João, que idealizaram este trabalho e ajudaram na execução do mesmo, além dos momentos de descontração;

- Às minhas amigas do grupo das Bãnanas e Saídas extrovertidas (WhatsApp), pelos encontros, almoços, festas, aniversários, desabafos e alegrias que foram fundamentais para minha saúde mental e deixaram toda a jornada muito mais leve.

- Aos parceiros de outras instituições, Marlene e Szabó (UFU), Mariana (UFES), Caio (UFES) e Labruna (USP) que colaboraram com materiais biológicos, reagentes, análises e ideias para a realização deste trabalho;

- Aos colegas do Grupo de Estudos em Bioquímica Aplicada (GEBQI), o qual foi importante para meu crescimento pessoal e intensificar a missão de que podemos e devemos fazer Extensão nas universidades;

- A todos os funcionários do Departamento de Bioquímica e Biologia Molecular (DBB), pelas conversas nos períodos do café e auxílio com documentações;

- À Fernanda Albuini, por ter feito parte da chapa 1 para representantes dos discentes junto ao colegiado, cujas conversas e opiniões para resolvermos e votarmos sobre o interesse dos nossos colegas, foram muito construtivas para mim.

- À Coordenação de Aperfeiçoamento de Pessoal de Nível Superior (CAPES), pela concessão da bolsa de estudos.

RESUMO

ARAÚJO, Fernanda Sales de, D.Sc., Universidade Federal de Viçosa, maio de 2021. **Análise da expressão gênica e perfil metabólico de carrapatos *Amblyomma sculptum* infectados com *Rickettsia amblyommatis***. Orientador: Cláudio Lísias Mafra de Siqueira. Coorientadores: Edvaldo Barros, Humberto Josué de Oliveira Ramos e Tiago de Oliveira Mendes.

Os carrapatos são artrópodes parasitas hematófagos, pertencentes à ordem Acari e distribuídos em três famílias: Ixodidae, Argasidae e Nuttalliellidae. Espécie comumente encontrada do sul dos Estados Unidos ao norte da Argentina, o *Amblyomma sculptum* pertence à família Ixodidae. O gênero *Rickettsia* pode permanecer no intestino, ovário, hemocele e glândulas salivares, dentre os patógenos que infectam carrapatos, pulgas e piolhos. Os carrapatos são capazes de manter estas bactérias por várias gerações, as quais possuem um sistema metabólico limitado, dependendo de intermediários adquiridos por quando da hematofagia e suas reações metabólicas. Para análise do peso, número de cópias de bactéria, e expressão de enzimas-chave do metabolismo utilizando a reação em cadeia da polimerase em tempo real quantitativa, carrapatos fêmeas *A. sculptum* foram alimentados com sangue, sangue adicionado de células VERO, e sangue adicionado de células VERO infectadas com *Rickettsia amblyommatis*, durante 12, 24, e 48 horas. Outro grupo foi alimentado com os mesmos tratamentos por 48 horas para análise do perfil metabólico utilizando a cromatografia gasosa acoplada ao espectrômetro de massas e os aplicativos *TargetSearch* e *Metaboanalyst*. Verificamos no intestino médio dos carrapatos infectados que o número de cópias da bactéria apresentou um aumento significativo de 24 para 48 horas. Nos tratamentos não infectados, a diferença de peso após a alimentação revelou um aumento de massa. Na presença de riquétsia, verificou-se diminuição ou não aumento do peso. Na análise da expressão relativa, enzimas escolhidas da via glicolítica, ciclo do ácido tricarboxílico, fosforilação oxidativa, beta-oxidação, transporte de ácidos graxos e dos metabolismos de aminoácidos e nucleotídeo foram alteradas quando da presença da bactéria nos diferentes tempos de alimentação. Diversos compostos identificados na análise do perfil metabólico estavam envolvidos no metabolismo de aminoácidos, purina, pirimidina, carboidratos, ciclo do ácido tricarboxílico, lipídeos, ácidos graxos, nicotinato, nicotinamida e pentose fosfato. Com a elucidação do nível de expressão das enzimas-

alvo e a abundância dos metabólitos identificados, demonstramos com mais detalhes que diversas vias são alteradas e direcionadas para o favorecimento de componentes essenciais para a sobrevivência e manutenção da riquétsia no intestino médio dos carrapatos ou resposta protetiva contra o patógeno. Estudos posteriores permitirão avançar nestes conhecimentos, potencialmente contribuindo para uma melhor compreensão da relação parasito- hospedeiro, selecionando novos alvos para o controle destes agentes e na bioprospecção de novas moléculas.

Palavras-chave: *Amblyomma sculptum. Rickettsia amblyommatis.* Metabolismo.

ABSTRACT

ARAÚJO, Fernanda Sales de, D.Sc., Universidade Federal de Viçosa, May, 2021. **Gene expression analysis and metabolic profile of *Amblyomma sculptum* ticks infected with *Rickettsia amblyommatis***. Adviser: Cláudio Lísias Mafra de Siqueira. Co-advisers: Edvaldo Barros, Humberto Josué de Oliveira Ramos and Tiago de Oliveira Mendes.

Ticks are hematophagous parasitic arthropods, belonging to the order Acari and distributed in three families: Ixodidae, Argasidae, and Nuttalliellidae. A species commonly found from the southern United States to northern Argentina, *Amblyomma sculptum* belongs to the Ixodidae family. Rickettsia genus can remain in the midgut, ovary, hemocele, and salivary glands, among the pathogens that infect ticks, fleas and lice. Ticks can maintain these bacteria for several generations, which have a limited metabolic system, depending on intermediates acquired during the hematophagy and its metabolic reactions. For weight analysis, bacterial copy number, and expression of critical enzymes using the quantitative real-time polymerase chain reaction, female *A. sculptum* ticks were fed with blood, blood + VERO cells, and blood + infected VERO cells *Rickettsia amblyommatis* for 12, 24, and 48 hours. Another group was fed with the same treatments for 48 hours to analyze the metabolic profile using gas chromatography coupled to the mass spectrometer and the applications TargetSearch and Metaboanalyst. We found in the midgut of infected ticks that the number of copies of the bacterium increased significantly from 24 to 48 hours. In uninfected treatments, the difference in weight after feeding revealed an increase in mass. In the presence of rickettsia, there was a decrease or no increase in weight. In the relative expression analysis, enzymes chosen from the glycolytic pathway, tricarboxylic acid cycle, oxidative phosphorylation, beta-oxidation, fatty acid transport, amino acid, and nucleotide metabolism were altered when the bacteria were present at different feeding times. Several compounds identified in the metabolic profile analysis were involved in the metabolism of amino acids, purine, pyrimidine, carbohydrates, tricarboxylic acid cycle, lipids, fatty acids, nicotinate, nicotinamide, and pentose phosphate. With the elucidation of the level of expression of the target enzymes and the abundance of the identified metabolites, we demonstrated in more detail that several pathways are altered and directed towards favoring essential components for the survival and

maintenance of rickettsia in the tick's midgut or protective response against the pathogen. Further studies will allow advancing this knowledge, potentially contributing to a better understanding of the parasite – host relationship, selecting new targets for the control of these agents and the bio prospecting of new molecules.

Keywords: *Amblyomma sculptum. Rickettsia amblyommatis.* Metabolism.

LISTA DE ILUSTRAÇÕES

Capítulo 1

Capítulo 2

LISTA DE TABELAS

Capítulo 1

Capítulo 2

LISTA DE ABREVIATURAS E SIGLAS

TCA	Ácido tricarboxílico
UFV	Universidade Federal de Viçosa
UFU	Universidade Federal de Uberlândia
BOD	Demanda biológica de oxigênio
KCl	Cloreto de potássio
CEUA	Comitê de Ética no Uso de Animais
DNA	Ácido desoxirribonucleico
RNA	Ácido riboxirribonucleotídeo
cDNA	Ácido desoxirribonucleico complementar
TAE	Tris-Acetato-EDTA
EDTA	Etilenodiamino tetra-acético
V	Volt
°C	Grau Celsius
PCR	Reação em cadeia da polimerase
UV	Ultravioleta
NB	Nível de biossegurança
USP	Universidade de São Paulo
FMVZ	Faculdade de Medicina Veterinária e Zootecnia
USA	Estados Unidos da América
LB	Luria Bertani
µl	Microlitros
g	Gramas
mg	Miligramas
ng	Nanogramas
ml	Mililitros
xg	Força G
CS	Citrato sintase
N.M	Massa do nucleotídeo
bp	Pares de base
CXR	Referência passiva interna
Ct	*Cycle Threshold*
DMEM	Meio Eagle Dulbecco Modificado
CO_2	Dióxido de carbono
%	Porcentagem
mM	Milimolar
$MgCl_2$	Cloreto de magnésio
dNTP	Desoxirribonucleotídeo fosfato
M-MuLV	Vírus da leucemia murina Moloney
U	Unidade de atividade enzimática
qPCR	Reação em cadeia da polimerase quantitativa
log	Logaritmo

KS	Kolmogorov-Smirnoff
ANOVA	Análise de variância
S.D	Desvio padrão
min	Mínimo
max	Máximo
INF	Infectado
Cr	Concentração relativa
PFK	Fosfofrutoquinase
PK	Piruvato quinase
PEPCK	Fosfoenolpiruvato carboxiquinase
FBP	Frutose bifosfato
PDH	Piruvato desidrogenase
IDH	Isocitrato desidrogenase
AKGD	Alfa-cetoglutarato desidrogenase
NADH	Nicotinamida adenina dinucleotídeo
NDH	NADH desidrogenase
ATP	Adenosina Trifosfato
ATPS	Adenosina Trifosfato Sintase
CoA	Coenzima A
AD	Acil-CoA
ECHD	Enoil Co-A hidratase
CPTI	Carnitina O-palmitoiltransferase
HAL	Histina amonia liase
AAAH	Aminoácido aromático hidroxilase
ASNase	Asparaginase
OAT	Ornitina aminotransferase
AspAT	Aspartato aminotransferase
purF	Glutamina fosforibosil pirofosfato aminotransferase
RPPK	Ribose fosfato pirofosfoquinase
dCMP	Deoxicitiilato deaminase
PNP	Purina nucleosídeo fosforilase
FUNARBE	Fundação Arthur Bernardes
FAPEMIG	Fundação de Amparo à Pesquisa do Estado de Minas Gerais
CNPq	Conselho Nacional de Desenvolvimento Científico e Tecnológico
CAPES	Coordenação de Aperfeiçoamento de Pessoal de Nível Superior
GC-MS	Cromatografia gasosa acoplada ao espectrômetro de massas
RT	Tempo de retenção
RI	Índice de retenção
CDF	Formato de documento computável
GMD	*Golm Metabolome Database*
FD	Fold change
PCA	Análise de componente principal
KEGG	*Kyoto Encyclopedia of Genes and Genomes*

SUMÁRIO

1. INTRODUÇÃO GERAL

Os carrapatos são artrópodes hematófagos parasitas obrigatórios, pertencentes à ordem Acari, taxonomicamente distribuídos em três famílias: Ixodidae, Argasidae e Nuttalliellidae. Conhecidos por sua capacidade de parasitar vários hospedeiros vertebrados, como gado, cavalos, cães, aves, capivaras e o homem, eles podem ser encontrados em diferentes ecossistemas, incluindo a Antártica (FRENOT et al., 2001; WILLE et al., 2020).

Amblyomma sculptum é a espécie comumente distribuída no norte da Argentina, Bolívia, Paraguai e Brasil (MARTINS et al., 2016), a qual está inserida na família Ixodidae (OLIVER, 1989). Este artrópode é considerado importante para a saúde humana e veterinária devido ao enorme potencial vetorial de agentes infecciosos, como a bactéria *Rickettsia rickettsii* (causadora da febre maculosa brasileira).

As bactérias do gênero *Rickettsia* infectam artrópodes, tais como: carrapatos, pulgas e piolhos, permanecendo no intestino, ovário, hemocele e glândulas salivares (RAOULT & ROUX, 1997). Há também relatos desse gênero infectando mosquitos (ZHANG et al., 2016; BARUA et al., 2020), traças (ARAÚJO et al., 2021) e insetos (BEHAR et al., 2010). Os carrapatos são capazes de manter estas bactérias por várias gerações desde a transmissão transovariana ou transestadial, permitindo a propagação para os outros animais através da alimentação por sangue. Após a ingestão da bactéria pela hematofagia, esta necessita ultrapassar a barreira intestinal do artrópode e circular pela hemocele, as quais serão fagocitadas pelos hemócitos, importante componente do sistema imune dos carrapatos (BURGDORFER & BRINTON, 1975).

Rickettsia amblyommatis pertence ao grupo da febre maculosa (*spotted fever group* – SFG) e possui potencial patogênico associado a carrapatos com ampla distribuição no Brasil, cuja infecção já foi observada em *A. cajennense s.s*, *A. oblongoguttatum, A. sculptum*, entre outras espécies (LABRUNA et al., 2004; AGUIRRE et al., 2018). De acordo com Snellgrove et al. (2021), a infecção de cobaias com *R. amblyommatis, R. bellii e R. montanensis* pode causar respostas inflamatórias subclínicas ou leves após a introdução da bactéria por inoculação intraperitonial, sugerindo uma baixa patogenicidade para animais. Em humanos, as manifestações

clínicas identificadas em pacientes infectados com *R. amblyommatis* foram leves, apresentando-se febre, cefaleia e mialgia (DELISLE et al., 2016).

Em muitos modelos biológicos, bactérias são capazes de coexistirem em um organismo e de produzirem metabólitos, os quais são encontrados naturalmente em menores quantidades no vetor. Este processo ocorre, por exemplo, em moscas tsé-tsé, cuja bactéria *Wigglesworthia glossinidius* (encontrada no citoplasma de células epiteliais do intestino) possibilita o equilíbrio metabólico e maior sobrevivência das moscas no ecossistema (NOGGE, 1981; AKMAN *et al*., 2002). Em outras situações, diversas bactérias não possuem uma maquinaria própria de síntese de intermediários metabólicos essenciais para a sua propagação e sobrevivência no ambiente em que vivem. Este modelo ocorre, por exemplo, em carrapatos *Ixodes scapularis*, cuja presença da bactéria *Anaplasma phagocytophilum*, é capaz de aumentar a expressão gênica de enzimas envolvidas na degradação de glicose no intestino, inibindo a expressão de enzimas envolvidas no ciclo tricarboxílico (TCA) e gliconeogênese (CABEZAS-CRUZ *et al*., 2017).

A interação da *Rickettsia* e sua atuação na expressão gênica de componentes metabólicos presentes no intestino de carrapatos *Amblyomma sculptum* foram demonstradas a partir da análise transcriptômica realizada anteriormente pelo nosso grupo de pesquisa, cujo trabalho intitulado “Anotação e montagem de transcriptomas de intestino médio e ovários do carrapato *Amblyomma sculptum*, antes e após a infecção por *Rickettsia amblyommii”*, possibilitou a seleção de alvos diretamente relacionados com o processo metabólico de carboidratos, lipídeos, aminoácidos e nucleotídeos. No trabalho, um total de 348 sequências codificantes (CDS) foram relacionadas com o mecanismo de infecção de riquétsia no intestino médio dos carrapatos *A. sculptum,* das quais 185 eram mais abundantes na condição infectada em comparação com os carrapatos não infectados para diferentes classes de proteínas. O número de CDS com expressão gênica aumentada foi maior na condição de infecção com a bactéria para enzimas relacionadas com o metabolismo e digestão de carboidratos (principalmente para via glicolítica, ciclo do ácido tricarboxílico e via das pentoses fosfato), lipídeos (enzimas relacionadas com a beta-oxidação de ácidos graxos e metabolismo de esteroides), aminoácidos (utilizados na maquinaria proteica) e nucleotídeos (síntese de DNA) (MOREIRA et al., 2017).

Diversos estudos têm usado diferentes ferramentas para a construção de vias metabólicas a partir do genoma (MIN el al., 2008), análises comparativas do genoma

de espécies de riquétsias (RENESTO et al., 2005), metabolômica da interação carrapato - *Borrelia* durante uma refeição de sangue de carrapato (HOXMEIER et al., 2017), transcriptômica comparativa (NARRA et al., 2020), caracterização do carrapato-patógeno por proteômica (VILLAR et al., 2012) e metabolômica (QUIROZ-CASTAÑEDA et al., 2020), para avaliar a interação de bactérias e carrapatos.

Entender quais vias e metabólitos são necessários e essenciais para a sobrevivência e efetiva relação parasito-hospedeiro é crucial para que possamos indicar potenciais alvos para o desenvolvimento de estratégias de intervenção terapêutica (MIN et al., 2008). No entanto, estudos de expressão e perfil metabólico ainda são mínimos para mostrar a interação entre *R. amblyommatis* e *A. sculptum*.

Neste estudo, utilizamos diferentes abordagens para investigar a diferença de peso encontrada em carrapatos infectados com *R. amblyommatis*. Primeiro, enzimas-alvo do metabolismo central foram selecionadas para a análise da expressão gênica nos diferentes tempos de alimentação com e sem infecção utilizando a reação em cadeia da polimerase em tempo-real quantitativa. A segunda abordagem foi traçada para a análise e identificação dos metabólitos no intestino médio dos carrapatos, os quais foram analisados por cromatografia gasosa acoplada a espectrometria de massas (GC-MS). Com a elucidação do nível de expressão das enzimas-alvo e a comparação na abundância dos metabólitos identificados, demonstramos que diversas vias são alteradas na presença da riquétsia e direcionadas para o seu favorecimento, cuja sobrevivência e manutenção no intestino médio dos carrapatos depende da disponibilidade destes intermediários. Mais estudos permitirão avançar nestes conhecimentos, potencialmente contribuindo no conhecimento da interação parasito – hospedeiro, na bioprospecção de novas moléculas e seleção de novos alvos para o controle destes agentes, a fim de diminuir a disseminação dessas bactérias, limitando sua permanência nesses artrópodes e reduzindo a transmissão para outros animais.

2. OBJETIVOS

2.1 Objetivo Geral

Analisar a expressão gênica de enzimas envolvidas no metabolismo de diversas vias no intestino médio de carrapatos *A. sculptum* alimentados e infectados com *R. amblyommatis* e elucidar o perfil metabólico da interação parasito - hospedeiro.

2.2 Objetivos Específicos

- Realizar a infecção experimental dos carrapatos fêmeas *A. sculptum* durante 12, 24 e 48 horas de alimentação com tratamentos não infectados *e* infectados *com R. amblyommatis* para a análise de expressão, e somente 48 horas para a análise do perfil metabólico;
- Avaliar o número de cópias de bactéria presente no intestino médio e o peso dos carrapatos em diferentes tempos de alimentação nos respectivos tratamentos;
- Analisar a expressão gênica das enzimas selecionadas da via glicolítica, ciclo do ácido tricarboxílico, fosforilação oxidativa, beta-oxidação, transporte de ácidos graxos, metabolismo de aminoácidos e nucleotídeos;
- Analisar os metabólitos extraídos utilizando a cromatografia gasosa acoplada ao espectrômetro de massas (GC-MS);
- Elucidar o envolvimento da bactéria *R. amblyommatis* com os metabólitos identificados em maior abundância comparado ao tratamento não infectado.

CAPÍTULO 1

GENE EXPRESSION OF ENZYMES INVOLVED IN THE METABOLISM OF TICKS *Amblyomma sculptum* INFECTED WITH *Rickettsia amblyommatis*

Gene expression of enzymes involved in the metabolism of ticks *Amblyomma sculptum* infected with *Rickettsia amblyommatis*

Fernanda Sales de Araújo [1], Ananda Pereira Aguilar [1], João Pedro Vianna Braga [1], Lucas da Silva Lopes [1], Larissa da Silva Teutschebein [1], Carollyne Caldas Veras [1], Thaís Lourenço Martins Guimarães [1], Tiago Antônio de Oliveira Mendes [1], Cláudio Mafra [1*]

[1] Department of Biochemistry and Molecular Biology, Federal University of Viçosa, Brazil

* mafra@ufv.br

ABSTRACT

Ticks are obligatory hematophagous parasitic arthropods known for their ability to parasitize several vertebrate species. *Amblyomma sculptum* is considered significant for human and animal health due to its tremendous vectorial potential of infectious agents. Rickettsiaceae organisms remain to parasitize various organs of that arthropod. In the present study, ticks were infected with *Rickettsia amblyommatis* using artificial feeding during varying times. The weight was observed before and after feeding. The number of copies of bacteria after infection and the relative expression of the main pathways affected in the treatments were predicted by quantitative polymerase chain reaction (qPCR) in real-time. We selected target enzyme genes involved in carbohydrate, energy, lipids, amino acids, and nucleotide metabolism. The association of weight and infection studies has answered questions about bacteria and vector interaction. We reported changes in the tick metabolism in response to *R. amblyommatis* infection. The obtained results showed that pathogen infection affected glucose metabolic pathways, gluconeogenesis, TCA cycle, energy, lipid, amino acid, and nucleotide metabolism. Studies involving pathogens and their host metabolites are advancing, highlighting the importance of gene expression evaluation to provide more information on the complex metabolic integration between the host-parasite relations.

1. INTRODUCTION

Ticks are arthropods obligatory hematophagous parasitic, belonging to the order Acari, taxonomically distributed in three families: Ixodidae, Argasidae, and Nuttalliellidae. Known for their ability to parasitize various vertebrate hosts, such as cattle, horses, dogs, capybaras, birds, and man, they can be found in different ecosystems, including Antarctica (FRENOT et al., 2001; WILLE et al., 2020).

Amblyomma sculptum is commonly distributed in northern Argentina, Bolivia, Paraguay, and Brazil (MARTINS et al., 2016), which is inserted in the family Ixodidae (OLIVER, 1989). There are also reports of this genus infecting mosquitoes (BARUA et al., 2020), moths (ARAÚJO et al., 2021), and insects (BEHAR et al., 2010). Ticks are considered very important for human and veterinary health due to the tremendous vectorial potential of infectious agents, such as the *Rickettsia rickettsii* bacterium (which causes Brazilian Spotted Fever).

Rickettsiaceae are parasites and infect arthropods, such as ticks, fleas, and lice, remaining in the midgut, ovary, cytoplasm, hematocele, and salivary glands (RAOULT & ROUX, 1997). Ticks can maintain these bacteria for several generations since transovarial or trans stadial transmission, allowing the spread to other animals through blood-feeding.

In order to establish a good model of feeding in hosts and infection of ticks with bacteria of the *Rickettsia* genus, several approaches have been used since feeding in rabbits, natural and artificial membranes (BONNET & LIU, 2012), capillary tubes (RANGEL et al., 2008), and plastic tips (RIBEIRO et al., 2014). In this study, the feeding of ticks with plastic tips helped in our approaches using infected and uninfected treatments to assess the weight difference (after and before) in the established times and to investigate the results through the analysis of gene expression of enzymes involved in the metabolism of ticks.

Rickettsiales have a limited metabolic capacity, requiring intermediaries from the host as nutrient and intracellular development (MIN et al., 2008). Several metabolic pathways and enzymes lack the *Rickettsia*, of which 51 host-acquired metabolites were identified by DRISCOLL et al. (2017), using phylogenomic and computational analysis, as molecules needed to compensate the incomplete and absent pathways and as essential intermediates in the host-dependent rickettsial metabolism. This study aimed to analyze the impacts of the *R. amblyommatis* infection in the gene expression

of primary *A. sculptum* ticks metabolism, like glycolysis, gluconeogenesis, TCA cycle, energy, lipid, amino acid, and nucleotide pathways.

2. MATERIAL AND METHODS

2.1 Tick collection

Adult *A. sculptum* female ticks were obtained from colonies maintained in the Ixodology Laboratory at the Faculdade de Medicina Veterinária of the Federal University of Uberlândia (UFU), Minas Gerais State, Brazil, kindness provided by Prof. Matias Szabó.

At the Laboratory of Parasitology and Molecular Epidemiology of the Department of Biochemistry and Molecular Biology of the Federal University of Viçosa (UFV), Minas Gerais State, Brazil, ticks were kept by approximately 20 days inside an incubator bio-oxygen demand (BOD) with a temperature of 28°C, in a regime of 16 hours of light/8 hours dark, stored in desiccators containing a saturated solution of potassium chloride (KCl) for the maintenance of relative humidity around 85% (WIKEL, 1979), until the time of artificial feeding, as previously described (BECHARA et al., 1995).

2.2 Blood Samples

This study was approved by the Ethics Commission on the Use of Animals (CEUA) from the Federal University of Viçosa (UFV) under protocol number 40/2018.

The blood used for artificial feeding was aseptically collected by puncturing the New Zealand rabbits' orbital venous sinus with a hematocrit capillary tube's aid. The blood samples were placed in collection tubes containing sodium heparin and kept under refrigeration at 4ºC, heated to 37ºC just before artificial feeding. A blood aliquot was tested to verify the absence of the *Rickettsia* infection. According to the manufacturer's protocol for blood, DNA was extracted with the QIAamp DNA Mini Kit (Qiagen, Hilden, Germany). Each blood sample was processed by polymerase chain reaction (PCR) using the primers CS 78 (5 '- GCA AGT ATC GGT GAG GAT GTA AT - 3') and CS 323 (5 '- GCT TCC TTA AAA TTC AAT AAA TCA GGA T - 3') that amplify a 401 bp fragment of the citrate synthase (gltA) gene for *Rickettsia* spp. (LABRUNA et al., 2004).

PCRs were performed in a thermocycler (Biocycler model MJ25+, Biosystems®), whose final reaction volume was 25 µl consisting of 10 mM of each primer, 200 ng genomic DNA extracted, 2 mM dNTPs, 1.25 mM $MgCl_2$, and 2 U of Taq

Polymerase. Cycling conditions were carried out with one cycle initial at 95ºC for 5 min, followed by 40 cycles at 95ºC for 30 s, 48ºC for 30 s, and 72ºC for 30 s, with the final extension of the primers at 72ºC for 7 min (LABRUNA et al., 2004). Negative and positive controls were included. The amplification product was analyzed using 5 µl of the PCR product in 1% agarose gel prepared with 1X TAE (tris-acetate-EDTA), ethidium bromide (1 µg/ml) stained, and placed in an electrophoretic well at 96 V for 45 min. After the PCR product's migration in the gel, it was visualized under ultraviolet (UV) light. All samples were analyzed in duplicates.

2.3 Processing, cloning, and bacterial transformation of *R. amblyommatis*

Due to the low pathogenicity of *R. amblyommatis* for humans and the *A. sculptum* tick its natural host, the bacterium was chosen as the adequate infection model according to the recommendations required for NB-2 and guidelines for biosafety and the available infrastructure condition. The inoculum was kindness provided by Dr. Marcelo B. Labruna of the Parasitology Laboratory, Faculty of Veterinary Medicine and Animal Science (FMVZ-USP), São Paulo State, Brazil.

According to the manufacturer's protocol for tissues, DNA from the infected inoculum was extracted using the QIAamp DNA Mini Kit (Qiagen, Hilden, Germany). Subsequently, the extracted DNA was used as a template for the PCR. The amplification product was analyzed as previously described (LABRUNA et al., 2004).

Confirming the presence of *R. amblyommatis*, the PCR products were purified using the PureLink ™ PCR Purification Kit (Invitrogen, USA) following the protocol provided by the manufacturer. According to the manufacturer's recommendations, the purified PCR products were cloned into the pGEM®-T Easy system (Promega, USA).

The transformation of the *Escherichia coli* DH5α with the recombinant plasmid was carried out by thermal shock as described by CARUSO (2007). Subsequently, it was immediately placed on ice for 2 min, and 1 ml of Luria Bertani (LB) medium was added to the incubation stage at 37ºC for 1 hour under agitation at 180 rpm. The microtubes were centrifuged for 10 min at 5.000 xg, and a final volume of 100 µl was used for plating on solid LB agar medium containing 20 µl of antibiotic ampicillin at 100 mg/ml. The mixture was incubated at 37ºC for 16 hours. After this procedure, the colonies' growth was verified for later scraping of them with plastic tip and insertion in liquid LB medium with antibiotic ampicillin, incubated under the agitation of 140 xg at 37ºC until the solution became cloudy, showing the growth of the transformed bacteria.

After confirmed bacterial cells' growth in the liquid LB medium, the extraction of plasmid DNA Miniprep was performed by alkaline lysis, described by BIRNBOIM & DOLY (1979).

The quality of the extraction was analyzed by electrophoresis on 1% agarose gel and confirmation of rickettsia's presence by PCR, using the primers CS 78 and CS 323, as previously described (LABRUNA et al., 2004).

2.4 Plasmid DNA quantification and standard curve of *R. amblyommatis*

Plasmid DNA was quantified using the Qubit® fluorometer (Invitrogen, USA), using a sample of 0.5 µl of each sample.

To calculate the number of copies present in 1 µl of each solution containing plasmid DNA, we used the following formula obtained by YUN et al. (2006):

$$numberofcopies = \frac{DNAconc\left(\frac{g}{\mu l}\right)X6{,}022x10^{23}\left(\frac{bp}{mol}\right)}{totalbpconstructed}theplasmidX660\left(\frac{g}{mol}\right)$$

Total base pairs (Bp) constructed from the plasmid = 3,162

DNA conc = DNA concentration obtained by Qubit®

Next, DNA mass was determined for each plasmid copy with the formula:

$$DNAmass = totalbpconstructedXN.M$$

N.M = nucleotide mass = 1,096 x 10^{21} g

After calculating the number of copies per µl of the solution and the total mass for one copy of plasmid present, the initial amount of DNA was established for performing serial dilutions from 1.4 x 10^{10} to 1.4 x 10^{4} copies of *R. amblyommatis*, which were performed in 0.2 ml microtubes for later use.

Serial dilutions were carried out to detect the bacteria and obtain cycle threshold (Ct) values through quantitative PCR. For it, using an internal fluorogenic TaqMan probe [5´ - 6FAM - CAT TGT GCC ATC CAG CCT ACG GT - BHQ 1 - 3 ´] (Hellixa Genomics, Brazil) and primers CS-5 (5´-GAG AGA AAA TTA TAT CCA AAT GTT GAT-3´) and CS-6 (5´- AGG GTC TTC GTG CAT TTC TT-3´) to obtain a 147 bp fragment of the gene encoding citrate synthase (gltA) for *Rickettsia* spp., as described by LABRUNA et al. (2004). For each reaction, a concentration of 10 mM of primers, 0.255 µM of the probe, 2 µl of serial dilutions, 5 µl of GoTaq® Probe qPCR Master Mix 2X (Promega, USA), and 0.17 µl of passive reference dye (CXR) were used. Serial dilutions with *Rickettsia* were done in duplicate. The machine program was carried out

with an initial 2 min at 95ºC followed by 50 cycles of 15 s at 95ºC, 30 s at 50ºC, and 30 s at 60ºC with the aid of the StepOne™ Real-Time PCR System (Applied Biosystems, USA).

The average of the Ct values obtained from the duplicates and the serial dilution log were plotted on a graph to obtain the absolute standard curve used in the quantification procedures.

2.5 Cultivation of *Rickettsia amblyommatis* in Vero cells

Rickettsia amblyommatis was grown up in Vero cells (fibroblastic cells of the kidneys of the African green monkey - *Cercopithecus aethiops*), according to PHELAN & MAY (2015).

For the spread of rickettsia and activation of the virulence, was used the protocol described by AMMERMAN et al. (2008) with modifications. Approximately 1 ml of the bacterial stock solution maintained under -80ºC was transferred to a Vero cell flask (10^6 cells/ml). After the transfer of *R. amblyommatis* to the Vero cell monolayers, the flasks were placed in a shake for 4 hours to allow the bacteria to enter the adhered cells. After this procedure, the infected cells were kept in Dulbecco's Modified Eagle Medium (DMEM) and incubated in the incubator with 5% CO_2 at 28ºC to prevent further Vero cells concerning the bacteria.

After 24 hours of infection, the flasks were visualized to check the monolayer's destruction and subsequent propagation to new flasks of uninfected cells. The culture medium was removed from the infected flasks, and a cell scraper was used to remove the monolayer. Subsequently, uninfected flasks with Vero cells monolayers with 90% confluence had the culture medium removed, adding 1 ml of the infected cell suspension, followed by incubation under 5% CO_2 atmosphere at 28ºC, with verification 24 hours after the procedure. The infected and uninfected Vero cells were analyzed and tested in duplicates to previously verify the presence/absence of the *Rickettsia*, using DNA extraction and real-time PCR, as previously described (LABRUNA et al., 2004).

2.6 Preparation of Vero cells uninfected and infected with *R. amblyommatis* solutions for tick feeding

With the Vero cell monolayer showing 100% infectivity (cells detached from the cell culture flasks), four aliquots of 1.5 ml were transferred to 2 ml tubes for

centrifugation at 5,000 xg for 10 min. The tubes were sealed with cling film to prevent any aerosol contamination.

Another three aliquots of 1.5 ml were removed for the absolute quantification of the bacteria. The remaining volume of infected Vero cells (aliquots of 1.5 ml) was distributed to each uninfected Vero cell flask to maintain the bacteria's spread.

DNA extraction and quantitative PCR were performed in duplicates with three aliquots of 1.5 ml, whose protocols were previously described (LABRUNA et al., 2004). The mean Ct values obtained were used in the standard curve equation. According to these values, in 1.5 ml of infected medium, there were 2.312 x 10^6 copies of *R. amblyommatis*.

The pellets obtained from the four centrifuged aliquots were reserved and resuspended with rabbit blood heated to 37ºC in a water bath. Blood samples placed in contact with the infected cells' pellets were transferred to the collection tubes to obtain a final volume of 3 ml of blood added with infected Vero cells, with approximately 7.7 x 10^4 copies/100 µl of *R. amblyommatis*.

For treatment with uninfected Vero cells, 1 ml (equivalent to 10^6 cells) was removed from the cell culture flask and centrifuged at 5,000 xg for 10 min. The pellet formed was resuspended with 1 ml of rabbit blood at 37ºC and transferred to the collection tubes, whose final volume was 3 ml.

2.7 Artificial feeding and dissection of adult female *A. sculptum* ticks

Adult female ticks were quickly dipped in distilled water three times and dried with paper towels. Then, the ticks were individually weighed, been separated by weight range into experimental groups, such as Treatment 1 (T1) with 30 female ticks fed only with heparinized blood; Treatment 2 (T2) with 30 ticks fed with heparinized blood + Vero cells; and Treatment 3 (T3) with 30 female ticks fed with heparinized blood + Vero cells infected with *R. amblyommatis*. For each treatment, 30 ticks were distributed into three groups containing ten ticks. These ticks were fed 12, 24, and 48 hours been maintained with separated desiccators as previously described (BECHARA et al., 1995).

Ticks were fed and infected using the artificial feeding method with 1,000 µl plastic tips, filled with 100 µl according to the treatment described by VALIM et al. (2017) (Figure 1). Each tip was replaced every 12 hours of feeding to prevent obstruction.

Figure 1: Artificial feeding of ticks *Amblyomma sculptum* with sterile 1,000 µl plastic tips positioned at an angle of approximately 45º, filled with 100 µl according to the treatment.

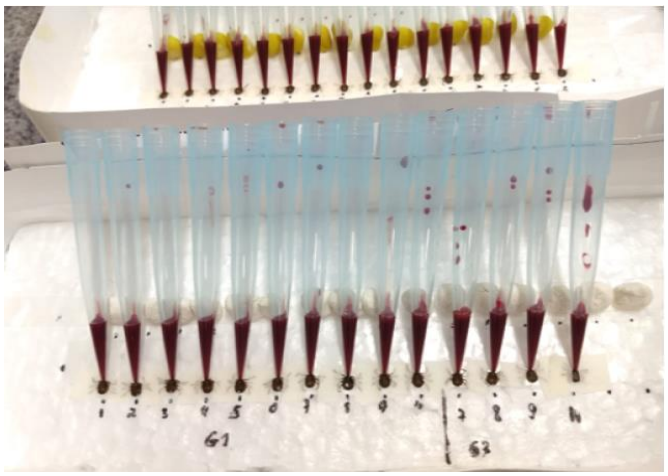

Source: own authorship.

After the first feeding period (12 hours), ticks were removed, washed with distilled water, dried with paper towels, and weighed. New ticks were then weighed and fed for 24 hours and others for 48 hours. The dissection of the females was performed according to ANATRIELLO et al. (2010). After this procedure, the midgut was placed in 0.2 ml microtubes containing 100 µl of RNA later solution (Ambion, USA) stored at -20ºC.

2.8 RNA and DNA extraction, quantification of infected and uninfected *A. sculptum* tick midgut samples

According to the manufacturer's protocol, the total RNA was extracted from each midgut using the RNeasy Mini Kit (Qiagen, Hilden, Germany). The RNA pellet was resuspended in 20 µl of RNAse-free water. To check the quality of the obtained RNA samples, 2 µl of each sample was applied in 1% agarose gel, as previously described (in section blood samples). For the RNA quantification, 2 µl of each sample was used for reading on a SpectraMax M5 spectrophotometer (Molecular Devices, USA), checking the values of the 260/280 and 260/230 ratio, considering as acceptable values between 1.8 and 2.2, and estimating their concentration in ng/µl.

According to the manufacturer's protocol for tissues, DNA was extracted working with the individual pellet formed from the RNA extraction (first step) using the QIAamp DNA Mini Kit (Qiagen, Germany).

For the absolute quantification of *Rickettsia* in each infected midgut sample, quantitative PCR was performed using the internal fluorogenic probe TaqMan and the DNA extracted from each organ, as previously described (LABRUNA et al., 2004). For uninfected DNA samples (ticks fed with blood or blood + uninfected Vero cells), the same procedure was performed, whose Ct value above 35 was considered as negative for the presence of *Rickettsia*. All the samples were analyzed in duplicate. *Rickettsia* copies were calculated with the average Ct values obtained from the DNA samples extracted from the infected midgut.

After obtaining the number of rickettsia copies present in each midgut, the RNA samples were grouped according to the replicates, feeding time (12, 24, and 48 hours) and treatment (blood, blood + uninfected Vero cells, and blood + infected Vero cells) in pools of ten samples with a total volume of 20 µl per microtube each, which replicates identified as Group 1 (G1), Group 2 (G2) and Group 3 (G3). A total of 27 samples were quantified (ng/µl) for reading on a SpectraMax M5 spectrophotometer (Molecular Devices, USA) for further treatment with DNAse and complementary DNA (cDNA) synthesis.

2.9 Treatment of RNA samples with DNase and cDNA synthesis

Extracted RNA was treated with DNAse I (Promega, USA) to remove any contamination with genomic DNA, following the manufacturer's specifications. A volume corresponding to 1 µg of RNA was used for the treatment. Verifying the absence of DNA in the samples, 1 µl of treated RNA was used as a template for PCR using primers A8 (5'- GAG CGA GAC TGG AAG GC - 3') and A12 (5' – TGT GCG CAG CAC AGT TTG G – 3') that amplify a 404 bp fragment in the presence of DNA of the *A. cajennense* (*A. sculptum*). PCR was performed in a thermocycler (Biocycler model MJ25+, Biosystems®), whose final reaction volume was 20 µl consisting of 10 mM of each primer, 1 µl of treated RNA, 2 mM dNTPs, 50 mM $MgCl_2$, and 2 U of Taq Polymerase and nuclease-free water to complete the reaction. Cycling conditions were carried out with one cycle initial at 94ºC for 3 min, followed by 29 cycles at 95ºC for 45 s, 59ºC for 1 min, and 72ºC for 1 min, with the final extension of the primers at 72ºC for 5 min (AGOSTINI, 2008). A DNA sample from the tick *A. sculptum* was used as a positive control of the reaction. Posteriorly, M-MuLV reverse transcriptase enzyme (New England Biolabs, USA) was used for the synthesis of cDNA with 20 µl of the treated RNA, dNTP (10 mM), oligo (dT) (100mM), RNAse inhibitor (40 U/µl), whose

reaction was performed according to the manufacturer's protocol. The synthesized cDNA was stored at -20ºC for further analysis.

2.10 Selection of candidate genes involved in metabolic processes in the midgut of *A. sculptum* ticks and primer design

From the evaluation of the infection and the weight difference of the ticks between treatments, candidate genes involved in metabolism were selected to elucidate the changes found between ticks infected for 12, 24, and 48 hours uninfected with the exact feeding times.

The genes chosen for the analysis were identified as differentially expressed by MOREIRA (2017) in the transcriptome of midguts, ovaries, and salivary glands of *A. sculptum* ticks infected and not infected by *R. amblyommatis*. The criterion for selecting the genes was obtained by verifying the difference between infected and uninfected treatments by observing the differential expression (log_2 - Fold change) in the midgut with values above 2.5 and below 9.2. Thus, for the analysis of gene expression under different feeding treatments and time, four genes were selected for carbohydrate metabolism (glycolysis and gluconeogenesis), five genes for energy metabolism (tricarboxylic acid cycle and oxidative phosphorylation), three genes for lipids metabolism, five genes for amino acids metabolism, and four genes for nucleotide metabolism, whose transcriptome showed significant difference between infected and non-infected following the cut-off values established. According to AGUILAR (Unpublished results), primers for endogenous genes and target enzyme genes were synthesized and noted in Supplementary Table 1.

To primers design, parameters included were 60% of G/C ratio limit, base pair (bp) size between 15 and 25, melting temperature (Tm) in the range 55 to 60°C not differing by more than 1 - 2°C (BUSTIN, 2004), using Primer3web version 4.1 (https://primer3.ut.ee/) (ROZEN & SKALETZKY, 2000). The OligoAnalyzer package (OWCZARZY et al., 2008) was used to discard problems with self-dimer and hairpin. Sequence manipulated suite (STOTHARD, 2000) was used to determine the product size expected (Supplementary Table 1) to the PCR, aligning the primers in the *A. sculptum* transcriptome sequences previously obtained (MOREIRA, 2017).

2.11 Primer testing and PCR amplification efficiency

Each primer's efficiency was tested through real-time PCR using serial cDNA dilutions ranging from 50 to 1.5625 ng/µl. In duplicate reactions, a concentration of 10

mM of primers, 1 µl of serial dilutions, 6 µl of GoTaq® qPCR Master Mix (Promega A6001, USA), and 0.12 µl of passive reference dye (CXR) were used. The program in the StepOne™ Real-Time PCR System (Applied Biosystems, USA) was carried out with initial 95ºC for 10 min followed by 40 cycles with 95ºC for 30 s, 60ºC for 1 min, and a melt curve was generated by *heating* from 60 to 95°C with either 1°C increments for 30 s.

Graphs with Ct (x) versus $\log_{10}$ concentration of cDNA dilutions (y) were produced for each primer pair. The slope of the obtained curve was used to calculate the amplification efficiency with the formula: $[10^{(-1/slope)} -1] * 100$ (PFAFFL, 2001), being the obtained equation (Supplementary Table 2) used to calculate the log of cDNA concentration.

2.12 Gene expression analyses by real-time quantitative PCR (qPCR)

The real-time quantitative PCR (qPCR) was performed using StepOne™ Real-Time PCR System (Applied Biosystems, USA). Reactions were prepared in duplicate containing 1 µl (12.5 ng) of cDNA, 0.5 µl of each primer (10 mM), 6 µl of GoTaq® qPCR Master Mix (Promega A6001, USA), 0.12 µl of passive reference dye (CXR), and nuclease-free water to complete a total of 12 µl. For the negative control, nuclease-free water was used in the absence of cDNA. A program was carried out with initial 95ºC for 10 min followed by 40 cycles with 95ºC for 30s, 60ºC for 1 min, and a melt curve generated by heating from 60 to 95°C with either 1°C increments for 30s. Each assay was performed with technical duplicates for each biological sample triplicate (G1, G2, and G3).

The efficiency values verified for the primers used in this study varied by more than 5% in relation to the primers related to endogenous genes, as recommended by LIVAK & SCHMITTGEN (2001). To calculate the relative expression between treatments, we used the standard curves of each gene.

The equation from the standard curve for each endogenous and target showed by Aguilar (Unpublished results) and in this study (Supplementary Table 2) was used to calculate the logarithm (log) of cDNA concentration from the Cts observed in real-time qPCR.

The relative concentration of the treatments and chosen endogenous was calculated from $10^{\text{log of cDNA concentration}}$. The relative expression was calculated using the mean ratio from $\frac{Relativeconcentrationtarget}{Relativeconcentrationendogenous}$ with three endogenous used in this study.

2.13 Statistical analysis

The statistical analysis of the data obtained for weight, number of copies of *R. amblyommatis* present in the tick's midgut, and gene expression were performed using the GraphPad Prism version 5 (GraphPad Software, Inc.).

The rickettsia copy number data were grouped according to the ticks' artificial feeding time (12 h, 24 h, and 48 h). The acquired values were evaluated to verify whether the samples come from a population with a normal distribution, whose statistical tests were: Kolmogorov-Smirnoff (KS), Normality Pearson omnibus and D'Agostino, and Normality Shapiro Wilk. Once the non-normality of the data was verified, the non-parametric option was checked for the later choice of the Kruskal-Wallis test and Dunns post-test, comparing all the data in pairs of columns with significance level $\alpha \leq 0.05$.

For the weight data, the weight difference was taken into account before and after artificial feeding with the treatments blood, blood + uninfected Vero cells, and blood + infected Vero cells. Testing the hypothesis, it was first verified whether the data followed a normal distribution. After assessing the data normality, the inferential Analysis of Variance test (ANOVA) was chosen due to the total number of comparisons defined for the three groups of artificial feeding treatments. The post-test chosen was Bonferroni's, comparing all data pairs from the columns with significance level $\alpha \leq 0.05$.

To verify whether the number of copies of bacteria could affect the weight of ticks from 12 to 48 hours, a Spearman's correlation was performed with a confidence interval of 0.05.

For the gene expression evaluation, were considered the normal distribution of data. The ANOVA was chosen with a post-test Bonferroni parameter comparing all data pairs from the columns with a significance level $\alpha \leq 0.05$.

3. RESULTS

3.1 Analysis of the number of copies of *R. amblyommatis* in the midgut of ticks *A. sculptum*

With mean Ct values obtained from the serial dilutions real-time PCR, the number of *Rickettsia* copies was calculated from the equation $y = -3.2452x + 47.851$, $R^2 = 0.9998$, which y = mean Ct values and x = logarithm (number of copies).

The mean number of copies of *R. amblyommatis* in the infected midguts after 48 hours of infection ranged from 1.525×10^6 to 4.90×10^6 (mean = 3.07×10^6). In the

midguts 24 hours infected, the number of copies ranged from 1.5225 x 10^5 to 8.617 x 10^5 (mean = 3.41 x 10^5). For the time of infection of 12 hours, the copy number ranged from 1.059 x 10^5 to 3.413 x 10^5 (mean = 1.97 x 10^5). It was observed that all treatments had a number of copies above the initial transferred to the blood (7.7 x 10^4 copies) (Figure 2).

Figure 2: Number of *Rickettsia amblyommatis* copies for each midgut at different feeding times. Significant values for α ≤ 0.05.

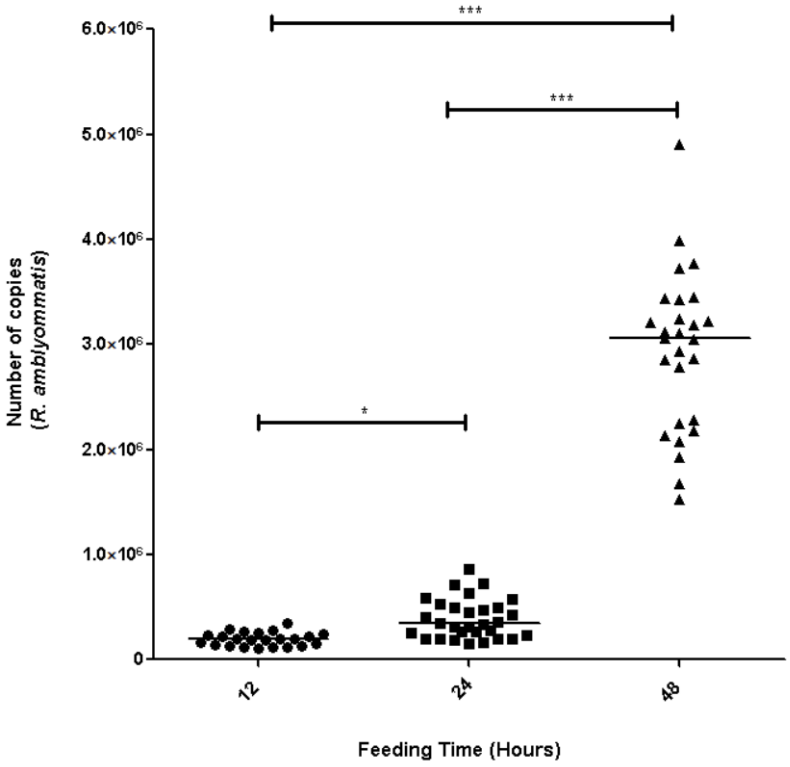

Source: own authorship.

For treatments of blood + infected Vero cells, was observed in the midgut an increase in the mean number of copies of *R. amblyommatis,* whose feeding time of 24 hours presented 1.73 times more rickettsia compared to 12 hours. The treatment of 48 hours showed a significant increase, whose difference between 48 and 24 hours was nine times, and the difference between 48 and 12 hours was 15.58 times.

3.2 Difference in the weight of ticks before and after artificial feeding

After analyzing the normality of the data and applying ANOVA, the weight differences after and before fed were noted (Supplementary Table 3) and plotted according to each tick and the respective treatment (Figure 3).

Figure 3: Difference in tick weights after - before artificial feeding with treatments: blood, blood + Vero cells and blood + infected Vero cells (INF Vero), with 12 hours (A), 24 hours (B), and 48 hours (C). Significance level α ≤ 0.05.

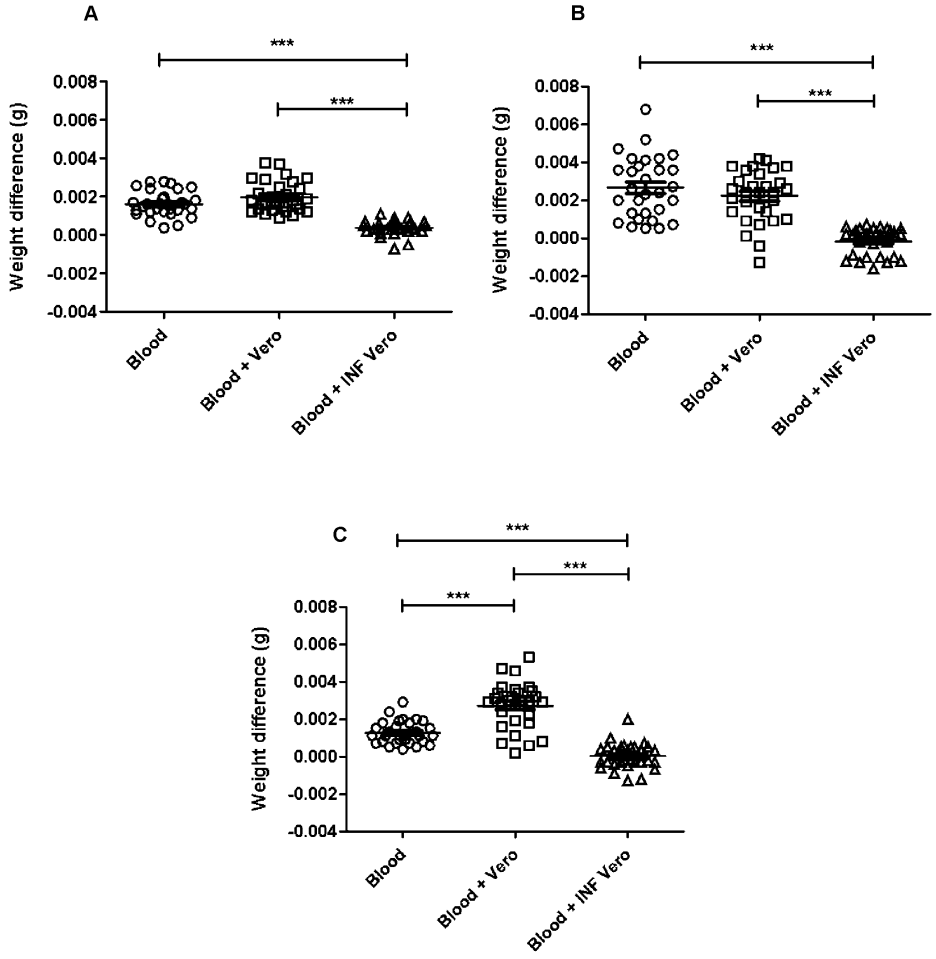

Source: own authorship.

Ticks fed 12 and 24 hours with blood or blood + Vero cells showed no statistical difference in the weight gain (Figure 3A and 3B). However, the mean weight gain of ticks fed 12 hours with blood + Vero cells was 1.21 times bigger than ticks fed only blood at the same time. Ticks fed 24 hours with blood + Vero cells showed the mean weight gain 0.82 times bigger than ticks fed only blood. Ticks fed with Vero cells during 48 hours showed the mean weight gain 2.252 times bigger than ticks fed only blood (Supplementary Table 3). The addition of Vero cells in the diet did not negatively influence the final weight of the ticks.

Comparing mean weight difference between the same treatments times, groups of ticks fed 24 hours with blood, it was observed that the mean weight increased 1.62

times compared with the treatment of 12 hours. The ticks fed 48 hours with blood showed the main weight decreased 1.29 times compared with 12 hours and 2.09 times compared with 24 hours. This result can be justified by the appearance of a white and red excretion after 48 hours of feeding, which was removed by cleaning the ticks before weighing (data not showed).

Several ticks showed a negative mean weight difference with the treatment of blood + Vero cells infected for 12, 24, and 48 hours, compared to treatments without infection (Figure 3A, 3B, and 3C). To verify whether the increase in the number of copies of bacteria could affect the weight of ticks from 12 to 48 hours, a graph was plotted using Spearman's correlation. The R_s of -0.2243 suggests a negative relationship, showing that increased copies of rickettsia in the midgut may impair ticks' weight gain. The correlation was significant (p-value = 0.0368), being the increase in the time of exposure of ticks to bacteria from 12 to 48 hours affected the weight gain (Figure 4).

Figure 4: Spearman's rank correlation coefficient correlation for the variables number of copies and weight difference. Rs = - 0.2243 and p-value = 0.0368.

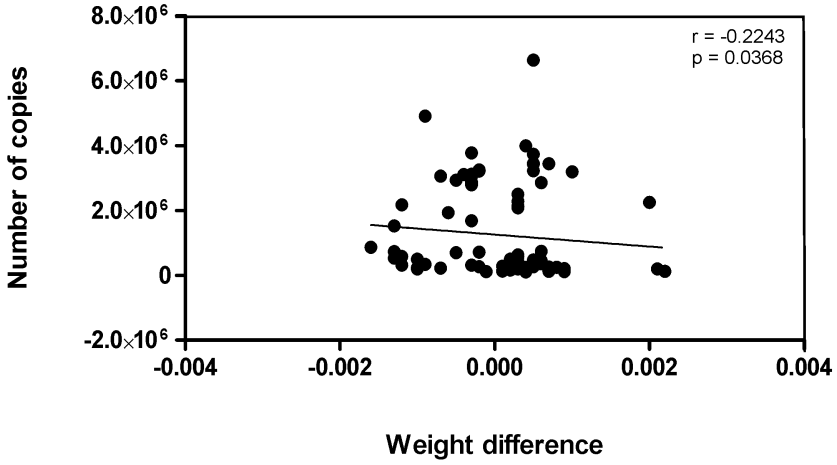

Source: own authorship.

3.3 Analysis of the genes relative expression of the enzymes involved in the metabolism of ticks by real-time qPCR

The relative concentrations of each target gene were normalized with the relative concentrations of the endogenous genes (Cr Target / Cr endogenous), calculating the mean of the three values obtained, whose final value was named relative expression.

3.3.1 Expression of gene targets involved in carbohydrate metabolism

The expression of four genes involved in carbohydrate metabolism was analyzed. Two of them participating in the beginning (g1215 - phosphofructokinase - PFK) and end (g1125 - pyruvate kinase - PK) of the glycolytic pathway. Two others from enzymes that participate initially (g385 - phosphoenolpyruvate carboxykinase - PEPCK) and end (G734 - fructose - 1,6 bisphosphatase - FBP) of gluconeogenesis.

In the first 12 hours of feeding, it was observed in the glycolytic pathway a low relative expression of PFK and PK, whose both treatments without infection showed statistically significant compared to blood + infected Vero cells for PFK and statistically lower for PK (Figures 5A, 5D). After 24 hours of feeding, an increase in PFK and PK's relative expression was significant for uninfected treatments. However, PFK and PK's relative expression was significantly lower for infected treatments (Figures 5B, 5E). With 48 hours of feeding, a slight change in uninfected treatments was observed compared to the previous time (24 h) for PFK. There was also a significant increase in the relative expression of PFK for the infected treatment (Figure 5C). For PK’s relative expression during 48 hours, the uninfected treatment significantly increased compared with the infected treatment group. A small difference was observed between blood and blood + Vero cells (Figure 5F).

Figure 5: Relative expression of enzymes involved in the glycolytic pathway at different feeding times with blood, blood + uninfected Vero cells (Blood+VERO), and blood + infected Vero cells (Blood+INF VERO). **A - C** relative expression of PFK at 12, 24, and 48 hours of feeding, **D – F** relative expression of PK at 12, 24, and 48 hours of feeding. Significance level α ≤0.05.

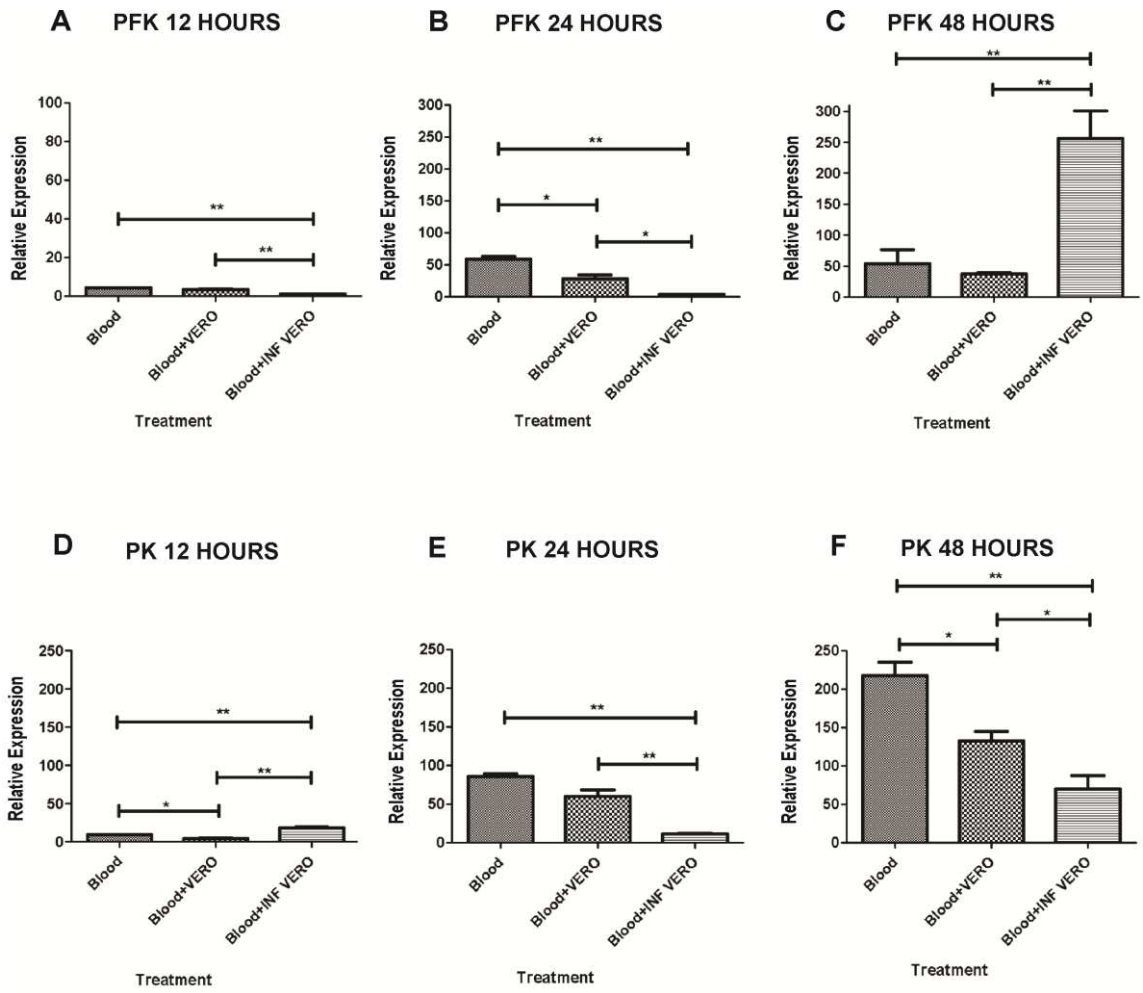

Source: own authorship.

The enzymes involved in gluconeogenesis (FBP and PEPCK) showed lower relative expression (x-axis) about enzymes of the glycolysis (PFK and PK). In 12 hours of feeding, a low relative expression of FBP and PEPCK was observed, whose treatments without infection showed statistically significant compared to blood + infected Vero cells for PEPCK and statistically lower for FBP (Figures 6A, 6D). With 24 hours of feeding, an increase in the relative expression of FBP and PEPCK was significant for uninfected treatments, and blood + infected Vero cells' relative expression was lower compared to the others (Figures 6B, 6E). Also, there was a significant increase in the relative expression of FBP and PEPCK for the infected

treatment within 48 hours (Figures 6C, 6F). A slight difference was observed between blood and blood + Vero cells for PEPCK (Figures 6E, 6F).

Figure 6: Relative expression of enzymes involved in the gluconeogenesis at different feeding times with blood, blood + uninfected Vero cells (Blood+VERO), and blood + infected Vero cells (Blood+INF VERO). **A - C** relative expression of FBP at 12, 24, and 48 hours of feeding, **D – F** relative expression of PEPCK at 12, 24, and 48 hours of feeding. Significance level α ≤0.05.

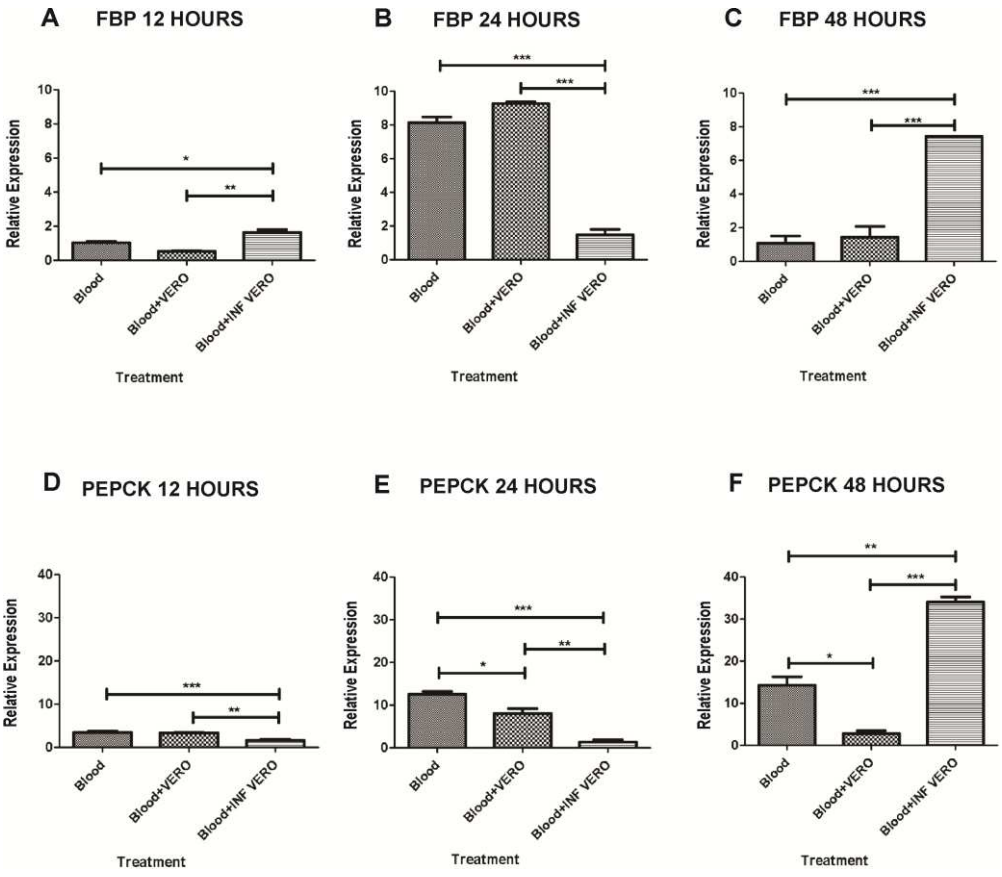

Source: own authorship.

3.3.2 Gene expression of targets involved in energy production

Five genes involved in energy production were analyzed; three of them related to enzymes that participate in the tricarboxylic acid (TCA) cycle, such as g3922 - pyruvate dehydrogenase (PDH), g642 - isocitrate dehydrogenase (IDH), and g1116 - α-ketoglutarate dehydrogenase (AKGD). Other evaluated genes are related to oxidative phosphorylation called g1474 - NADH dehydrogenase (NDH) and the g1394 - α subunit ATP synthase (ATPS) (Figure 7).

Figure 7: Relative expression of enzymes involved in the TCA cycle at different feeding times with blood, blood + uninfected Vero cells (Blood+VERO), and blood + infected Vero cells (Blood+INF VERO). **A - C** relative expression of PDH at 12, 24, and 48 hours of feeding, **D – F** relative expression of IDH at 12, 24, and 48 hours of feeding, **G – I** relative expression of AKGD at 12, 24, and 48 hours of feeding. Significance level α ≤0.05.

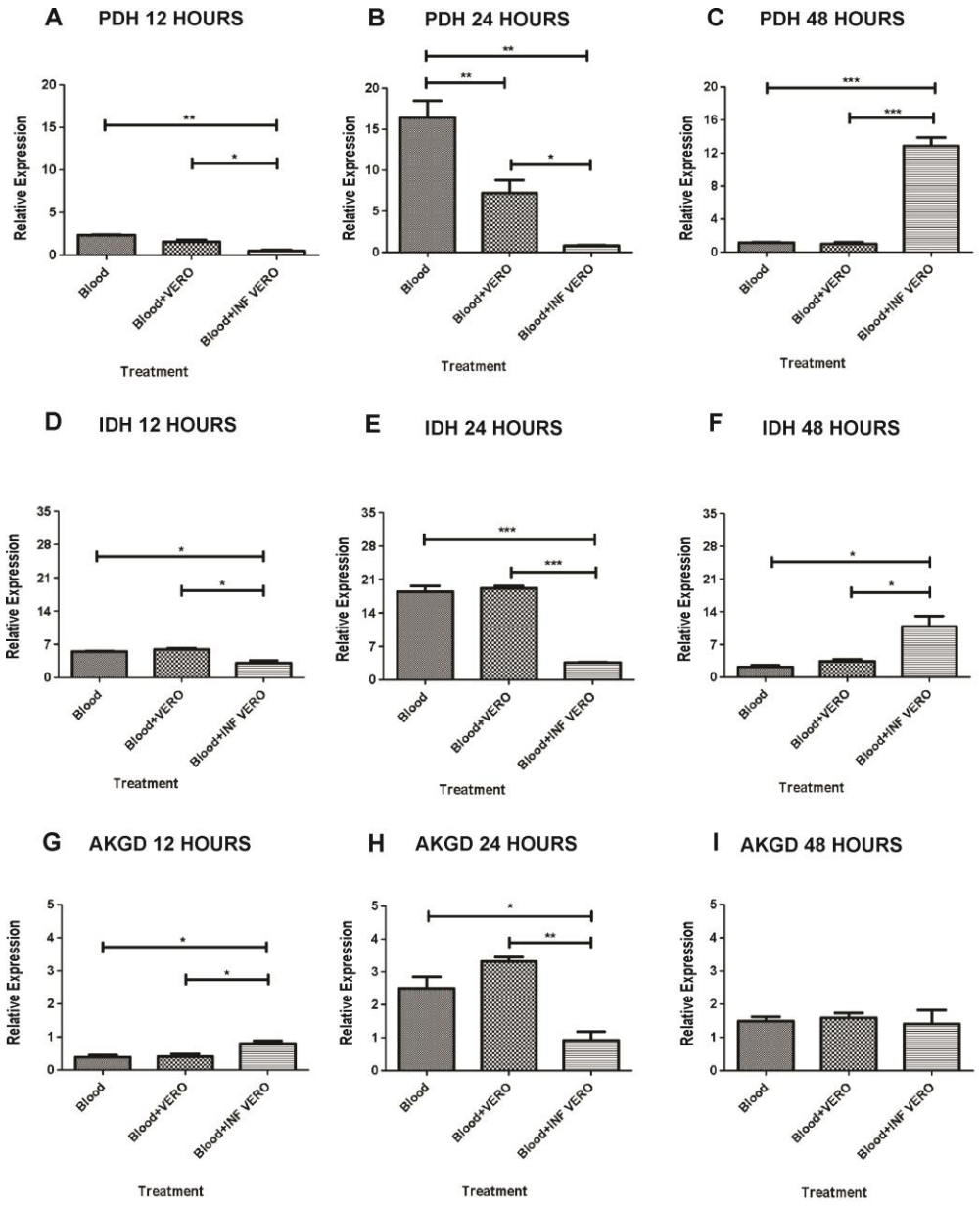

Source: own authorship.

The relative expression of the AKGD was lower compared to PDH and IDH. The group with 12 hours of feeding without infection was statistically more significant than blood + infected Vero cells for PDH and IDH and statistically lower for AKGD (Figures 7A, 7D, and 7G). With 24 hours of feeding, an increase in the relative expression of PDH, AKGD, and IDH was significant for uninfected treatments, and relative

expression of blood + infected Vero cells remained diminished (Figures 7B, 7E, and 7H). In contrast, PDH and IDH showed a more significant relative expression in the treatment infected with 48 hours (Figures 7C and 7F). AKGD showed lower relative expression at 48 hours compared to 24 hours in the uninfected treatment. In 48 hours, there was no statistical difference between infected and uninfected ticks (Figure 7I).

For oxidative phosphorylation, NDH showed smaller relative expression in the treatment with blood + infected Vero cells at 12 and 24 hours (Figures 8A and 8B), whose presence of bacteria was significant at 48 hours feeding, significantly increasing relative expression of this gene (Figure 8C).

Figure 8: Relative expression of enzymes involved in the energy metabolism at different feeding times with blood, blood + uninfected Vero cells (Blood+VERO), and blood + infected Vero cells (Blood+INF VERO). **A - C** relative expression of NDH at 12, 24, and 48 hours of feeding, **D – F** relative expression of ATP synthase at 12, 24, and 48 hours of feeding. Significance level α ≤0.05.

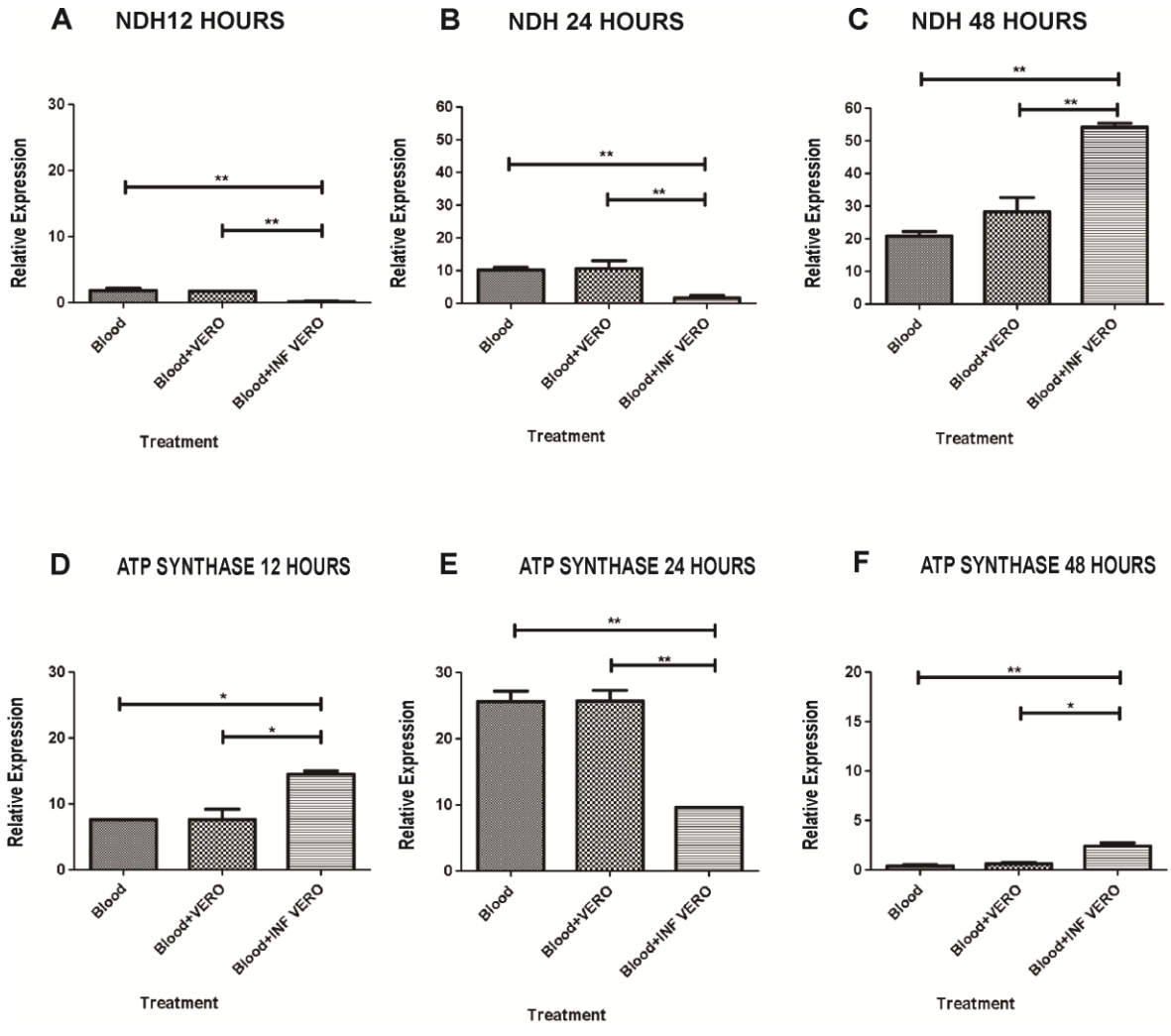

Source: own authorship.

For ATP synthase, the first hours of feeding, the relative expression was more significant in the treatment group with blood + infected Vero cells (Figure 8D). In 24 hours of feeding, treatments uninfected had their relative expression increased, and the treatment infected remained low (Figure 8E). In contrast, in 48 hours of feeding, the relative expression of ATPS was decreased in all treatments (Figure 8F).

3.3.3 Gene expression of targets involved in lipids metabolism

Three genes involved in lipids metabolism were analyzed, two of them expressed in enzymes that participate in the beta-oxidation as g5381 – acyl-CoA dehydrogenase (AD) and g1825 – enoyl-CoA hydratase (ECHD), and one involved in the transport of long-chain fatty acids into the mitochondrial matrix as g3006 - carnitine O-palmitoyltransferase (CPTI) (Figure 9).

The relative expression of the AD gene was up-regulated when compared to ECHD and CPTI genes. In 12 hours of feeding, treatments without infection showed statistically lower than blood + infected Vero cells for AD and ECHD (Figures 9A and 9D). With 24 hours of feeding, an increase in the relative expression of AD and ECHD was significant for uninfected treatments, and relative expression of blood + infected Vero cells remained diminished (Figures 9B and 9E). In contrast, AD and ECDH showed a more significant relative expression in the treatment infected for 48 hours (Figures 9C and 9F). CPTI showed more significant relative expression for transport of long-chain fatty acids only in the first 12 hours of feeding, whose infected treatment presented greater relative expression (Figure 9G). In the other times, CPTI remained smaller than for uninfected treatment (Figure 9H and 9I).

Figure 9: Relative expression of enzymes involved in the lipid metabolism at different feeding times with blood, blood + uninfected Vero cells (Blood+VERO), and blood + infected Vero cells (Blood+INF VERO). **A - C** relative expression of AD at 12, 24, and 48 hours of feeding, **D – F** relative expression of ECHD at 12, 24, and 48 hours of feeding, **G – I** relative expression of CPTI at 12, 24, and 48 hours of feeding. Significance level α ≤0.05.

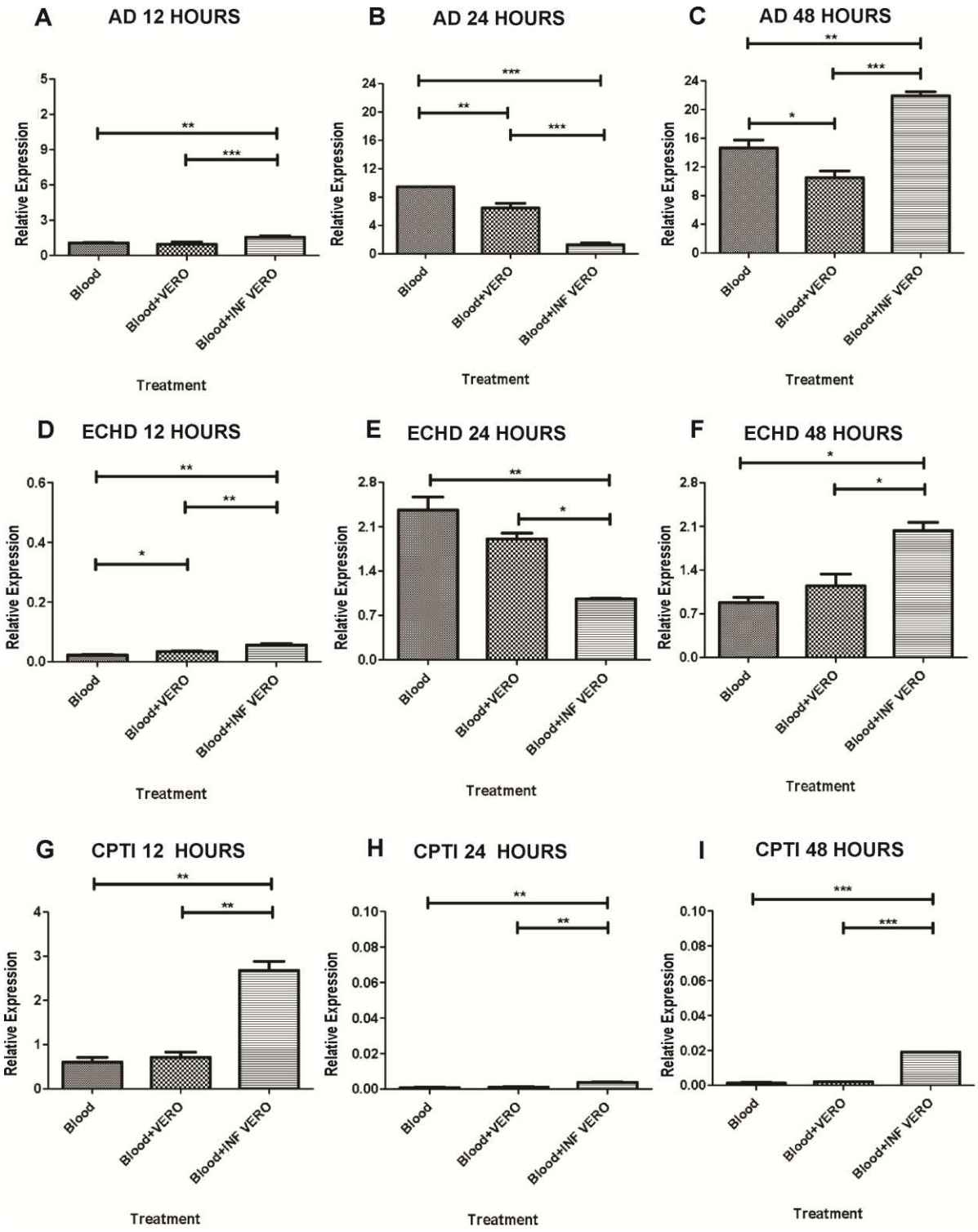

Source: own authorship.

3.3.4 Gene expression of targets involved in amino acids metabolism

Five genes involved in amino acids metabolism were analyzed, and the relative expression measured for g673 – Putative aromatic amino acid hydroxylase (AAAH), g465 – Histidine ammonia-lyase (HAL), g3515 – Asparaginase (ASNase), g3339 - Putative ornithine aminotransferase (OAT), and g486 - Aspartate aminotransferase (AspAT).

The relative expression of the AAAH, HAL, OAT, and AspAT was more significant when compared to ASNase. In 12 hours of feeding, treatments without infection showed statistically lower than in the treatment group blood + infected Vero cells for AAAH, HAL, ASNase, AspAT, and statistically significant for OAT (Figures 10A, 10D, and 10G; Figures 11A and 11D). With 24 hours of feeding, an increase in the relative expression of AAAH, HAL, ASNase, and OAT was significant for uninfected treatments, whose relative expression of blood + infected Vero cells remained diminished (Figures 10B, 10E and 10H; Figures 11B and 11E). AspAT showed a more significant relative expression in the treatment infected 24 hours (Figure 11E). Blood + Vero cells' relative expression was bigger than blood treatment for AAAH, HAL, and ASNase (Figures 10B, 10E, and 10H). With 48 hours of feeding, an increase in the relative expression of AAAH, HAL, ASNase, and OAT was significant for infected treatment, with uninfected had a decrease compared to 24 hours (Figures 10C, 10F, and 10I; Figures 11C and 11F). AspAT showed a decrease in all treatments' relative expression in the time of 48 hours compared to 24 hours (Figure 11F).

Figure 10: Relative expression of enzymes involved in the amino acid metabolism at different feeding times with blood, blood + uninfected Vero cells (Blood+VERO), and blood + infected Vero cells (Blood+INF VERO). **A - C** relative expression of AAAH at 12, 24, and 48 hours of feeding, **D – F** relative expression of HAL at 12, 24, and 48 hours of feeding, **G – I** relative expression of ASNase at 12, 24, and 48 hours of feeding. Significance level α ≤0.05.

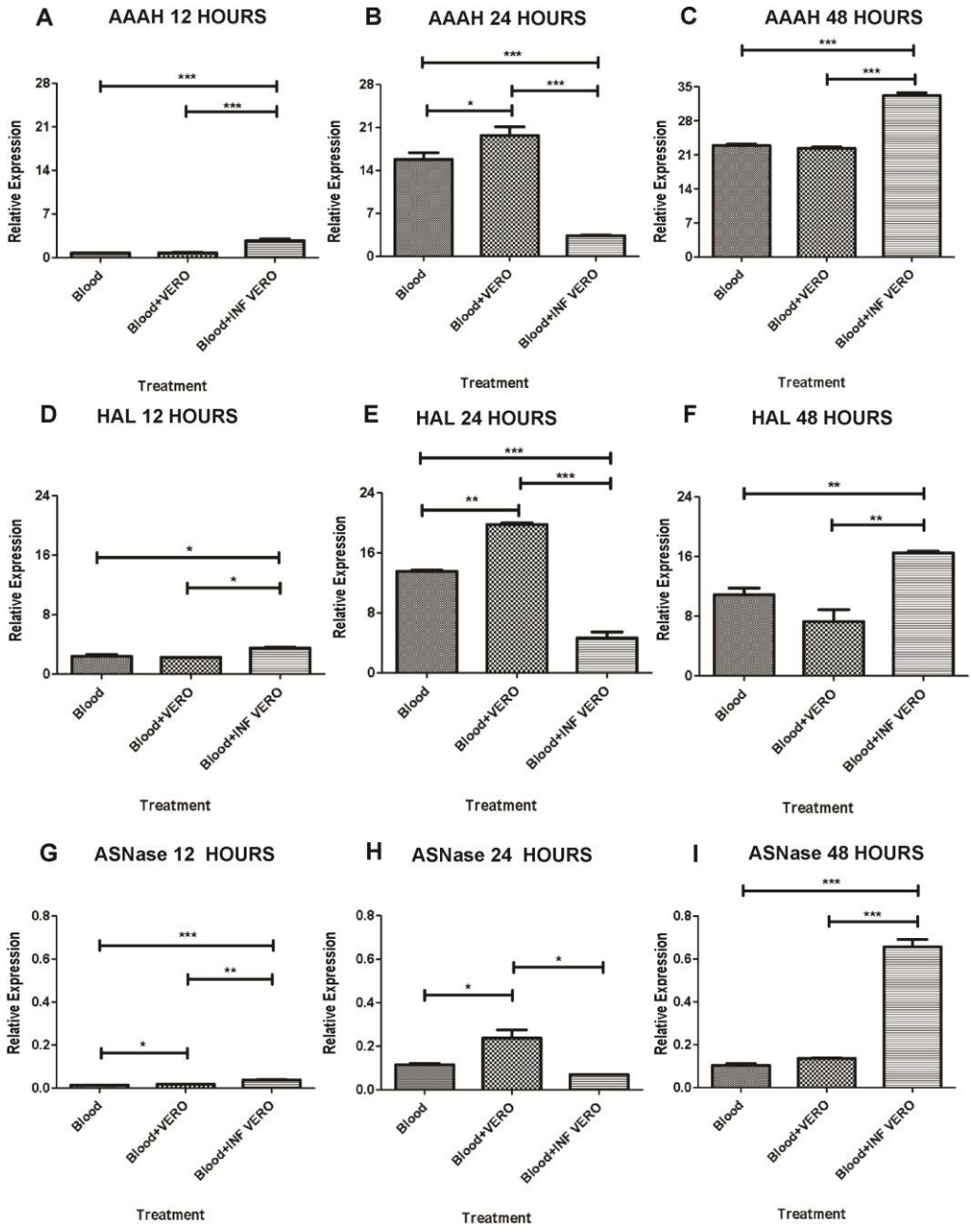

Source: own authorship

Figure 11: Relative expression of enzymes involved in the amino acid metabolism at different feeding times with blood, blood + uninfected Vero cells (Blood+VERO), and blood + infected Vero cells (Blood+INF VERO). **A - C** relative expression of OAT at 12, 24, and 48 hours of feeding, **D – F** relative expression of AspAT at 12, 24, and 48 hours of feeding. Significance level α ≤0.05.

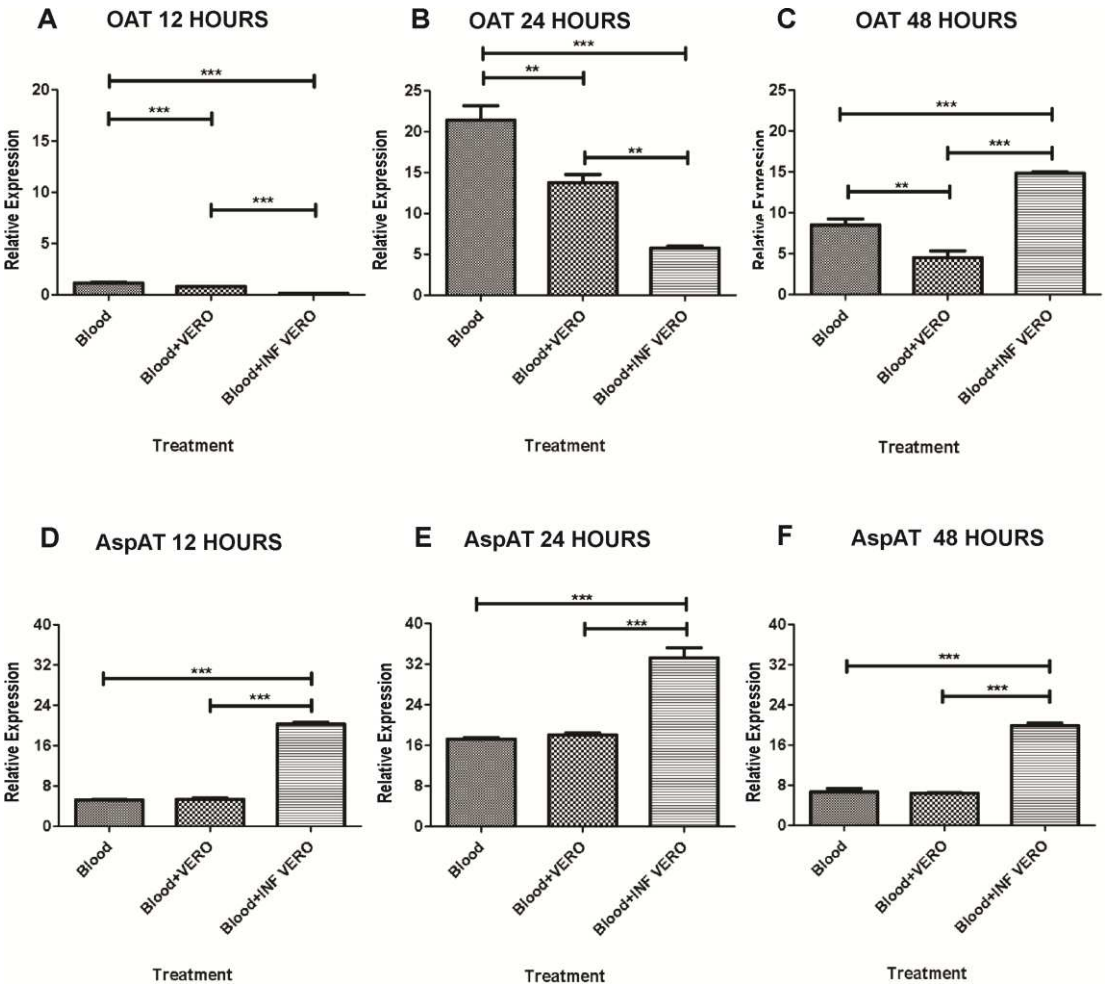

Source: own authorship.

3.3.5 Gene expression of targets involved in nucleotide metabolism

Four genes involved in nucleotide metabolism were analyzed: g130 – Putative glutamine phosphoribosyl pyrophosphate amidotransferase (purF), g971 – Putative ribose-phosphate pyrophosphokinase (RPPK), g8171 – Putative deoxycytidylate deaminase (dCMP deaminase), and g2871 - Purine nucleoside phosphorylase (PNP).

The expression of purF and RPPK were more significant compared to dCMP deaminase and PNP. In 12 hours of feeding, treatments without infection showed

statistically more significant than blood + infected Vero cells for purF and dCMP deaminase (Figures 12A and 13A) and statistically lower for PNP (Figures 13D).

With 48 hours of feeding, there was an increase in the relative expression of purF, RPPK, and dCMP deaminase for infected treatment; uninfected had an increase compared to 24 hours for RPPK and PNP (Figure 12C, 12F; Figure 13C, 13F). In contrast, PNP showed a lower relative expression in the treatment infected 48 hours (Figure 13F).

Figure 12: Relative expression of enzymes involved in the nucleotide metabolism at different feeding times with blood, blood + uninfected Vero cells (Blood+VERO), and blood + infected Vero cells (Blood+INF VERO). **A - C** relative expression of purF at 12, 24, and 48 hours of feeding, **D – F** relative expression of RPPK at 12, 24, and 48 hours of feeding. Significance level α ≤0.05.

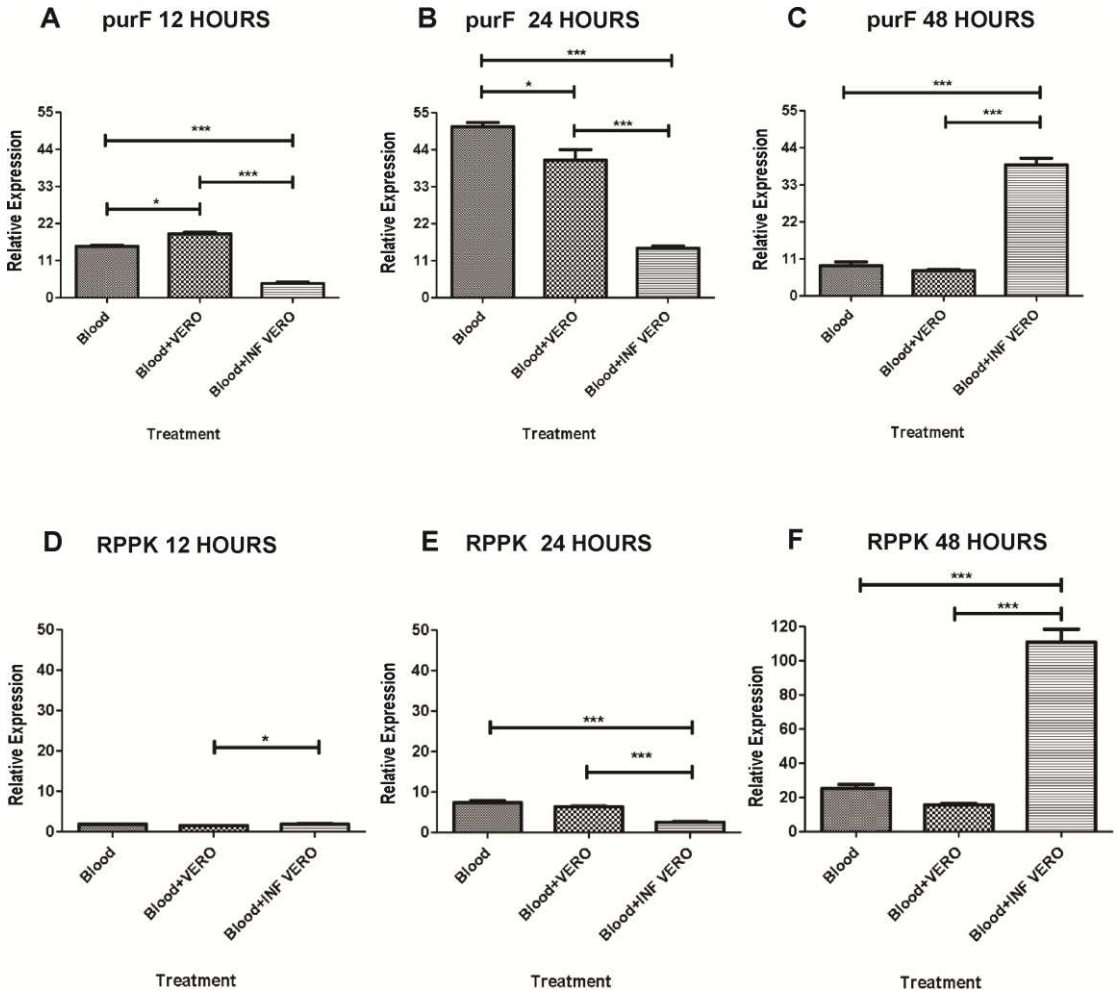

Source: own authorship.

Figure 13: Relative expression of enzymes involved in the nucleotide metabolism at different feeding times with blood, blood + uninfected Vero cells (Blood+VERO), and blood + infected Vero cells (Blood+INF VERO). **A - C** relative expression of dCMP deaminase at 12, 24, and 48 hours of feeding, **D – F** relative expression of PNP at 12, 24, and 48 hours of feeding. Significance level α ≤0.05.

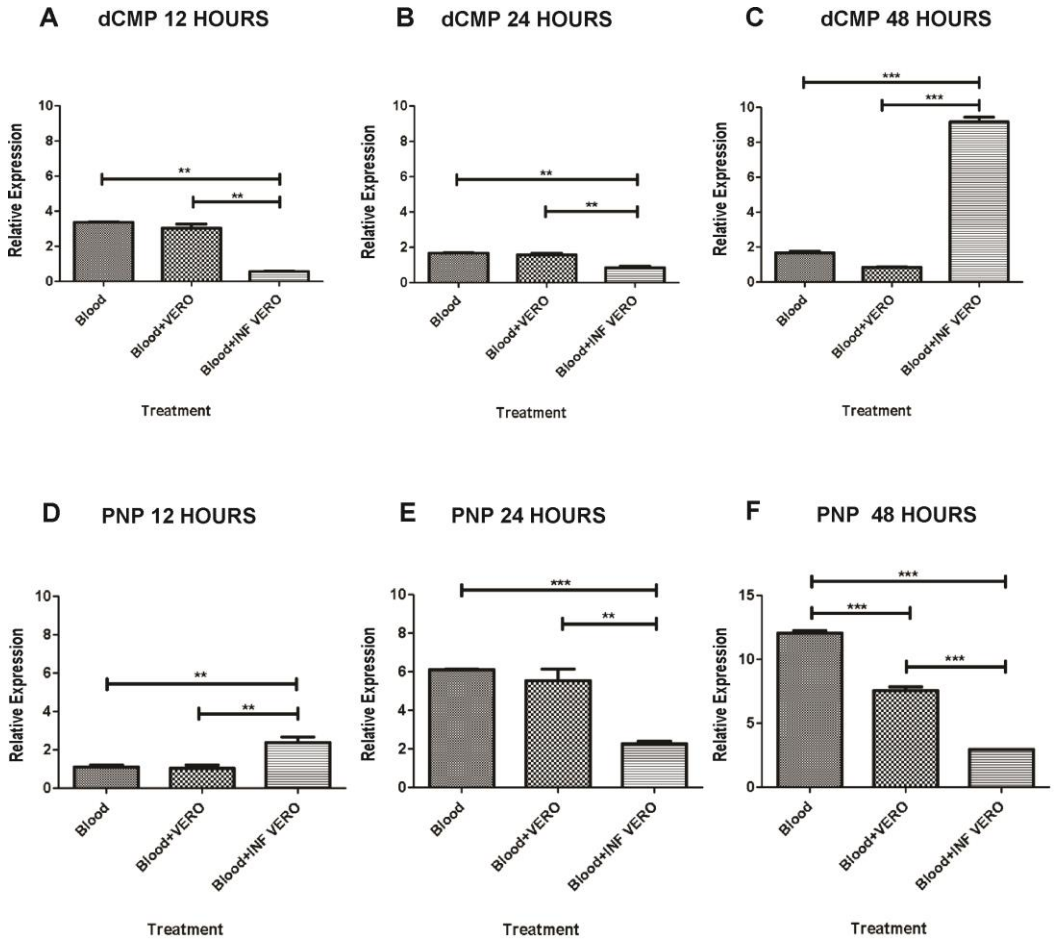

Source: own authorship.

4. DISCUSSION

After determining the mean number of copies of rickettsia present in the tick's midgut, a significant increase from 12 to 24 hours of feeding was observed. The first interaction site between a rickettsia-free and a tick is the midgut when the arthropod feeds in an infected vertebrate host (SOCOLOVSCHI et al., 2009). In sequence, the bacteria cross the midgut barrier and escape from the tick's immunology cells, invading hemocytes, present in the hemolymph. After this process, the bacteria can enter the epithelial cells and start their replication. Thus, bacteria invade salivary glands and ovaries for replication and permanence. These steps were described in detail by

SOCOLOVSCHI et al. (2009), which also showed that the more infected blood the tick ingests, the greater the probability of infection and the more significant number of bacteria are found. This observation corroborates with the results presented for the infection for 48 hours.

The weight results presented with blood and blood + Vero cells feedings at 12 and 24 hours showed that the first contact of ticks with blood (20 days after the molting process for the adult stage) was efficient using plastic tips as an alternative to replace vertebrate hosts, whose weight difference was positive. This result corroborates the knowledge that ixodid ticks during the first hours of feeding ingest a significant amount of blood (SONENSHINE, 1991). The most used experimental methodology for infection by rickettsiae in free ticks is still the management of susceptible mammalian hosts, but models like the one presented here have been tested to standardize the technique (PURNELL, 1970; WALKER et al., 1979; VALIM et al., 2017) that in the future may replace the use of animal hosts in different approaches (RANGEL et al., 2011).

The significant decrease in the weight of ticks in the presence of *R. amblyommatis* for 12, 24, and 48 hours of feeding, indicated an interaction between the arthropod and the bacteria in the midgut negatively impacting the increased weight and making its ability to store nutrients unfeasible. In the work of HARRIS et al. (2017), the tick of the species *Amblyomma maculatum* was exposed to *R. rickettsii*, *R. parkeri*, *R. amblyommatis*, *R. montanensis,* or *R. felis*, with mass weight-reducing difference by up to 30% between after and before feeding treatments.

The weight of ticks fed with blood for 48 hours was lower than 24 hours (Figure 4A). This result can be justified by the appearance, after 48 hours of feeding, of a white and red excretion in ticks. According to SONENSHINE (1991), the excreta can be composed of undigested hemoglobin right after feeding, which justifies the red color, and guanine, a white residual excretion product. Cleaning the ticks after the feeding time, discarded these substances. During artificial feeding with capillary tubes performed by ABEL et al. (2008), the mean weight of ticks fed 48 hours was also lower than ticks fed for 24 hours, whose excretion was also observed and considered a limiting factor weight gain after 24 hours of feeding.

In this study, the addition of Vero cells in the diet increased to the components ingested by the tick, whose digestion may have allowed the ticks to increase in weight compared to the diet with blood. This experimental model was used to rule out any

negative influence of uninfected Vero cells during tick feeding, stating that the bacteria's presence could limit the weight gain of the tick and not the presence of the Vero cell.

We chose to analyze the gene expression of enzymes involved in tick metabolism to understand the tick phenotypic change (weight difference between infected and uninfected treatments).

The lower expression of PFK in the infected treatment during 12 and 24 hours of feeding suggests that the tick interfered negatively in the expression of this gene to decrease the availability of intermediates of the glycolytic pathway to hinder the permanence and survival of *R. amblyommatis* inside the midgut. Within 48 hours, the tick and bacteria's energy requirement was sufficient to increase the expression of PFK in the infected treatment. According to RENESTO et al. (2005), many Rickettsiae do not have the enzymes necessary to break carbohydrates. Thus, they need to capture such intermediates present in the hosts as a primary source of carbon. If the intermediates are present, rickettsia can regulate the gene expression of crucial tick enzymes to increase their degradation, increasing their medium availability. This result suggests that the simple use of the tick's carbon sources is insufficient to maintain and survive the bacteria in the midgut. Besides that, the product of the reaction catalyzed by PFK, fructose 1,6 bisphosphate, can be used by bacteria to form glycerol-3-phosphate, which will be internalized by rickettsia's transporters and transformed into glycerophospholipid, the main constituent of the cell membrane (DRISCOLL et al., 2017).

The high relative expression of PK for uninfected treatments fed for 48 hours favors pyruvate formation, an essential component for the beginning of the TCA cycle. In the infected treatment, PK's lower expression can benefit the accumulation of phosphoenolpyruvate in the cytoplasm, which may be captured and converted to pyruvate phosphate dikinase (PPDK), present in Rickettsiaceae (RENESTO et al., 2005).

Up expression of PEPCK presented in the infected treatment corroborates phosphoenolpyruvate formation from pyruvate (gluconeogenesis), confirming that there was a modification in the gene expression of the enzyme to enrich an important intermediary used by bacteria in their own TCA cycle. *Rickettsia* possesses the necessary enzymes to synthesize TCA intermediates, unlike the glycolytic pathway (RENESTO et al., 2005). Besides that, a small part of the fructose 1,6 biphosphate

formed from the glycolysis reaction can be transformed into fructose phosphate by the enzyme FBP, whose intermediary plays an essential role in the pentose phosphate pathway. It was reported that the *Rickettsia* genus has a deficiency in this pathway's enzymes (RENESTO et al., 2005), which is considered necessary in the synthesis of nucleotides (MIN et al., 2008).

The low availability of pyruvate in the midgut of infected ticks affected the relative expression of the PDH enzyme, which presented a more significant expression only 48 hours of feeding. This result suggests that the lower expression of PDH can be attributed to lower pyruvate availability in the cytoplasm, which enters the mitochondria to form acetyl-CoA. Pyruvate is the most critical product of glycolysis, which distribution favored rickettsia in the first moment. If this substrate's low availability hinders pyruvate conversion to acetyl- CoA, the TCA cycle, and the other reactions that depend on this intermediate can be adversely affected. The negative or low weight difference presented in this study in the infected treatment may be related to the difficulty of the tick in obtaining energy to maintain the vital reactions to survival and later storage of metabolites.

In the TCA cycle, the more significant relative expression of PDH, IDH, and AKGD for uninfected treatments (24 hours) maintains the indication that the availability of pyruvate at the beginning of this pathway is greater for uninfected, due to the entry of phosphoenolpyruvate in the TCA cycle of the bacteria in the infected treatment. According to REN et al. (2019), when ticks enter the blood-feeding stage, the TCA cycle and other energy metabolism pathways become more active. The ticks can immediately convert carbohydrates, fats, and proteins from the blood of the host into ATP by the respiratory chain. Most organs in ticks can develop rapidly after a short duration of feeding. In this study, the decrease in the relative expression of enzymes in the TCA cycle at 12 and 24 hours may have impaired the development of ticks and consequently decreased the weight gain of these arthropods. This pathway is indispensable to provide energy during feeding and is considered essential to the rapid expansion of the tick body (REN et al., 2019).

In 48 hours of feeding, the decrease in the relative expression of the enzymes PDH, IDH, and AKGD in uninfected treatments, suggests that the tick met its energy (ATP) requirement and started the synthesis of other essential metabolites for survival, whose expression of the enzymes involved in the TCA cycle was suppressed. In the infected treatment, PDH and IDH showed an increase considered late. Here, we

believe that the bacteria could increase PK's relative expression, resulting in greater cytosolic pyruvate availability, which was converted to Acetyl-CoA by PDH, whose expression was also increased. This observation indicates that suppressing these enzymes at 12 and 24 hours may impair other reactions for tick survival. If that expression remained suppressed, the bacteria could lead its host to death.

After the TCA cycle, oxidative phosphorylation is the next step for the synthesis of ATP. The more significant relative expression of NDH in uninfected treatments indicates that NADH molecules obtained by the TCA cycle were utilized to sequentially transfer electrons of the complex I to complex V (NDH participates of the complex I and ATP synthase participates of the complex V). The lower relative expression of NDH in infected treatment reveals a deficiency of NADH due to the low acquisition during the suppression of the TCA cycle. As we saw earlier to the other enzymes, with 48 hours of feeding with rickettsia, the relative expression of NDH was increased to compensate for low relative expression in the early hours.

ATP is an essential energetic molecule for prokaryotic and eukaryotic organisms. ATP synthase relative expression was increased (12 hours of feeding) with the presence of the bacteria. With this observation, we infer that rickettsia can influence the gene expression of the tick in order to capture host ATP already generated through ATP/ADP translocases and changing for bacterial ADP, which are present in Rickettsiaceae (SCHMITZ-ESSER et al., 2004), including the information that the *Rickettsia* possesses genes for oxidative phosphorylation and ATP synthase complex (MIN et al., 2008). In 48 hours of feeding, all treatments had a lower relative expression of ATP synthase. This result corroborates with the observation described previously that the tick met its energy (ATP) requirement and started synthesizing other essential metabolites for survival.

AD catalyzes the conversion of acyl-CoA to enoyl-CoA inside mitochondria. This reaction is the first in the beta-oxidation pathway, which occurs when necessary to produce energy, using fatty acids as substrate. ECHD participates in the second reaction of beta-oxidation, which converts enoyl-CoA to 3-hydroxy acyl-Coa.

In lipid metabolism, most genes are present in members of the Rickettsiales order (MIN et al., 2008). AD and ECHD relative expression were lower in infected treatment with 24 hours of feeding. These enzymes form acetyl-CoA from fatty acids, whose suppression decreased their formation and participation in the TCA cycle, suggesting that the tick restricted key metabolites for *R. amblyommatis*. In contrast,

the relative expression of CPTI considered the gatekeeper of free fatty acid oxidation (ZANG et al., 2005) increased during the first and late feeding for infected treatment. This result demonstrates that the low amount of glucose in fasting ticks favored the degradation pathway of fatty acids to obtain energy, whose regulation is for survival for long periods without feeding. After 12 hours of feeding, the relative expression decreased in all treatments. According to ZANG et al. (2005), increased concentration of glucose from food increases malonyl-CoA formation. It diminishes fatty acid oxidation by the action of the enzyme acetyl-CoA carboxylase, favoring malonyl-CoA formation and inhibiting the carnitine system.

The decrease or low weight gain of ticks fed with *Rickettsia* may also be linked to the increase enzymes AD, ECDH, and CPTI expression. According to RUPASINGHE et al. (2016), the increase in fatty acid β-oxidation is negatively correlated with the increased body mass index.

AAAH are members of enzymes that use a mononuclear nonheme Fe center to catalyze various challenging reactions, in which O_2 is used in the oxidative transformation of substrates (McCRAKEN, 2015). HAL is the first enzyme in L-histidine's degradation pathway, whose reaction can be catalyzed for other enzymes until conversion to L-glutamate (KOHLMEIER, 2015). OAT is involved in the biosynthesis pathway of proline and glutamate from ornithine (GINGUAY et al., 2017). AspAT catalyzes the interconversion of aspartate and α-ketoglutarate to oxaloacetate and glutamate. L-glutamate serves as a donor of amino groups for the excretion pathways that lead to eliminating nitrogen products or for the biosynthetic pathways of arginine, glutamine, proline, and polyamines (CABEZAS-CRUZ et al., 2017).

It has been described that the *Rickettsia* genus possesses a deficiency in the amino acid metabolism pathways. Aromatic amino acids (tyrosine, phenylalanine, and tryptophan) and histidine are provided by cell medium or host cell (MIN et al., 2008). This study showed a more significant relative expression of AAAH, HAL, and ASNase in the blood + Vero cells treatment at 24 hours of feeding. The addition of only Vero cells in the blood as second control for infection treatment showed once again a positive response for gene expression, whose Vero cells were able to supply amino acids in the blood meal composition of ticks and to increase the relative expression of essential enzymes involved in the formation of dopamine, serotonin, tyrosine, and glutamate. In the infected treatment for 48 hours, the relative expression was more considerable compared to uninfected treatment. This result pointed out that the lower

expression in the first times (12 and 24 hours) may have affected obtaining amino acids, which was compensated late. If the bacteria cannot acquire these amino acids required for growth, their proliferation may be limited and compromised.

We verified that AspAT showed relative expression bigger than uninfected treatment in all-time (Figure 11D, 11E, and 11F). BONTEMPS-GALLO et al. (2016) suggested that L-glutamate and proline are osmoprotective molecules whose blood meal osmolarity may affect virulence factors and may serve as a physiological signal to migrate *Borrelia burgdorferi* from the midgut to salivary glands of *Ixodes* ticks. Further studies are needed to confirm that the increase of the relative expression of AspAT (all time) and OAT (48 hours) for glutamate production in the presence of *R. amblyommatis* had as objective promote their growth in the high or low osmolarity (blood meal) and to sense environmental osmotic pressure, mechanism seen in *Salmonella typhimurium* (BOTSFORD et al., 1994), *B. burgdorferi* (BONTEMPS-GALLO et al., 2016) and *Escherichia coli* (EPSTEIN, 1986). In *Rickettsia*, glutamate also participates in histidine metabolism, nitrogen metabolism, glutathione metabolism, glyoxylate, and dicarboxylate metabolism, among other reactions based on the Kyoto Encyclopedia of Genes data and Genomes (KEGG). One of the products of the reaction involving AspAT, oxaloacetate, still may be intermediate for glutamate, aspartate, and lysine formation, in addition to cofactors for ticks, indicating an essential role for both host and bacteria.

ASNase converts asparagine into aspartate, which is an essential substrate to the formation of glutamate with the participation of AspAT. In 48 hours of feeding, the infected treatment showed a more significant relative expression of ASNase than uninfected treatment. This result indicates that aspartate may be used as a substrate for the reaction of glutamate formation, whose relevance has been demonstrated in other studies (RENESTO et al., 2005; MIN et al., 2008).

The enzyme purF participates in the biosynthesis pathway for purine and thiamine. It is known that purF catalyzes the synthesis of phosphoribosylamine (PRA) from phosphoribosyl pyrophosphate (PRPP) and glutamine (KOENIGSKNECHT et al., 2007). RPPK converts ribose 5-phosphate into phosphoribosyl pyrophosphate (PRPP), whose ribose 5-phosphate is produced from glucose-6-phosphate of the glycolytic pathway. The enzyme dCMP deaminase is responsible for the main pathway of pyrimidines synthesis, providing the nucleotide substrate for thymidylate synthase

(WEINER et al., 1993). PNP catalyzes the phosphorolysis of purine nucleosides and converts inosine to hypoxanthine and guanosine to guanine.

Studies of nucleotide metabolism revealed that host-acquired ribonucleotides serve as precursors for RNA synthesis and deoxyribonucleotide production (WINKLER et al., 1999). In the uninfected tick's midgut, the relative expression of PNP, dCMP deaminase, RPPK, and purF was more significant than the infected treatment for 24 hours. The low relative expression of purF and RPPK in infected ticks during 12 and 24 hours revealed a decrease in *de novo* purine synthesis regulated by product phosphoribosyl amine and glutamine conversion glutamate during the reaction. *Rickettsia* depends on the host to obtain nucleotides such as adenine and guanine, and the suppression of purF and RPPK expressions show a possible mechanism of defense from the tick in order to hinder the process of obtaining these nucleotides by bacteria for the *de novo* nucleotide synthesis pathway (MIN et al., 2008). In contrast, in the last feeding time, the relative expression was more significant in infected treatment, indicating that the initial suppression may be compensated for the synthesis of DNA, RNA, ATP, and coenzymes for ticks, growth, and virulence for bacteria. For the synthesis of pyrimidines catalyzed for dCMP deaminase, the bacteria presence decrease the relative expression, suggesting a reduction in the availability of resources to prevent the spread of bacteria, whose mechanism is not sustained within 48 hours.

PNP is one of the enzymes involved in the purine degradation pathway, which converts inosine to hypoxanthine, and converts guanosine to guanine when DNA is metabolized (based on KEGG). The synthesis of guanine, a regular tick excretory product (KAMEL et al., 1982), and hypoxanthine, may have been decreased by the tick not to favor the use of these intermediaries in the formation of molecules in the purine salvage pathway, whose product may be used by *Rickettsia* (RENESTO et al., 2004; MIN et al., 2008). Ticks fed 48 hours with blood showed an excretion after feeding, which contained hemoglobin (red) and guanine (white). This observation may justify the more significant relative expression of PNP in the last time of feeding with the excretory product seen, whose ticks showed lower mean weight difference after clean and weighting (Figure 3C).

5. CONCLUSION

In the present study, *A. sculptum* female ticks were infected with *R. amblyommatis* using artificial feeding during 12, 24, and 48 hours, which weight was

observed before and after feeding. The protocol of artificial feeding of ticks with plastic tips allowed the exclusion in the use of vertebrate hosts, who would have to go through a process of infection with rickettsia, requiring an adequate infrastructure for the procedure. With artificial feeding, an increase in mass in treatments with blood and blood added with VERO cells was observed. However, there was a decrease in weight in the infected treatment, pointing out that rickettsia interfered with the tick's metabolism mechanisms.

The number of copies of the bacterium increased significantly from 24 to 48 hours in the infected treatment, showing its adaptation and spread in the last hours of established treatment.

Rickettsiae are obligatory intracellular bacteria whose behavior within the host will dictate their survival and spread, with a high capacity for invasion into other tissues. The association of weight and infection studies has answered questions about the tick and vector interaction. Other bacteria of the genus *Rickettsia* should be studied to evaluate the phenotypic behavior and response when in contact with its vectors.

This study also reported changes in the tick metabolism in response to *R. amblyommatis* infection at different feeding times. This experimental approach pointed out which chosen metabolic pathways may be affected by *R. amblyommatis* infection in the midgut, resulting in a tick’s weight loss. The results demonstrated that pathogen infection affected glucose metabolic pathways, gluconeogenesis, TCA cycle, energy, lipid, amino acid, and nucleotide metabolism. These results supported the lower mean weight gain found in ticks fed with blood + infected Vero cells. Then, providing answers of how the pathogen can benefit from the tick changing the gene expression of key metabolic enzymes and how ticks can change the gene expression of enzymes involved in their metabolism to difficult the permanence and propagation of the bacteria in phenotypic consequence as weight gain.

Studies involving metabolites of pathogens and their hosts are advancing, but future work using bioinformatics and metabolomics approaches will provide more information on the complex metabolic integration, in this very interesting parasite – host interaction, highlighting the importance of gene expression evaluation to provide more information on the complex metabolic integration between the host-parasite relation.

6. ACKNOWLEDGMENT

This work was supported by Fundação Arthur Bernardes (FUNARBE), Fundação de Amparo à Pesquisa do Estado de Minas Gerais (FAPEMIG), Conselho Nacional de Desenvolvimento Científico e Tecnológico (CNPq) and Coordenação de Aperfeiçoamento de Pessoal de Nível Superior (CAPES). C.M. is Productive Research grant recipient from Brazilian National Council for Scientific and Technological Development (CNPq).

7. REFERENCES

ABEL, I., CORRÊA, F. N., CASTRO, A. A., CUNHA, N. C., MADUREIRA, R. C., FONSECA, A. H. Artificial feeding of *Amblyomma cajennense* (Acari: Ixodidae) fasting females through capillary tube technique. Rev. Bras. Parasitol. Vet. 17, 128-132, 2008.

AGOSTINI, M. M. Marcadores moleculares para identificação de carrapatos vetores de agentes infecciosos. 2008. Dissertação (Mestrado em Bioquímica Agrícola). Universidade Federal de Viçosa, Viçosa, MG, 2008.
Disponível em:
https://www.locus.ufv.br/bitstream/123456789/2447/1/texto%20completo.pdf. Acesso em: 22 jan.2021.

AGUILAR, A. P. (Unpublished results). Caracterização de expressão gênica em glândulas salivares, intestinos e ovários de *Amblyomma cajennense* infectados com *Rickettsia amblyommii* sob pressão de agentes antimicrobianos inibidores da síntese de proteínas, por meio da validação por PCR quantitativo, de genes codificantes de enzimas chave em diferentes vias metabólicas de *Amblyomma cajennense*. Universidade Federal de Viçosa, Viçosa, MG, 2019.

AGUIRRE, A. A. R.; GARCIA, M. V.; COSTA, I. N.; CSORDAS, B. G.; RODRIGUES, V. S.; MEDEIROS, J. F.; ANDREOTTI, R. New records of tick-associated spotted fever group Rickettsia in an Amazon-Savannah ecotone, Brazil. Ticks and tick-borne diseases, v. 9, n. 4, 1038-1044 p, 2018.

AKMAN, L., YAMASHITA, A., WATANABE, H., OSHIMA, K., SHIBA, T., HATTORI, M., et al. Genome sequence of the endocellular obligate symbiont of tsetse flies, Wigglesworthia glossinidia. Nat Genet 32, 402–407, 2002.

AMMERMAN, N. C., BEIER-SEXTON, M., AZAD, A. F. Laboratory maintenance of *Rickettsia rickettsii*. Curr. Prot. Microbiol. 11, 1-27, 2008.

ANATRIELLO, E., RIBEIRO, J. M. C., MIRANDA-SANTOS, I. K. F., BRANDÃO, L. G., ANDERSON, J. M., VALENZUELA, J. G., MARUYAMA, S. R., SILVA, J. S., FERREIRA, B. R. An insight into the sialotranscriptome of the brown dog tick, *Rhipicephalus sanguineus*. BMC Genomics. 11,1-17, 2010.

ARAÚJO, F.S., BARCELOS, R.M., MENDES, T.A.O., MAFRA, C. Molecular Evidence of *Rickettsia felis* in *Phereoeca* sp. Braz. J. Vet. Parasitol. 30(1): e015620, 2021.

BARUA, S., HOQUE, M. M., KELLY, P. J., POUDEL, A., ADEKANMBI, F., KALALAH, A., YANG, Y., & WANG, C. First report of *Rickettsia felis* in mosquitoes, USA. Emerg. Microbes. Infect. 9(1), 1008–1010, 2020.

BECHARA, G. H., SZABÓ, M. P. J., FERREIRA, B. R., GARCIA, M. V. *Rhipicephalus sanguineus* tick in Brazil: feeding and reproductive aspects under laboratorial conditions. Rev. Bras. Parasitol. Vet. 4, 61-66, 1995.
BEHAR, A., MCCORMICK, L. J., & PERLMAN, S. J. *Rickettsia felis* infection in a common household insect pest, *Liposcelis bostrychophila* (Psocoptera: Liposcelidae). Appl. Environ. Microbiol. 76(7), 2280–2285, 2010.

BIRNBOIM, H. C., DOLY, J. A rapid alkaline extraction procedure for screening recombinant plasmid DNA. Nucleic Acids Res. 7, 1513-1523, 1979.

BONNET S., LIU, X. Y. Laboratory artificial infection of hard ticks: A tool for the analysis of tick-borne pathogen transmission. Acarol. 52, 453-464, 2012.

BONTEMPS-GALLO, S., LAWRENCE, K., GHERARDINI, F. C. Two different virulence-related regulatory pathways in *Borrelia burgdorferi* are directly affected by osmotic fluxes in the blood meal of feeding *Ixodes* Ticks. PLoS Pathog. 12, e1005791, 2016.

BOTSFORD, J. L., ALVAREZ, M., HERNANDEZ, R., NICHOLS, R. Accumulation of glutamate by *Salmonella typhimurium* in response to osmotic stress. Appl. Environ. Microbiol. 60, 2568-74, 1994.

BURGDORFER, W., BRINTON, L. P. Mechanisms of transovarial infection of spotted fever Rickettsiae in ticks. Annals of the New York Academy of Sciences, 266: 61-72, 1975.

BUSTIN, S. A. (Ed.). A-Z of Quantitative PCR. IUL Press, 2004. 830pp.

CABEZAS-CRUZ, A., ESPINOSA, P. J., OBREGÓN, D. A., ALBERDI, P., DE LA FUENTE, J. *Ixodes scapularis* tick cells control *Anaplasma phagocytophilum* infection by increasing the synthesis of phosphoenolpyruvate from tyrosine. Front Cell Infect Microbiol. 7, 375, 2017.

CARUSO, C. S., 2007. Clonagem, expressão e caracterização de proteínas recombinantes de *Xylella fastidiosa*. PhD thesis. Universidade de São Paulo, São Paulo.
Disponível em:
http://www.teses.usp.br/teses/disponiveis/75/75132/tde-29082007-111527/. Acesso em: 15 abr. 2021.

DRISCOLL, T. P., VERHOEVE, V. I., GUILLOTTE, M. L., LEHMAN, S. S., RENNOLL, S. A., BEIER-SEXTON, M., RAHMAN, M. S., AZAD, A. F., GILLESPIE, J. J. Wholly Rickettsia! Reconstructed metabolic profile of the quintessential bacterial parasite of eukaryotic cells. MBio 8, 00859-17, 2017.

EPSTEIN, W. Osmoregulation by potassium transport in *Escherichia coli*. FEMS Microbiol. Lett. 39, 73-78, 1986.

ESTRADA-PEÑA, A., MARTINEZ, J. M., ACEDO, C. S., QUILEZ, J., DEL CACHO, E. Phenology of the tick, *Ixodes ricinus*, in its southern distribution range (central Spain). Med. Vet. Entomol. 18, 387-397, 2004.

FRENOT, Y., DE OLIVEIRA, E., GAUTHIER-CLERC, M., DEUNFF, J., BELLIDO, A., VERNON, P. Life cycle of the tick *Ixodes uriae* in penguin colonies: relationships with host breeding activity. Int. J. Parasitol. 31, 1040-1047, 2001.

GINGUAY, A., CYNOBER, L., CURIS, E., NICOLIS, I. Ornithine Aminotransferase, an Important Glutamate-Metabolizing Enzyme at the crossroads of multiple metabolic pathways. Biology (Basel) 6, 18, 2017.

HARRIS, E. K., VERHOEVE, V. I., BANAJEE, K. H., MACALUSO, J. A., AZAD, A. F., MACALUSO, K. R. Comparative vertical transmission of *Rickettsia* by *Dermacentor variabilis* and *Amblyomma maculatum*. Ticks tick Borne Dis. 8, 598-604, 2017.

HOXMEIER, J., FLESHMAN, A., BROECKLING, C., PRENNI, J. E., DOLAN, M. C., GAGE, K. L., et al. Metabolomics of the tick-Borrelia interaction during the nymphal tick blood meal. Sci Rep 7, 44394, 2017.

KAMEL, M. Y., SHALABY, F. Y., GHAZY, A. M. Biochemical studies of tick embryogenesis DNA, RNA, haemoprotein, guanosine and guanine in developing eggs of *Hyalomma dromedarii*. Insect Biochem. 12, 15-23, 1982.

KOENIGSKNECHT, M. J.; RAMOS, I.; DOWNS, D. M. Glutamine phosphoribosylpyrophosphate amidotransferase-independent phosphoribosyl amine synthesis from ribose 5-phosphate and glutamine or asparagine. J. Biol. Chem. 282, 28379-28384, 2007.

KOHLMEIER, M. Amino Acids and nitrogen compounds. Nutr. Metabol. 2, 265-477, 2015.

LABRUNA, M. B., WHITWORTH, T., BOUYER, D. H., MCBRIDE, J. W., PINTER, A., POPOV, V., WALKER, D. H. *Rickettsia* species infecting *Amblyomma cooperi* ticks from an area in the state of São Paulo, Brazil, where Brazilian spotted fever is endemic. J. Clin. Microbiol. 42, 90-98, 2004.

LIVAK, K. J.; SCHMITTGEN, T.D. analysis of relative gene expression data using real-time quantitative PCR and the 2−ΔΔCT method. Methods 25, 402-408, 2001.

MARTINS, T. F., BARBIERI, A. R. M., COSTA, F. B., TERASSINI, F. A., CAMARGO, L. M. A., PETERKA, C. R. L., et al. Geographical distribution of *Amblyomma cajennense* (sensu lato) ticks (Parasitiformes: Ixodidae) in Brazil, with description of the nymph of *A. cajennense* (sensu stricto). Parasites Vectors 9, 186, 2016.

McCRACKEN, J. Structural characterization of the catalytic sites of mononuclear nonheme Fe hydroxylases using 2H-ESEEM. Methods Enzymol. 563, 285-309, 2015.

MIN, C., YANG, J., KIM, S., CHOI, M., KIM, I., CHO, N. Genome-based construction of the metabolic pathways of *Orientia tsutsugamushi* and comparative analysis within the Rickettsiales order. Comp. Funct. Genomics, 2008.

MOREIRA, H. N. S. Anotação e montagem de transcriptomas de intestino médio e ovários do carrapato *Amblyomma sculptum*, antes e após a infecção por *Rickettsia amblyommii*, PhD thesis, Universidade Federal de Viçosa, Viçosa, 2017. Disponível em: https://locus.ufv.br//handle/123456789/9368 Acesso em: 10 fev.2021.

NARRA, H.P., SAHNI, A., ALSING, J., SCHROEDER, C. L. C., GOLOVKO, G., NIA, A. M., et al. Comparative transcriptomic analysis of Rickettsia conorii during in vitro infection of human and tick host cells. BMC Genomics 21, 665, 2020.

NOGGE, G. Significance of symbionts for the maintenance of an optimal nutritional state for successful reproduction in hematophagous arthropods. Parasitology 82, 101–104, 1981.

OLIVER, J. R. Biology and systematics of ticks (Acari: Ixodida). Annu. Rev Ecol. Syst. 20, 397-430, 1989.

OWCZARZY, R., TATAUROV, A. V., WU, Y., MANTHEY, J. A., MCQUISTEN, K. A., ALMABRAZI, H. G., PEDERSEN, K. F., LIN, Y., GARRETSON, J., MCENTAGGART, N. O., SAILOR, C. A., DAWSON, R. B., PEEK, A. S. IDT SciTools: a suite for analysis and design of nucleic acid oligomers. Nucleic Acids Res. 36, W163–W169, 2008.

PFAFFL, M. W. A new mathematical model for relative quantification in real-time RT-PCR. Nucleic Acids Res. 29, 2002-2007.s, 2001.

PHELAN, K.; MAY, K. M. Basic techniques in mammalian cell tissue culture. Curr. Prot. Cell Biol. 66, 1.1.1-1.1.22, 2015.

PURNELL, R. Infection of the tick *Rhipicephalus appendiculatus* with *Theileria parva* using an artificial feeding technique. Vet. J. 11, 403-405, 1970.

QUIROZ-CASTAÑEDA, R. E.; COBAXIN-CÁRDENAS, M.; CUERVO-SOTO, L. I. Exploring the diversity, infectivity and metabolomic landscape of Rickettsial infections for developing novel therapeutic intervention strategies. Cytokine, [S.L.], v. 112, p. 63-74, 2018.

RANGEL, C. P., CUNHA, N. C., REZENDE, J., SILVA, F. J. M., CORRÊA, F. N., TEIXEIRA, R. C., SILVA, J. B., BAÊTA, B. A., FONSECA, A. H. Alimentação artificial por meio de tubos capilares de fêmeas parcialmente ingurgitadas do carrapato *Dermacentor* (*Anocentor*) *nitens*. Rev. Bras. Parasit. Vet. 17, 35-39, 2008.

RANGEL, C. P. Eficiência da alimentação in vitro de fêmeas de *Rhipicephalus microplus* (Acari: Ixodidae), PhD thesis, Universidade Federal Rural do Rio de Janeiro, Seropédica, 2011.
Disponível em:
http://r1.ufrrj.br/adivaldofonseca/wp-content/uploads/2014/06/Rangel-C-P-2011-Eficiencia-de-alimenta%C3%A7%C3%A3o-artificial-in-vitro-Tese.pdf Acesso em: 10 dez.2020.

RAOULT, D., ROUX, V. Rickettsioses as paradigms of new or emerging infectious diseases. Clin. Microbiol. Rev. 10, 694-719, 1997.

REN, S., ZHANG, B., XUE, X., WANG, X., ZHAO, H., ZHANGI, X., WANG, M., XIAO, Q., WANG, H., LIU, J. Salivary gland proteome analysis of developing adult female *Haemaphysalis longicornis* ticks: molecular motor and TCA cycle-related proteins play an important role throughout development. Parasit Vectors. 12, 613, 2019.

RENESTO, P., OGATA, H., AUDIC, S., CLAVERIE, J. M., RAOULT, D. Some lessons from *Rickettsia* genomics. FEMS Microbiol. Rev. 29,99-117, 2005.

RIBEIRO, C. C. D. U., BAÊTA, B. A., VALIM, J. R. A., TEIXEIRA, R. C., CEPEDA, P. B., DA SILVA, J. B., DA FONSECA, A. H. Use of plastic tips in artificial feeding of *Dermacentor* (*Anocentor*) *nitens* females Neumann, 1897 (Acari: Ixodidae). Ticks Tick Borne Dis. 6, 689-692, 2014.

ROZEN, S., SKALETZKY, H. J. Primer 3 on the WWW for general users and for biologist programmers. Methods Mol Biol. 132, 365-86, 2000.

RUPASINGHE, H. P. V., SEKHON-LOODU, S., MANTSO, T., PANAYIOTIDIS, M. I. Phytochemicals in regulating fatty acid β-oxidation: potential underlying mechanisms and their involvement in obesity and weight loss. Pharmacol. Ther. 165, 153-163, 2016.

SCHMITZ-ESSER, S., LINKA, N., COLLINGRO, A., BEIER, C. L., NEUHAUS, H. E., WAGNER, M., HORN, M. ATP/ADP Translocases: a common feature of obligate intracellular amoebal symbionts related to chlamydiae and rickettsiae. J. Bacteriol. 186, 683-691, 2004.

SOCOLOVSCHI, C., MEDIANNIKOV, O., RAOULT, D., PAROLA, P. The relationship between spotted fever group Rickettsiae and Ixodid ticks. Vet. Res. 40, 34, 2009.

SONENSHINE, D. E.,. Biology of ticks. Oxford University Press, New York, 1991. 447 pp.

STOTHARD, P. The sequence manipulation suite: javascript programs for analyzing and formatting protein and DNA sequences. Biotechniques 28, 1102-1104, 2000.

VALIM, J. R. A., RANGEL, C. P., BAÊTA, B. A., RIBEIRO, C. C. D. U., CORDEIRO, M. D., TEIXEIRA, R. C., CEPEDA, P. B., FONSECA, A. D. H. Using plastic tips in artificial feeding of *Rhipicephalus sanguineus* sensu lato (Acari: Ixodidae) females. Rev. Bras. Parasitol. Vet., 26, 110-114, 2017.

VILLAR, M.; POPARA, M.; BONZÓN-KULICHENKO, E.; AYLLÓN, N.; VÁZQUEZ, J.; LAFUENTE, J. Characterization of the tick-pathogen interface by quantitative proteomics. Ticks And Tick-Borne Diseases, [S.L.], v. 3, n. 3, p. 154-158, 2012.

WALKER, A., BROWN, C., BELL, L., MCKELLAR, S. Artificial infection of the tick *Rhipicephalus appendiculatus* with *Theileria parva*. Res. Vet. Sci. 26, 264-265, 1979.

WEINER, K. X., WEINER R. S., MALEY, F., MALEY, G. F. Primary structure of human deoxycytidylate deaminase and overexpression of its functional protein in *Escherichia coli*. J. Biol. Chem. 268, 12983-9, 1993.

WIKEL, S. K. Acquired resistance to ticks. Expression of resistance by C4-deficient guinea-pigs. Am. J. Trop. Med. Hyg. 28, 586-590, 1979.

WILLE, M., HARVEY, E., SHI, M., GONZALEZ-ACUÑA, D., HOLMES, E. C., HURT, A. C. Sustained RNA virome diversity in Antarctic penguins and their ticks. *ISME J.* 14, 1768-1782, 2020.

WINKLER, H. H., DAUGHERTY, R., HU, F. *Rickettsia prowazekii* Transports UMP and GMP, but Not CMP, as Building Blocks for RNA Synthesis. Am. Soc. Microbiol. 181, 3238-3241, 1999.

YUN, J. J., HEISLER, L. E., HWANG, I. I. L., WILKINS, O., LAU, S.K., HYRCZA, M.; JAYABALASINGHAM, B., JIN, J., MCLAURIN, J., TSAO, M., DER, S. D. Genomic DNA functions as a universal external standard in quantitative real-time PCR. Nucleic Acids Res. 34, e85, 2006.

ZANG, Y., WANG, T., XIE, W., WANG-FISCHER, Y. L., GETTY, L., HAN, J., CORKEY, B. E., GUO, W. Regulation of acetyl CoA carboxylase and carnitine palmitoyl transferase-1 in rat adipocytes. Obes. Res. 13, 1530-9, 2005.

ZHANG, J., JOHN, K. P., LU, G., CRUZ-MARTINEZ, L., WANG, C. Rickettsia in mosquitoes, Yangzhou, China. Emerg. Microbes Infect. 12;5(10):e108, 2016

Supplementary Table 1: Enzymes related to the metabolism of the uninfected and infected *A. sculptum* tick with *R. amblyommatis* and the endogenous genes.

CDS	Name	Pathway	ID (UniProtKB)	Primers sequence (5' – 3')	Estimated amplicon (bp)	Reference
g385	Phosphoenolpyruvate carboxykinase	Carbohydrate metabolism	A0A023FKA1	F- TTCCCAAGATCTTCCACGTC R- TTCTTGCAGCCAAAAGTCCT	248	Aguilar (2019)
g734	Fructose-bisphosphatase	Carbohydrate metabolism	A0A023FKC8	F- ACCCGGACATGAAGATCAAG R- AATATGCCGCCGTACTTCAG	193	Aguilar (2019)
g1125	Pyruvate kinase	Carbohydrate metabolism	A0A023FZY8	F- ACCTTGGACGTCAACCAGAC R- ATCGTGCCCTCATGGTACTC	170	Aguilar (2019)
g1215	Putative pfkb family carbohydrate kinase	Carbohydrate metabolism	A0A023FKH5	F- CTACACTGCTGGAGGTGCAA R- ACATTGACGCCAGCTTCTCT	150	Aguilar (2019)
g642	Isocitrate dehydrogenase	Energy metabolism	A0A023FMC1	F- CAACCCTATCGCATCCATCT R- GCTTCTTCCTCAGGTTGTCG	245	Aguilar (2019)
g1116	α-ketoglutarate dehydrogenase complex	Energy metabolism	A0A023FDJ6	F- CTGAGCTCCTCGTGGAAGAC R- ACTTTATGGTCCGCACTTCG	180	Aguilar (2019)
g1394	ATP synthase subunit alpha	Energy metabolism	A0A023FKR0	F- ACGCCCTCATCATTTACGAC R- GATCACTGGCAAAGCTGTCA	194	Aguilar (2019)
g1474	NADH dehydrogenase 1 alpha subcomplex	Energy metabolism	A0A023FQQ5	F- CAGGCTAACAGCCGAAAAAG R- TTGAAGCCCTTTTCATACCG	156	Aguilar (2019)
g3922	Pyruvate dehydrogenase E1 component	Energy metabolism	A0A023FZF0	F- GTGGCGACCTACCGGTACTA R- GCTTCCACCTCTGCTTTCAC	194	Aguilar (2019)

Supplementary Table 1 (continued)

g1825	Enoyl-CoA hydratase	Lipid metabolism	A0A4D5RMG2	F- CTCAACATCAAGCACGCAGT R- GTCTGGGGACGTCTTGTCAT	207	Aguilar (2019)
g3006	Carnitine O-palmitoyltransferase	Lipid metabolism	A0A023FNC9	F- TGCAGCTCGCCTACTACAGA R- TCCTGGTACCCTTTCTGGTG	217	Aguilar (2019)
g5381	Putative medium-chain acyl-coa dehydrogenase	Lipid metabolism	A0A023FLK4	F- TCGGAGGAGCAGAAGGAGTA R- ACCGTACTTTGCAGGAATGG	165	Aguilar (2019)
g465	Histidine ammonia-lyase	Amino acid metabolism	A0A023FNR7	F- ATCGAGTTCTTGCGTCCACT R- GGTCCATGTGTGGCTTAACA	175	Present Study
g486	Aspartate aminotransferase	Amino acid metabolism	A0A023FW96	F- AGATCGGCATGTTCTGCTT R- CACTTTGTGACTTGGTGCAT	163	Present Study
g673	Putative aromatic amino acid hydroxylase	Amino acid metabolism	A0A023FKJ2	F- GGAAGAAGTTGGTGCTTTGG R- TGCGACATGCTTTTGATCTC	180	Present Study
g3339	Putative ornithine aminotransferase	Amino acid metabolism	A0A023FLF8	F- TGCTCCCTATGAACACTGGA R- ATAGCTGGAAGGATCGGTTG	176	Present Study
g3515	Asparaginase	Amino acid metabolism	A0A1E1XG16	F- CGAAGTGACGGACGAGATAAT R- ACTCGAAACTCGTGCCCTAT	242	Present Study
g130	Putative glutamine phosphoribosylpyrophosphate amidotransferase	Nucleotide metabolism	A0A023GL61	F- TGCTACATGGGCATCAACAT R- TCGAGTTGGACGGGATAGTT	221	Present Study

Supplementary Table 1 (continued)

g971	Ribose-phosphate pyrophosphokinase	Nucleotide metabolism	A0A023FVX9	F- TGCACTGATCCACAAAGAGC R- CAAAGCAGGCATCGTTGAT	233	Present Study
g2871	Purine nucleoside phosphorylase	Nucleotide metabolism	A0A023GHV8	F- AGAAAATCGCCAACGAAGAA R- GATGAGAGAGAGCCCGAAAA	203	Present Study
g8171	Putative deoxycytidylate deaminase (Fragment)	Nucleotide metabolism	A0A023FEK6	F- GACTCGGCAGTGGAGACTAA R- GCTTGTCGTTGAGGAAGACT	181	Present Study
Endogenous						
G85	Putative actin-related protein 1	Cytoskeleton	A0A1E1X349	F- GACGCAGATCATGTTCGAGA R- AGGTAGTCGGTCAGGTCACG	210	Aguilar (2019)
G271	Glyceraldehyde-3-phosphate dehydrogenase (GAPDH)	Glycolysis	B5TMF7	F- CGTCTTCCAGGAGATGAAGC R- GGAGGCATTGCTCACAATCT	229	Aguilar (2019)
G463	α-tubulin	Microtubule component	A0A023FXC7	F- CAGGGTTTCCTCATCTTCCA R- GGAGTTGTAGGGTTCCACGA	165	Aguilar (2019)

Supplementary Table 2: Regression equation and R square (R2) value of the target genes' amplifications and endogenous genes.

Target Gene	Linear Regression Equation	R^2
g385	y = -3.5917x + 26.858	0.9972
g734	y = -3.8108x + 28.469	0.9936
g1125	y = -3.1448x + 32.887	0.9812
g1215	y = -3.4513x + 31.939	0.9975
g642	y = -2.5876x + 35.341	0.9744
g1116	y = -3.9166x + 32.62	0.9881
g1394	y = -3.4643x + 30.444	0.9847
g1474	y = -3.5274x + 29.435	0.993
g3922	y = -3.5823x + 30.881	0.9958
g1825	y = -3.5292x + 32.991	0.9758
g3006	y = -3.7383x + 26.431	0.9741
g5381	y = -3.5453x + 32.009	0.9772
g465	y = -3.228x + 29.858	0.9860
g486	y = -3.8003x + 32.535	0.9635
g673	y = -3.7742x + 30.706	0.9811
g3339	y = -3.703x + 31.544	0.9974
g3515	y = -3.0903x + 32.808	0.9673
g130	y = -3.5459x + 33.698	0.9862
g971	y = -3.6878x + 29.471	0.9714
g2871	y = -3.4605x + 29.612	0.9889
g8171	y = -3.5379x + 32.882	0.9686
Endogenous control		
g85	y = -3.3536x + 26.691	0.9952
g271	y = -3.7426x + 25.082	0.9981
g463	y = -3.6680x + 29.76	0.9910

*x = log concentration of cDNA (ng) e y = average of Ct

Source: own authorship.

Supplementary Table 3: Weight means before and after feeding ticks with the respective treatment and times, separated in replicates.

		Replicates		
Treatment		G1	G2	G3
Blood (12 hours)	Weight before mean (g) ± S.D (min - max)	0.00507 ± 0.000291 (0.005 - 0.0056)	0.00608 ± 0.000262 (0.0058 - 0.0066)	0.00612 ± 0.000297 (0.0057 - 0.0067)
	Weight after mean (g) ± S.D (min - max)	0.00637 ± 0.000365 (0.0059 - 0.0068)	0.00796 ± 0.000631 (0.0072 - 0.0092)	0.00785 ± 0.000799 (0.0067 - 0.0088)
	Weight gain mean (g) ± S.D (min - max)	0.00130[a] ± 0.0002494 (0.0009 - 0.0017)	0.00188[a] ± 0.0005138 (0.0013 - 0.0027)	0.00173[a] ± 0.00092 (0.0004 - 0.0028)
Blood (24 hours)	Weight before mean (g) ± S.D (min - max)	0.00644 ± 0.00024 (0.0061 - 0.0068)	0.00829 ± 0.00022 (0.0080 - 0.0086)	0.00679 ± 0.00036 (0.0064 - 0.0077)
	Weight after mean (g) ± S.D (min - max)	0.00802 ± 0.000127 (0.0068 - 0.0101)	0.0112 ± 0.000196 (0.009 - 0.0153)	0.01029 ± 0.0013 (0.0083 - 0.0124)
	Weight gain mean (g) ± S.D (min - max)	0.00158[a] ± 0.00117 (0.0005 - 0.002)	0.00291[a,b] ± 0.00186 (0.0006 - 0.0068)	0.0035[b] ± 0.0011 (0.0015 - 0.0052)

Supplementary Table 3 (continued)

Blood (48 hours)	Weight before mean (g) ± S.D (min - max)	0.00646 ± 0.00033 (0.0059 - 0.0069)	0.00732 ± 0.00028 (0.0070 - 0.0078)	0.00541 ± 0.00042 (0.0049 - 0.0062)
	Weight after mean (g) ± S.D (min - max)	0.00802 ± 0.00077 (0.0066 - 0.0093)	0.0847 ± 0.00064 (0.0076 - 0.0094)	0.00651 ± 0.00051 (0.0056 - 0.0068)
	Weight gain mean (g) ± S.D (min - max)	0.00156[a] ± 0.00079 (0.0005 - 0.0029)	0.00115[a] ± 0.00057 (0.0004 - 0.0020)	0.0011[a] ± 0.00033 (0.0007 - 0.0018)
Blood + Uninfected Vero cells (12 hours)	Weight before mean (g) ± S.D (min - max)	0.00715 ± 0.00026 (0.0068 - 0.0077)	0.00522 ± 0.00027 (0.0047 - 0.0056)	0.00611 ± 0.00036 (0.0056 - 0.0066)
	Weight after mean (g) ± S.D (min - max)	0.00849 ± 0.00037 (0.0079 - 0.0090)	0.00743 ± 0.00092 (0.0061 - 0.0091)	0.00851 ± 0.00073 (0.0075 - 0.0098)
	Weight gain mean (g) ± S.D (min – max)	0.00134[a] ± 0.000259 (0.0009 - 0.0017)	0.00221[b] ± 0.00096 (0.0010 - 0.0038)	0.00240[b] ± 0.00060 (0.0020 - 0.0032)

Supplementary Table 3 (continued)

	Weight before mean (g) ± S.D (min - max)	0.00807 ± 0.0003 (0.0077 - 0.0086)	0.0072 ± 0.00023 (0.0068 - 0.0075)	0.008 ± 0.00016 (0.0078 - 0.0082)
Blood + Uninfected Vero cells (24 hours)	Weight after mean (g) ± S.D (min - max)	0.01058 ± 0.001026 (0.0088 - 0.0116)	0.00907 ± 0.000178 (0.0070 - 0.0113)	0.01026 ± 0.0012 (0.0079 - 0.0116)
	Weight gain mean (g) ± S.D (min - max)	0.00251[a] ± 0.00115 (0.0007 - 0.042)	0.00187[a] ± 0.0017 (-0.0013 - 0.0041)	0.00220[a] ± 0.0013 (0.0001 - 0.0038)
	Weight before mean (g) ± S.D (min - max)	0.00815 ± 0.00023 (0.0077 - 0.0085)	0.00736 ± 0.00037 (0.0067 - 0.0078	0.00625 ± 0.00034 (0.0057 - 0.0067)
Blood + Uninfected Vero cells (48 hours)	Weight after mean (g) ± S.D (min - max)	0.01125 ± 0.00183 (0.0093 - 0.0151)	0.0104 ± 0.00135 (0.0091 - 0.0123)	0.00862 ± 0.00115 (0.0061 - 0.0103)
	Weight gain mean (g) ± S.D (min - max)	0.0031[a] ± 0.00181 (0.0008 - 0.0068)	0.00311[a] ± 0.00133 (0.00013 - 0.00017)	0.00237[a] ± 0.00106 (0.0002 - 0.0036)

Supplementary Table 3 (continued)

Blood + Infected Vero cells (12 hours)	Weight before mean (g) ± S.D (min - max)	0.00783 ± 0.00026 (0.0075 - 0.0083)	0.00707 ± 0.00021 (0.0067 - 0.0074)	0.00618 ± 0.00028 (0.0058 - 0.0066)
	Weight after mean (g) ± S.D (min - max)	0.00822 ± 0.00063 (0.0070 - 0.0094)	0.00754 ± 0.00026 (0.0072 - 0.0080)	0.00659 ± 0.00078 (0.0053 - 0.0080)
	Weight gain mean (g) ± S.D (min - max)	0.00039[a] ± 0.00059 (-0.0011 - 0.0011)	0.00047[a] ± 0.00025 (0.0003 - 0.0009)	0.00041[a] ± 0.00079 (-0.0007 - 0.0022)
Blood + Infected Vero cells (24 hours)	Weight before mean (g) ± S.D (min - max)	0.00618 ± 0.00026 (0.0060 - 0.0065)	0.00726 ± 0.00025 (0.0070 - 0.0076)	0.00818 ± 0.00025 (0.0077 - 0.0085)
	Weight after mean (g) ± S.D (min - max)	0.00649 ± 0.00079 (0.0043 - 0.0070)	0.00705 ± 0.00109 (0.0060 - 0.0092)	0.00783 ± 0.0008 (0.0064 - 0.0087)
	Weight gain mean (g) ± S.D (min - max)	0.00031[a] ± 0.00058 (0.0005 - 0.002)	-0.00021[a] ± 0.0010 (-0.0016 - 0.0021)	-0.00035[a] ± 0.00075 (-0.0013 - 0.0006)

Supplementary Table 3 (continued)

	Weight before mean (g) ± S.D (min - max)	0.00919 ± 0.000238 (0.0090 - 0.0097)	0.00920 ± 0.000316 (0.0087 - 0.0097)	0.01036 ± 0.00038 (0.0099 - 0.0109)
Blood + Infected Vero cells (48 hours)	Weight after mean (g) ± S.D (min - max)	0.00890 ± 0.00636 (0.0079 - 0.0098)	0.00935 ± 0.00659 (0.0085 - 0.0107)	0.01052 ± 0.00766 (0.0096 - 0.0119)
	Weight gain mean (g) ± S.D (min - max)	-0.00029[a] ± 0.000649 (-0.0013 - 0.0005)	0.00015[a] ± 0.00052 (-0.0005 - 0.0010)	0.00016[a] ± 0.00062 (-0.0009 - 0.002)

S.D = standard deviation
Min = minimum; Max = maximum
Different letters indicate statistical difference ($P < 0.05$) between replicates

Source: own authorship.

CAPÍTULO 2

METABOLIC PROFILE OF THE MIDGUT OF *Amblyomma sculptum* IN RESPONSE UNDER *Rickettsia amblyommatis* INFECTION

METABOLIC PROFILE OF THE MIDGUT OF *Amblyomma sculptum* IN RESPONSE UNDER *Rickettsia amblyommatis* INFECTION

Fernanda Sales de Araújo [1], Tiago Antônio de Oliveira Mendes [1], Caio Cezar Guedes Corrêa [2], Mariana Neves Catrinck[2], Nívea Moreira Vieira[3], João Pedro Vianna Braga [1], Lucas da Silva Lopes [1], Cláudio Mafra [1*]

[1] Department of Biochemistry and Molecular Biology, Federal University of Vicosa, Viçosa, MG, Brazil

[2] Department of Agronomy, Federal University of Espírito Santo, Alegre, ES, Brazil

[3]Department of Microbiology, Federal University of Vicosa, Viçosa, MG, Brazil

* mafra@ufv.br

ABSTRACT

Amblyomma sculptum is an important arthropod involved in human and animal health due to its vectorial potential of infectious agents. *Rickettsia* species can parasite various organs of that arthropod crossing the midgut barrier and escaping from the tick's immunology cells. Many Rickettsiae have limited metabolic capacity. Thus, they need to capture such intermediates synthesized by the hosts to use as a primary source of carbon and precursors of reactions that allow their survival, maintenance, and replication in the ticks. In the present study, female ticks were fed with different treatments: blood, blood + infected Vero cells with *Rickettsia amblyommatis,* and blood + Vero cells uninfected using artificial feeding during 48 hours. The metabolites were extracted and analyzed on a gas chromatograph coupled to a mass spectrometer (GC-MS). The chromatograms obtained were converted and analyzed using the package TargetSearch in R language to make baseline correction, conversion, and correction to retention index (RI). The metabolites were identified from the library Golm Metabolome Database (GMD). The 122 metabolites identified were normalized and inserted in Metaboanalyst software to perform principal component analysis (PCA), Volcano Plot, Metabolite Set Enrichment Analysis (MSEA), and heat maps. We reported changes in the metabolites identified in the tick midgut in response to *R. amblyommatis*. The results showed that pathogen infection affected several metabolites involved in the metabolism of amino acids, purine and pyrimidine, carbohydrates and TCA cycle, lipids and fatty acids, nicotinate, nicotinamide and pentose phosphate, among others. Our findings may assist in the study of new targets, to hinder the spread of these bacteria, limiting their permanence in these arthropods and reducing transmission for other animals.

1. INTRODUCTION

Ticks are obligatory hematophagous ectoparasitic arthropods, belonging to the phylum Arthropoda, subphylum Chelicerata, included in the class Arachnida and order Ixodida, exclusively distributed in three families: (a) Ixodidae, whose species are commonly known as hard ticks (BARROS-BATTESTI et al., 2006); (b) Argasidae, whose species are known as soft ticks (USPENSKY, 2005) and (c) Nuttalliellidae, only represented by *Nuttalliella namaqua*, found in Africa, whose morphological characteristics are shared by both soft and hard ticks (GUGLIELMONE et al., 2010).

The *Amblyomma sculptum* are inserted in the *Amblyomma cajennense* complex (consisting of *A. cajennense sensu stricto*, *Amblyomma tonelliae* n. sp., *Amblyomma interandinum* n. sp., *Amblyomma patinoi* n. sp. and *Amblyomma mixtum*) (NAVA et al., 2014), being distributed in the northern Argentina, contiguous regions of Bolivia and Paraguay, coastal and central-western region of Brazil (MARTINS et al., 2016). This species parasite several vertebrate hosts, such as cattle, horses, dogs, birds, capybaras, and humans (ESTRADA-PEÑA et al., 2004; FERREIRA et al., 2021).

Rickettsia is an obligate intracellular gram-negative bacterium, which parasites eukaryotic cells (WALKER, 1996). This genus currently represents 35 valid species that infect arthropods like mites, insects, and ticks (SÁNCHEZ-MONTES et al., 2021). The rickettsial species are divided into five groups: (a) basal group (BG) or ancestral group (AG), (b) the spotted fever group (SFG), (c) the typhus group (TG), (d) transitional group (TRG) and (e) intermedia group (IG) (SÁNCHEZ-MONTES et al., 2021).

Rickettsia amblyommatis, named *Rickettsia amblyomii previously*, belongs to the SFG, with prevalence in *Amblyomma americanum* and in other *Amblyomma* spp. (SANTIBÁÑEZ et al., 2018). This bacterium has been used in laboratory experiments due to low pathogenicity for male meadow voles (*Microtus pennsylvanicus*), being non-pathogenic to guinea pigs (*Cavia porcellus*) (RIVAS et al., 2015; KARPATHY et al., 2016). However, serological evidence suggests that humans have a robust immune response against this organism, with some patients showing only mild clinical illness (DELISLE et al., 2016).

The tick midgut is the first organ to receive the blood meal obtained from the host, whose Rickettsia (from the infected host) can multiply and proliferate, resisting the ticks' immune reactions, transposing that barrier, reaching the salivary gland and other organs (MARTINS et al., 2017). Moreover, the rickettsias' metabolic deficiency

explain why those organisms present reductive genome evolution and consequently depend on the animal host's metabolic products (DRISCOLL et al., 2017).

Studies have used several tools as genome construction of metabolic pathway (MIN el al., 2008), comparative genome analyses of rickettsia species (RENESTO et al., 2005), metabolomics of tick-*Borrelia* interaction during a tick blood meal (HOXMEIER et al., 2017), comparative transcriptomics (NARRA et al., 2020), characterization of tick-pathogen by proteomics (VILLAR et al., 2012) and metabolomics (QUIROZ-CASTAÑEDA et al., 2020), to assess the interaction of bacteria and ticks. Understanding which metabolites are necessary and essential for their survival can indicate potential targets for developing of therapeutic intervention strategies (MIN et al., 2008). However, metabolomics studies still are minimal to show the interaction between *R. amblyommatis* and *A. sculptum.*

In this study, we used a nontarget metabolomics approach to identify metabolites in the tick midgut unfed, fed with blood + Vero cells, and fed with blood + *R. amblyommatis* infected Vero cells, analyzed by gas chromatography coupled to mass spectrometry (GC-MS). A total of 122 metabolites were identified and classified functionally, of which the most abundant are involved in the amino acids metabolism, carbohydrate metabolism, fatty acids biosynthesis and degradation, purine and pyrimidine metabolism, and other pathways. We were also able to show the abundance of various metabolites through heat maps and statistical analysis to discuss their importance for *A. sculptum* and *R. amblyommatis* and how these bacteria may be able to modulate specific pathways for their use. Considering the metabolic changes observed in the midgut of infected ticks in relation to the uninfected control group, our findings may assist in the study of new targets to hinder the spread of these bacteria, limiting their permanence in these arthropods and reducing transmission for other animals.

2. MATERIAL AND METHODS

2.1 Ticks collection

Adult *A. sculptum* female ticks were obtained 20 days after molting process, kindness provided by Prof. Matias Szabó from the Ixodology Laboratory, at the Faculdade de Medicina Veterinária of the Federal University of Uberlândia (UFU), Minas Gerais State, Brazil.

Ticks were kept approximately 60 days inside incubator bio-oxygen demand (B.O.D) with a temperature of 20ºC, in a regime of 16 hours of light/ 8 hours of dark, stored in desiccators with a saturated solution of potassium chloride for maintenance of the relative humidity around 85%, until the artificial feeding (WIKEL, 1979; BECHARA et al., 1995) at the Laboratory of Parasitology and Molecular Epidemiology (LAPEM) of the Department of Biochemistry and Molecular Biology (DBB) of the Federal University of Vicosa (UFV), Minas Gerais State, Brazil.

2.2 Blood samples collection

The study was approved by the Ethics Commission on the Use of Animals (CEUA) from the Federal University of Viçosa (UFV) under protocol number 40/2018.

The blood used was aseptically collected by puncture using hematocrit capillary tubes in the New Zealand rabbits' orbital venous sinus. The blood samples were placed in vacuum tubes containing sodium citrate and kept under refrigeration at 4ºC, heated to 37ºC before artificial feeding. An aliquot was tested to verify the absence of the *Rickettsia* infection. Blood DNA was extracted using the QIAamp DNA Mini Kit (Qiagen, Hilden, Germany), according to the manufacturer's protocol. Each DNA sample extraction was processed by polymerase chain reaction (PCR) using the primers CS 78 (5'- GCA AGT ATC GGT GAG GAT GTA AT - 3') and CS 323 (5'- GCT TCC TTA AAA TTC AAT AAA TCA GGA T - 3') that amplify a 401 bp fragment of the citrate synthase (gltA) gene for *Rickettsia* spp. (LABRUNA et al., 2004).

The reaction was performed in a thermocycler (Biocycler model MJ25+, Biosystems®), whose final reaction volume was 25 µl presenting 10 mM of each primer, 200 ng genomic DNA extracted, 2 mM dNTPs, 1.25 mM MgCl2, and 2 U of Taq Polymerase. Cycling conditions were carried out with 1 initial cycle for 5 min at 95ºC, followed by 40 cycles for 30 s at 95ºC, 30 s at 48ºC, and 30 s at 72ºC, with the final extension of the primers for 7 min at 72ºC, as described by LABRUNA et al. (2004). Negative and positive controls were included. The amplification product was analyzed using 5 µl of the PCR product in 1% agarose gel prepared with 1X tris-acetate-EDTA (TAE), ethidium bromide (1 µg/ml) stained, and placed in an electrophoretic well for a run at 96 V for 40 min. After gel migration, PCR products were visualized under ultraviolet (UV) light. All samples were analyzed in triplicates.

2.3 *Rickettsia amblyommatis* cultivated in Vero cells

Rickettsia amblyommatis was grown up in Vero cells, described by Phelan & May (2015). The bacteria were kindness provided by Dr. Marcelo B. Labruna of the Parasitology Laboratory, Faculty of Veterinary Medicine and Animal Science (FMVZ-USP), São Paulo State, Brazil.

According to the manufacturer's protocol for tissues, DNA from the infected inoculum was extracted using the QIAamp DNA Mini Kit (Qiagen, Hilden, Germany). Subsequently, the extracted DNA was used as a template for the PCR. The amplification product was analyzed as previously described (LABRUNA et al., 2004). The PCR products with the confirmed presence of *R. amblyommatis* were purified using the PureLink™ PCR Purification Kit (Invitrogen, USA) following the protocol provided by the manufacturer. The PCR purified products were cloned into the pGEM®-T Easy system (Promega, USA), according to the manufacturer's recommendations. The transformation of the *Escherichia coli* DH5α with the recombinant plasmid was carried out by thermal shock as described by CARUSO (2007).

After confirmed bacterial cells' growth in the LB liquid medium, the plasmid DNA Miniprep extraction was performed by alkaline lysis, as described by BIRNBOIM & DOLY (1979). To calculate the number of copies in 1 µl of each solution containing plasmid DNA the formula was used as obtained by YUN et al. (2006). The serial dilutions from 1.4 x 10^{10} to 1.4 x 10^{4} copies of *R. amblyommatis* were performed in 0.2 ml microtubes for later use in the real-time PCR.

Approximately 1 ml of the bacterial stock solution maintained under -80ºC was transferred to a Vero cell flask (10^{6} cells/ml). The flasks were placed in a shake for 4 hours to ensure the entry of the bacteria inside the cells. After this protocol, Dulbecco's Modified Eagle Medium (DMEM) (Vitrocell, Brazil) was prepared according to the manufacturer's protocol. The culture medium was added to the infected cells and incubated in the incubator with 5% CO_2 at 28ºC (AMMERMAN et al., 2008).

After overnight infection, the flasks were visualized to check the infection (monolayer’s destruction), performing subsequent propagation to new flasks of uninfected cells. The culture medium was removed from the infected flasks, and a cell scraper was used to drop the monolayer. Posteriorly, uninfected flasks with Vero cells (approximately 90% confluence) had the culture medium removed, whose 1 ml of the

infected cell suspension was added and incubated under 5% CO_2 atmosphere at 28ºC, verifying the flask 24 hours after the procedure (AMMERMAN et al., 2009).

Aliquots of 1.0 ml of infected and uninfected Vero cells were analyzed and tested to previously verify the quantitation of *Rickettsia*, extracting the DNA with QIAamp DNA Mini Kit (Qiagen, Hilden, Germany), according to the manufacturer's recommendations and performing the real-time PCR using an internal fluorogenic TaqMan probe [5´ - 6FAM - CAT TGT GCC ATC CAG CCT ACG GT - BHQ 1 - 3 ´] (Hellixa Genomics, Brazil) and primers CS-5 (5´-GAG AGA AAA TTA TAT CCA AAT GTT GAT-3´) and CS-6 (5´- AGG GTC TTC GTG CAT TTC TT-3´) to obtain a 147 bp fragment of the gene encoding citrate synthase (gltA) for *Rickettsia* spp., as described by LABRUNA et al (2004). The reaction was performing with a concentration of 10 mM of primers, 0.255 µM of the probe, 2 µl of serial dilutions, 5 µl of GoTaq® Probe qPCR Master Mix 2X (Promega, USA), and 0.17 µl of passive reference dye (CXR). DNA samples were used in duplicate. The machine program was carried out with an initial 2 min at 95ºC followed by 50 cycles of 15 s at 95ºC, 30 s at 50ºC, and 30 s at 60ºC with the aid of the StepOne™ Real-Time PCR System (Applied Biosystems, USA).

DNA samples showing cycle threshold (CT) values above 35 were considered harmful for the presence of *Rickettsia* spp. The serial dilution of *R. amblyommatis* was plotted on a graph to obtain the absolute standard curve used in the quantification procedures. According to these values, in 1.0 ml of infected medium, there were 7.186 x 10^6 copies of *R. amblyommatis*.

2.4 Artificial feeding of adult female *A. sculptum* ticks and midgut dissection

Ticks were individually weighed, been separated by weight range into experimental groups with three replicates with 10 ticks each, such as C1 with female ticks unfed, S1 with female ticks fed only with citrated blood; SV with ticks fed with citrated blood + Vero cells; and SI with female ticks fed with citrated blood + Vero cells infected with *R. amblyommatis*. These ticks were fed for 48 hours been maintained separated by desiccators as previously described (BECHARA et al., 1995).

Aliquots of 1.0 ml of flasks containing infected and uninfected Vero cells were transferred to 2 ml tubes for centrifugation at 5,000 x g for 10 min. The tubes were sealed with cling film to prevent any aerosol contamination. The pellets obtained from the centrifuged aliquots were reserved and resuspended with rabbit blood heated to 37ºC in a water bath. Blood samples in contact with the infected cells' pellet were

transferred to the collection tubes to obtain a final volume of 3 ml of blood added with infected Vero cells, with approximately 2.3953 x 10^4 copies/100 µl of *R. amblyommatis*.

For treatment with uninfected Vero cells, 1 ml (equivalent to 10^6 cells) was removed from the cell culture flask and centrifuged at 5.000 x g for 10 min. The pellet formed was resuspended with 1 ml of rabbit blood at 37ºC and transferred to the collection tubes, whose final volume was 3 ml.

The artificial feeding method with 1,000 µl plastic tips was used to feed and infect ticks (VALIM et al., 2017), filled with 100 µl according to the treatment (S, SV, and SI). Tips were replaced every 12 hours of feeding to prevent obstruction and blood coagulation.

After the feeding period (48 hours), ticks were removed from the artificial feeding, weighted, washed with distilled water, dried with paper towels, placed individually in 1.5 mL tubes containing 300 µl of ice-cold 100% HPLC - grade methanol ≥99.9% (Sigma-Aldrich, USA) and stored at -80ºC to stop the metabolism (quenched process).

The dissection of the female ticks was performed according to ANATRIELLO et al. (2010). Briefly, the ticks were dissected with the aid of personal protective equipment and a stereoscope microscope with a direct light source (Motic SMZ-140) at LAPEM / DBB / UFV. After drying, each tick was individually fixed on a sterile paraffin base for total immobilization. For dissection, sterile disposable scalpels (number 11) and acupuncture needles attached to surgical forceps were used to remove internal organs. After dissection, a total of 10 midguts (according to each treatment) were placed in 1.5 ml microtubes containing 400 µL of ice-cold methanol, weighted and stored at -80ºC until the extraction of metabolites.

2.5 Processing and extraction of the midgut for analysis of metabolites

For extraction of the metabolites, the protocol described by LISEC et al. (2006) was followed with modifications. The pool of ten midguts (according to each treatment) was transferred for a 2.0 ml microtube, and the volume was completed to 1.4 µl with ice-cold 100% HPLC-grade methanol (Sigma-Aldrich, USA) and the mixture vortexed for 10 s. After this procedure, 60 µl of ribitol (0.2 mg/ml) was added, and the sample vortexed for 10 s. All samples were homogenized in the shake (Orbital Shaker, USA) for 10 min at 200 rpm and 4ºC (box with ice).

The final mixture was centrifuged at 11,000 x g for 10 min (4ºC). The supernatant was gently removed and transferred into a new microtube until confirmation of infection or not infection.

The formed pellet was used to confirm the infected/ uninfected treatment, whose DNA extraction was performed using QIAamp DNA Mini Kit (Qiagen, Hilden, Germany), according to the manufacturer's recommendations and performing the real-time PCR using an internal fluorogenic TaqMan probe [5´ - 6FAM - CAT TGT GCC ATC CAG CCT ACG GT - BHQ 1 - 3 ´] (Hellixa Genomics, Brazil) and primers CS-5 (5´-GAG AGA AAA TTA TAT CCA AAT GTT GAT-3´) and CS-6 (5´- AGG GTC TTC GTG CAT TTC TT-3´) to obtain a 147 bp fragment of the gene encoding citrate synthase (gltA) for *Rickettsia* spp., as described by LABRUNA et al. (2004) and written in the section 2.3 *Rickettsia amblyommatis* cultivated in Vero cells, in this manuscript. DNA samples with cycle threshold (CT) values above 35 were considered harmful for the presence of *Rickettsia* spp.

After confirming the infection or not infection in each midgut pool, the samples were identified as C1, C2, and C3 for ticks unfed; S1, S2, and S3 for ticks fed only with citrated blood; SV1, SV2, and SV3 for ticks fed with citrated blood + Vero cells; and SI1, SI2, and SI3 for ticks fed with citrated blood + Vero cells infected with *R. amblyommatis*.

To finish metabolites pool extraction, was added 375 µl of chloroform (-20ºC) and 750 µl of ultrapure H_2O (4°C) into each microtube vortexed for 10 s. After homogenization, the tubes were centrifuged at 2,200 x g for 15 min. Approximately 450 µl of the upper phase was transferred into a 1.5 ml microtube; and the metabolites samples were dried under overnight lyophilization in the lyophilizer (VirTis Wizard 2.0 Lyophilizer Controller, USA) following the parameters: 726 Torr, + 8.9º until + 41.2º, Avg = + 25.1º, Cond = - 42.7º under vac pump. The samples were stored at -80ºC until performing the analysis.

2.6 Gas Chromatography coupled to Mass Spectrometry Analysis

The sample derivatization and the following chromatographic analyses were performed according to the protocol described by LISEC et al. (2006) with minor modification. A mixture of alkanes (0.029% (v / v): n-dodecane, n-pentadecane, n-nonadecane, n-docosane, n-octacosane, n-dotriacontane, and n-hexatriacontane

dissolved in pyridine) was used as retention time standards instead of fatty acid methyl esters (ROESSNER-TUNALI et al., 2003).

Before the derivatization process, the samples stored at -80ºC were placed in a vacuum concentrator at 30ºC for 30 min. In the derivatization stage, 40 µl of the methoxyamine hydrochloride solution (20 mg/ml in pyridine) was added to each sample and heated up at 37ºC for 2 h and 900 rpm. Subsequently, 70 µl of N-methyl-N-(trimethylsilyl)trifluoroacetamide (MSTFA) + 8 µl of the retention time standard were added to the samples and these were incubated at 37ºC for 30 min in a shaker at 900 rpm. An aliquot of 100 µl was transferred to glass vials with a 250 µl insert and then, analyzed by gas chromatography coupled to mass spectrometry (GC-MS).The samples were analyzed on a gas chromatograph coupled to a mass spectrometer model GCMS-QP2010 SE with an automatic sampler model AOC-20s (Shimadzu, Kyoto - Japan). The chromatographic column DB-35MS (30 m x 0.25 mm x 0.25 µm, J & W Scientific, Folsom, CA, USA) was used. 1 µl of the sample was injected in splitless mode using helium as the carrier gas with 2 mL/min of constant flow. The temperature program was set as follows: isothermal at 80ºC for 2 min, followed by a 15ºC/min ramp to 330ºC, and remaining for 6 min at 330ºC. The electron ionization (EI) mode was used in 70 eV. The recorded mass range varied from m/z 70 to m/z 600 with an acquisition rate of 2000 scans/s. The temperature of the injector and the transfer line was set at 230ºC and 250ºC, respectively.

2.7 Data processing

Initially, all generated GC-MS chromatograms were converted to Computable Document Format (NetCDF). The package TargetSearch (CUADROS-INOSTROZA et al., 2009) present in R language (R Core Team, 2020) was used to make baseline correction, retention time (RT) conversion to retention index (RI), correction of RI, and identification of metabolites.

For RI correction, four alkanes found were used as compounds of internal standard, and the RT of standard markers were converted to RI using linear interpolation (VAN DEN DOOL & KRATZ, 1963). These standards were searched in the sample definition file, defining the RI marker, time window, and m/z values. Apex Data files were created to perform the library search, containing a peak list, retention times, and converted RIs (CUADROS-INOSTROZA et al., 2009). The metabolites were

identified from the library Golm Metabolome Database (GMD) (http://gmd.mpimp-golm.mpg.de/download/).

2.8 Statistical analysis and functional annotation

Only metabolites present in at least two replicates in three were accepted for differential analysis with the others treatments to guarantee processing quality. The peaks intensity data of the identified metabolites were initially corrected according to the initial weight of the pool of ten midguts (Supplementary Table 1).

The corrected data were analyzed, filtered by the interquantile range (IQR) with three normalization parameters. The first parameter utilized was sample normalization by the median, following by log transformation, and data scaling via Pareto scaling. Posteriorly, the processed data were analyzed in pairs using Volcano plot with p-value < 0.05 and Fold Change (FC) threshold = 1.5, with equal group variance. Aiming to assess possible patterns in groups and treatments, a principal component analysis (PCA) was conducted. Heatmaps of normalized intensities and values of Log_2 fold change were made using the Ward algorithm, with Euclidean distance and the t-test. Finishing, a Metabolite Set Enrichment Analysis (MSEA) was performed, with discrete (classification) group label, whose only metabolites sets containing at least three entries were accepted. These analyses were conducted using the software MetaboAnalyst (CHONG et al., 2018).

3. RESULTS

3.1 *Rickettsia*'s confirmation from the real-time PCR

In the first step, the pellets obtained from the metabolites pool extraction were used to validate the treatments. All treatments without infection and theirs replicates (C1, C2, and C3; S1, S2, and S3; SV1, SV2, and SV3) showed cycle threshold (CT) above 35 or undetermined in the real-time PCR, representing the absence of bacteria in the groups. Samples infected (SI1, SI2, and SI3) showed CT value between 29 and 30, confirming the infection with *Rickettsia* in the groups.

3.2 Nontarget metabolic analysis and identification from the library

A total of 122 individuals metabolites were identified in the treatments, whose name from the KEGG and the corrected peaks intensity (according to samples weight) was annotated (Supplementary Table 1).

Most of the metabolites were classified as amino acids metabolism (36), carbohydrate metabolism (six), fatty acids biosynthesis and degradation (eleven), glutathione metabolism (three), glycerolipid metabolism (two), glycerophospholipid metabolism (two), lipids (seven), nicotinate and nicotinamide metabolism (three), pentose phosphate pathway (three), purine metabolism (six), pyrimidine metabolism (nine), TCA cycle (three), vitamin digestion and absorption (three), dipeptides (two) and less representative classes (excreta, nitrogen elimination, ketone body biosynthesis, oxidative phosphorylation, and phenylpropanoid biosynthesis) (Supplementary Table 1).

The PCA plot analysis was performed to compare and evaluate the treatment tendencies. As a result, the fed uninfected treatments (S and SV) presented a close correlation, even when one replicate of S (S1) was distant from their respective treatment. On the order hand, the fed-infected treatment (SI) showed less proximity to the fed uninfected treatment (Figure 1A). In order to proceed with the analyzes, another PCA plot was performed comparing C, S, SV, and SI, whose treatment distribution was homogeneous and closer between S and SV, with greater variation in the C replicates, involving even the infected SI treatment (Figure 1B). It was observed that the profile of metabolites found in the midgut pool of fasting ticks (unfed - C) showed minor differences concerning the metabolites found in treatments infected with rickettsia (SI). Comparing the SI/C treatments by Volcano Plot (Figure 1C), we observed that ten metabolites were up-regulated and six down-regulated.

Figure 1: Principle component analysis (PCA) and Volcano Plot data showing difference between treatments. (A) Red color circle represents S treatment, green color circle represents SI treatment and blue color circle represents SV. B - Red color circle represents C treatment, green color circle represents S treatment, blue color circle represents SI and cyan color circle represents SV treatment. (C) – Volcano plot with up-regulated metabolites (red), down-regulated metabolites (blue), and insignificant (gray).

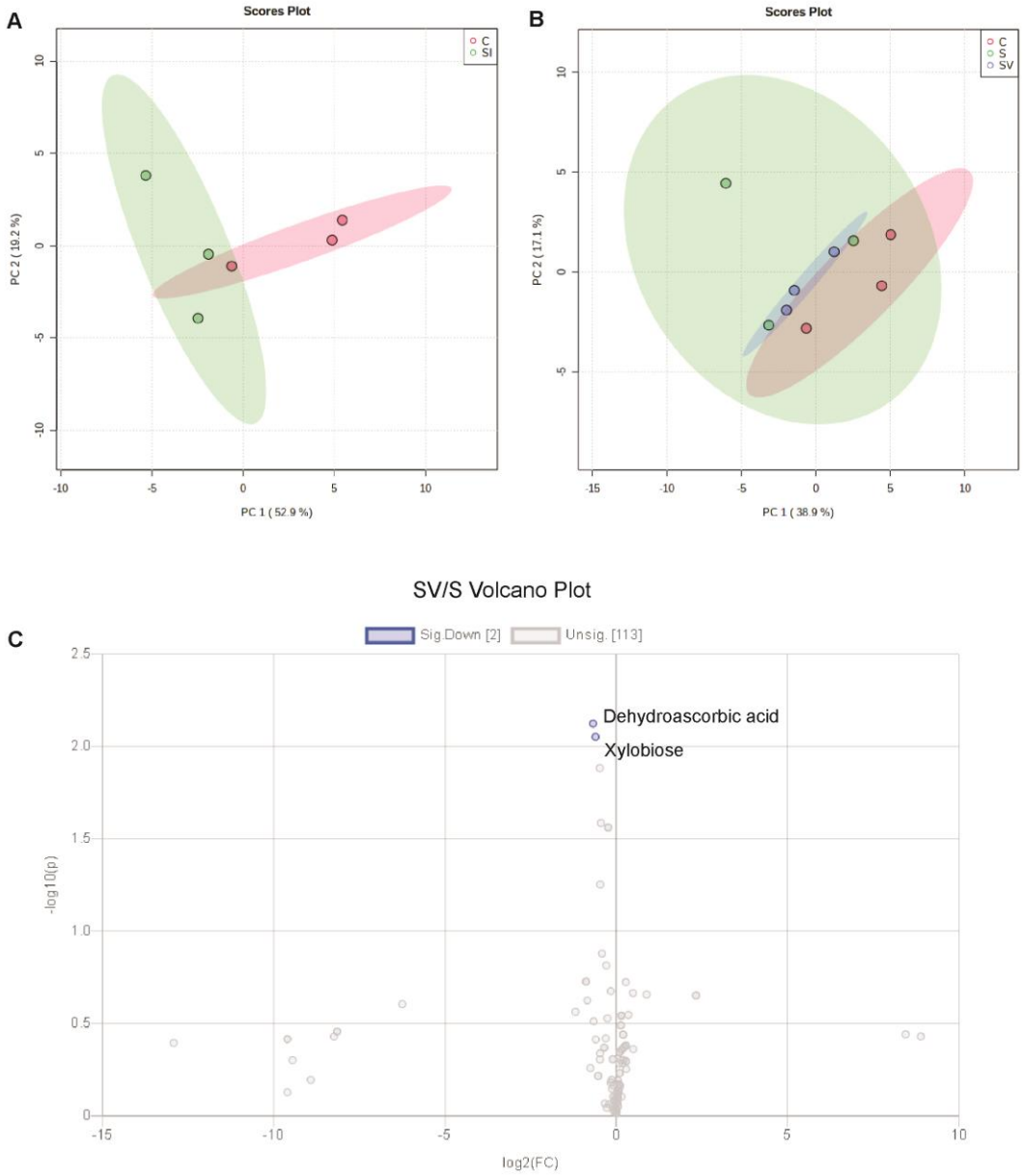

Source: own authorship.

In the PCA plot, SI and C clustered differently, showing a separation tendency, in which one replicate sample C was closer to the SI (Figure 2A). Comparing C, S, and SV treatments, the analysis with PCA showed proximity between the samples. However, a replica of S has shown a less homogeneous distribution concerning the others. SV and C samples were close to the S (Figure 2B).

Figure 2: Principle component analysis (PCA) and Volcano Plot data showing the difference between treatments. (A) Red color circle represents C treatment, green color circle represents SI treatment. B - red color circle represents C treatment, green color circle represents S treatment, blue color circle represents SV. (C) – Volcano plot with up-regulated metabolites (red), down-regulated metabolites (blue), and insignificant (gray).

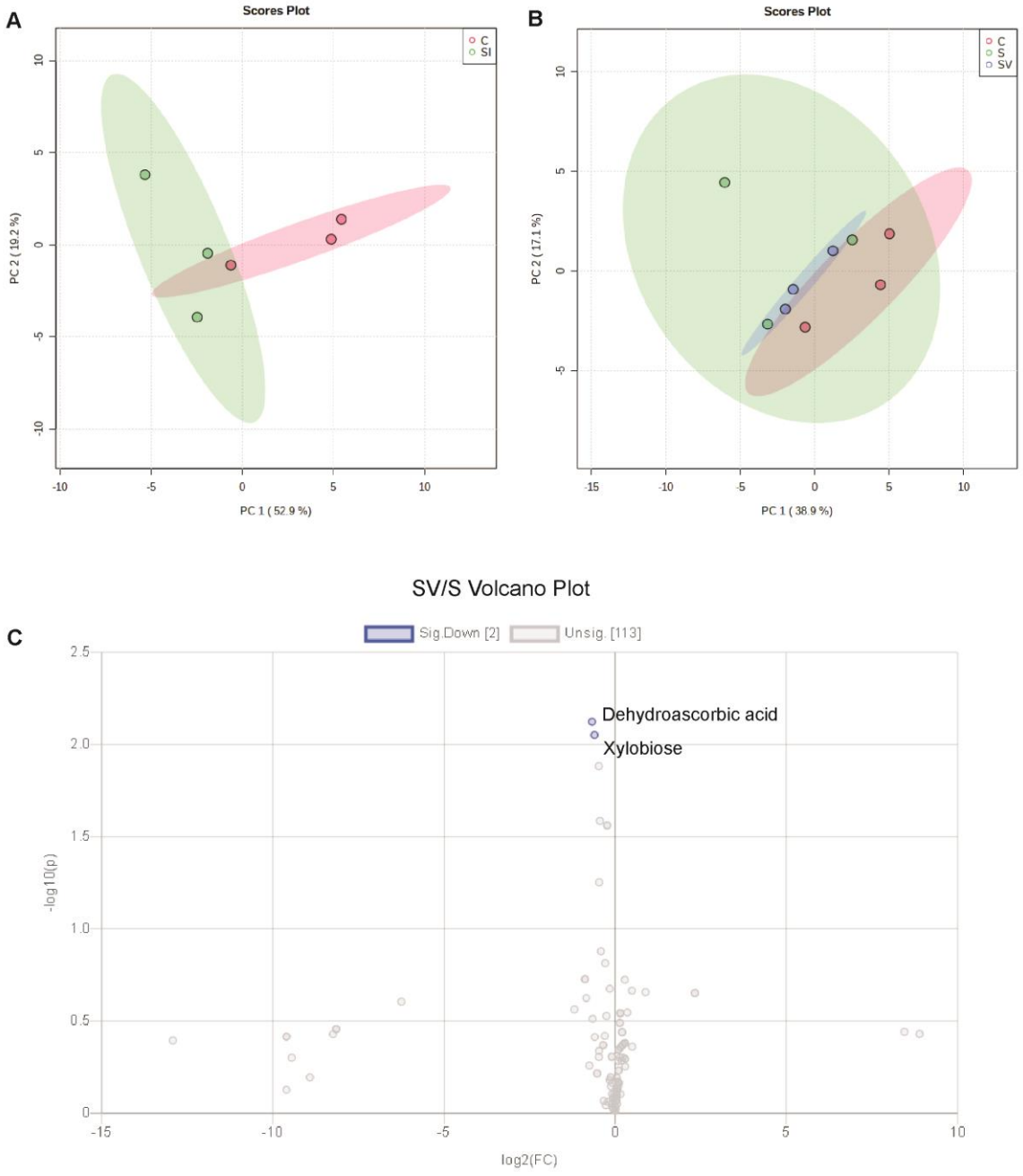

Source: own authorship.

In this study, after PCA plot comparations and treatments analyses in pairs with all possibles variations, we chose to work and discuss the data acquired from the SI and SV treatments to describe the metabolic profile of tick's midgut infected by *R.*

amblyommatis and uninfected. This choice was due to the results found comparing treatments S and SV, which showed only two metabolites with a significant difference using Volcano Plot (Fold Change threshold = 1.5; p-value threshold = 0.05) (Figure 2C).

3.3 PCA, Volcano plot, MSEA and heatmap comparative analyses between SV and SI treatments

The PCA plot of SI/SV samples showed a considerable distance and separation between treatments fed with blood + Vero cells infected and uninfected. As shown in Figure 3A, two distinct groups were formed with PC1 covering 50.6% of the variables and PC2 covering 21.8%. In the Volcano plot analyses, 21 metabolites (17.21% of total identified) showed statistical significance (p-value < 0.05) and magnitude of change (Fold change threshold = 1.5) comparing SI against SV (Figure 3B). Of these 21 metabolites, 17 compounds were up-regulated and four down-regulated.

Figure 3: Principle Component Analysis (PCA) and Volcano Plot data showing the difference between SI and SV treatment. A – red color circle represents SI treatment and green color circle represents SV treatment. B – Volcano plot with up-regulated metabolites (red), down-regulated metabolites (blue), and insignificant (gray).

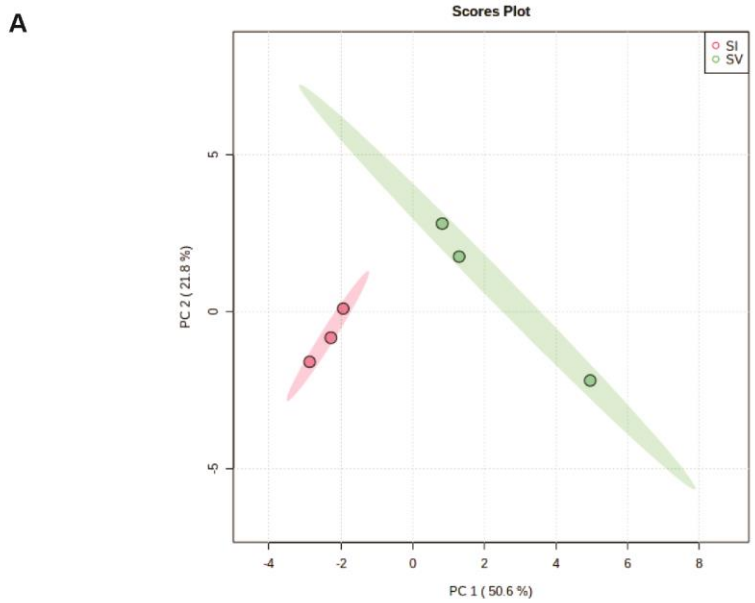

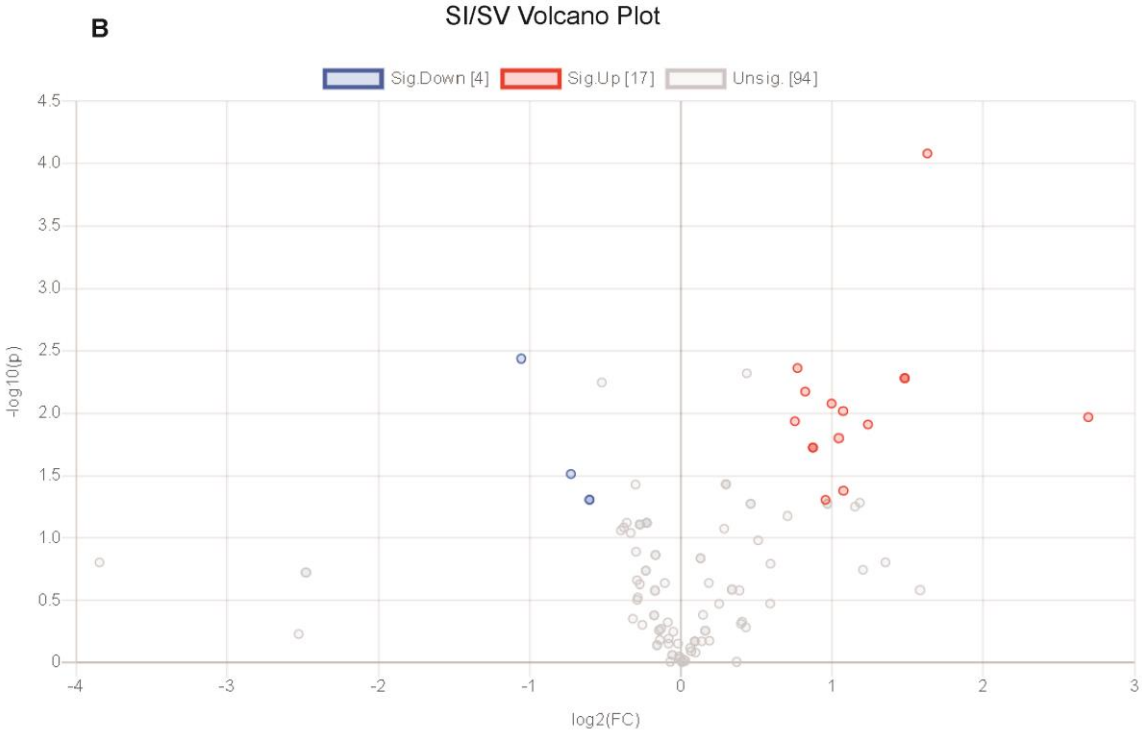

Source: own authorship.

To understand and identify the metabolic pathways involved in the relation SI/SV, a Metabolite set enrichment analysis (MSEA) was performed. As a result, we observed that the top six pathways were: pantothenate and CoA biosynthesis, propanoate, beta-alanine, butanoate, pyrimidine metabolism and, TCA cycle (Figure 4).

Figure 4: Metabolite Set Enrichment (MSEA) analysis of SI compared to SV. A total of six pathways were indicated in the overview, using metabolites sets containing at least two entries.

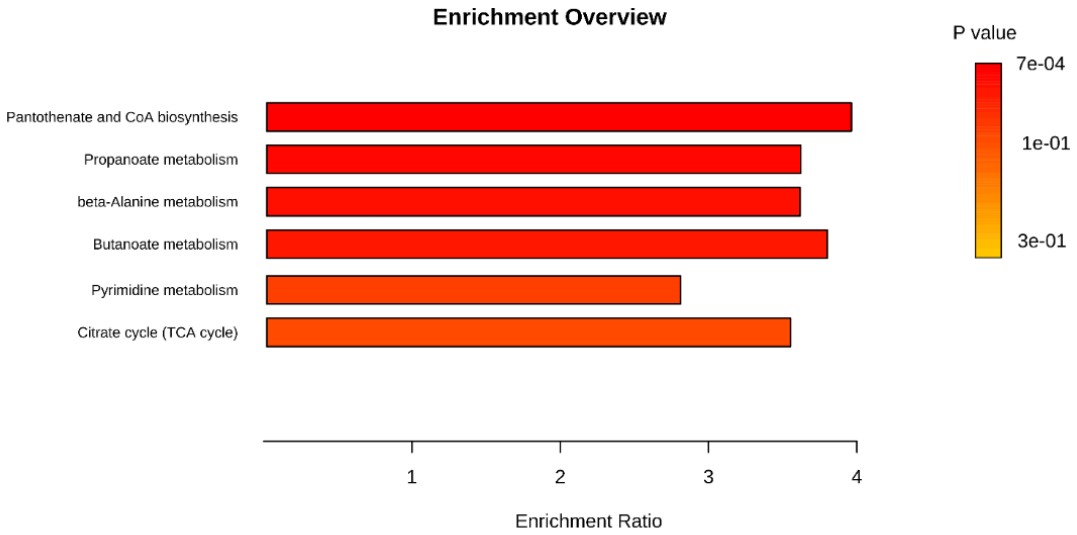

Source: own authorship.

Heat map analysis was performed, grouping the metabolites belonging to correlated pathways. According to our results, in the metabolism of amino acids, 24 metabolites were increased, and nine metabolites were decreased in at least two replicates in SI treatment. We highlight Homovanillate, 4-Hydroxyphenylpyruvate, Melatonin, Phenylglycine, Creatinine, N-Acetylmethionine, Spermidine, N-Acetylputrescine, Serotonin, 1-Pyrroline-2-carboxylate, Spermine, N-Acetyl-L-glutamate, and N6-Acetyl-L-lysine, among the increased amino acids. In the SV treatment, 31 metabolites were decreased in at least two replicates, and three metabolites were increased. A total of six metabolites were down-regulated in both treatments, while one metabolite was up-regulated (Figure 5). The identified amino acids participate in the metabolism of arginine, proline, tryptophan, cysteine, glycine, serine, threonine, histidine, lysine, phenylalanine, valine, leucine, and isoleucine.

Figure 5: Heat map displaying 34 metabolites involved in the amino acid metabolism found in the SI replicates (SI1, SI2, SI3) and SV (SV1, SV2, SV3) with different abundances. At the top, the dendrogram clustered treatments based on the similarity of the metabolites, whose red color represents SI treatment and green color represents SV treatment. Changes in abundance are shown by red color (increased) and blue (decreased).

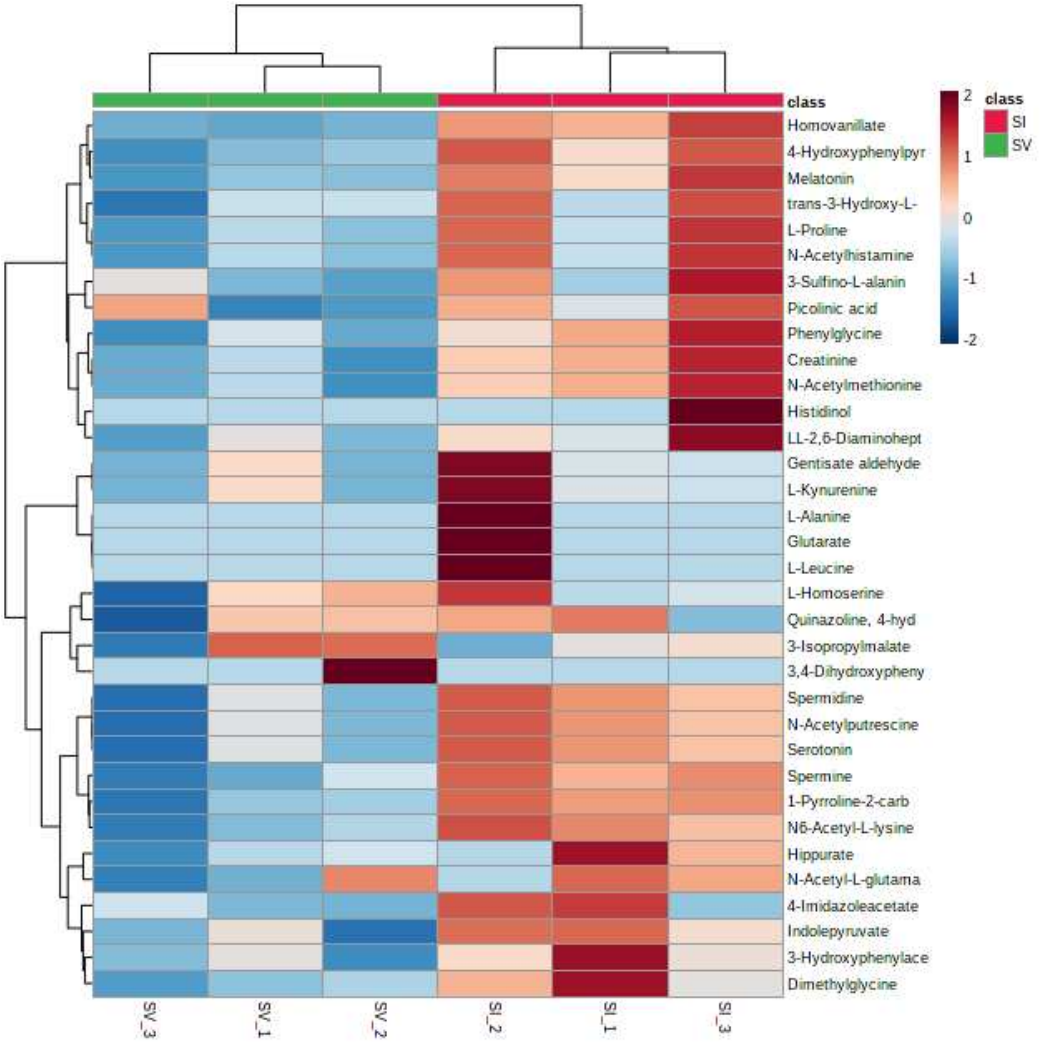

Source: own authorship

In the univariate analysis, the fold change was performed using threshold = 1.5, in which log2 FC > 0.5849625 was considered up-accumulated metabolites and log2 FC < - 0.5849625 down-accumulated, considering the fold result between SI and SV treatments in the individuals pathways. As a result, eleven metabolites were up accumulated in the amino acid metabolism, and one down accumulated (Figure 6).

Figure 6: Changes in the median of metabolites abundance in the SI (red) and SV (green) treatments to the amino acid metabolism. The distribution with inter-quartile and the replicates are shown.

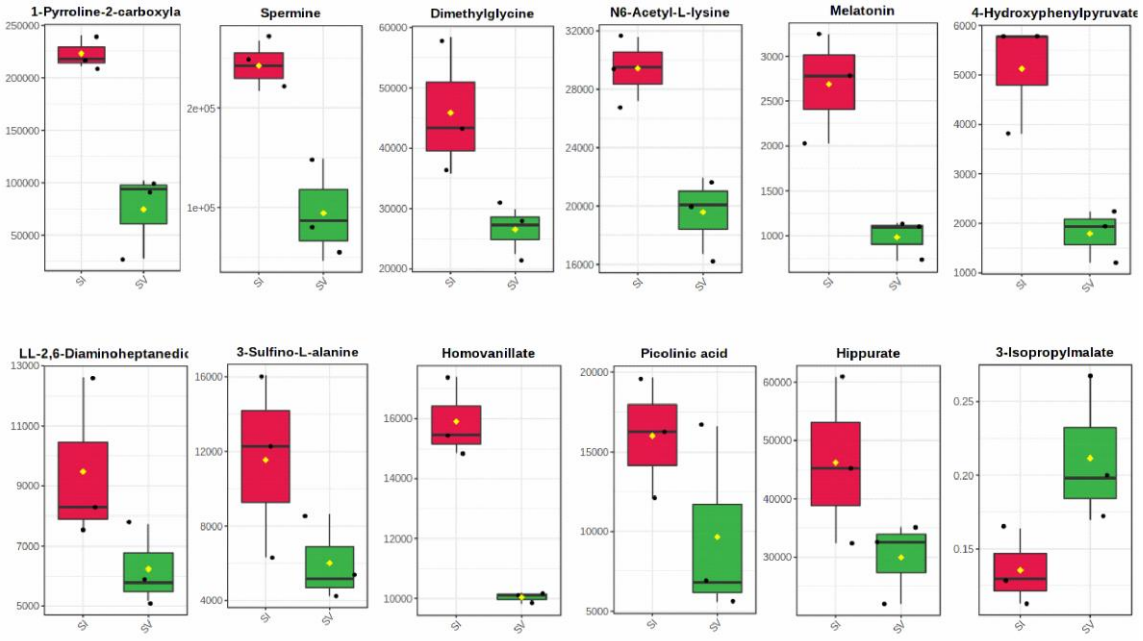

Source: own authorship.

In Figure 7A, the heat map showed that all metabolites were down in at least two replicates to the SV treatment in the metabolism of purine and pyrimidine. In contrast, the SI treatment showed 16 metabolites with up abundance and one decreased. We can notice a homogeneous separation between down-regulated metabolites majority in SV and up in SI in this group,. Another pathway with a similar result was carbohydrate and TCA cycle metabolism, which showed six metabolites decreased, and two increased in SV treatment. In the SI treatment, all metabolites identified were increased in at least two replicates (Figure 7B).

Figure 7: Heat map displaying metabolites involved in the purine and pyrimidine metabolism (A), carbohydrate and TCA cycle (B) found in the SI replicates (SI1, SI2, SI3) and SV (SV1, SV2, SV3) with different abundances. At the top, the dendrogram clustered treatments based on the similarity of the metabolites, whose red color represents SI treatment and green color represents SV treatment. Changes in abundance are shown by red color (increased) and blue (decreased).

(A)

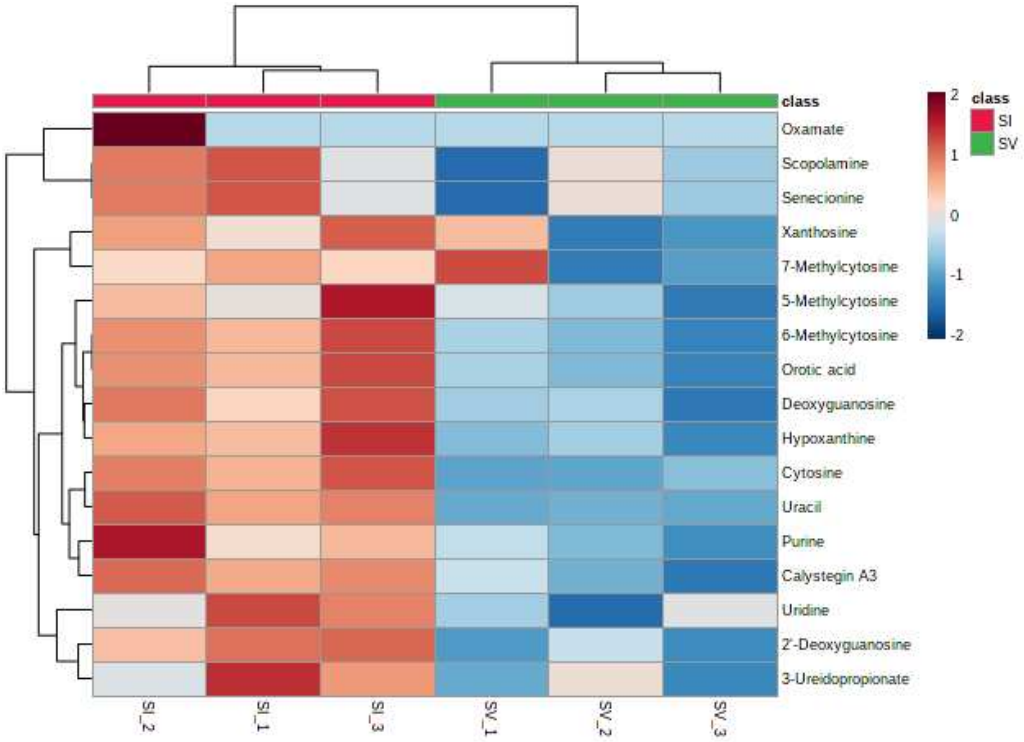

(B)

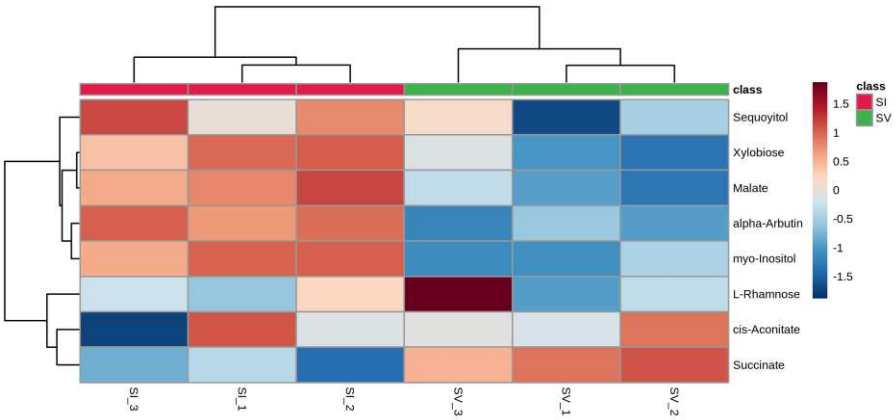

Source: own authorship.

In the fold change analysis, ten metabolites were considered up-accumulated in the SI/SV ratio to the purine and pyrimidine metabolism (Figure 8A). In the carbohydrate and TCA cycle, only four metabolites were significantly up and one down accumulated (Figure 8B).

Figure 8: Changes in the median of metabolites abundance in the SI (red) and SV (green) treatments to the purine and pyrimidine metabolism (A), carbohydrate and TCA cycle (B). The distribution with inter-quartile and the replicates are shown.

(A)

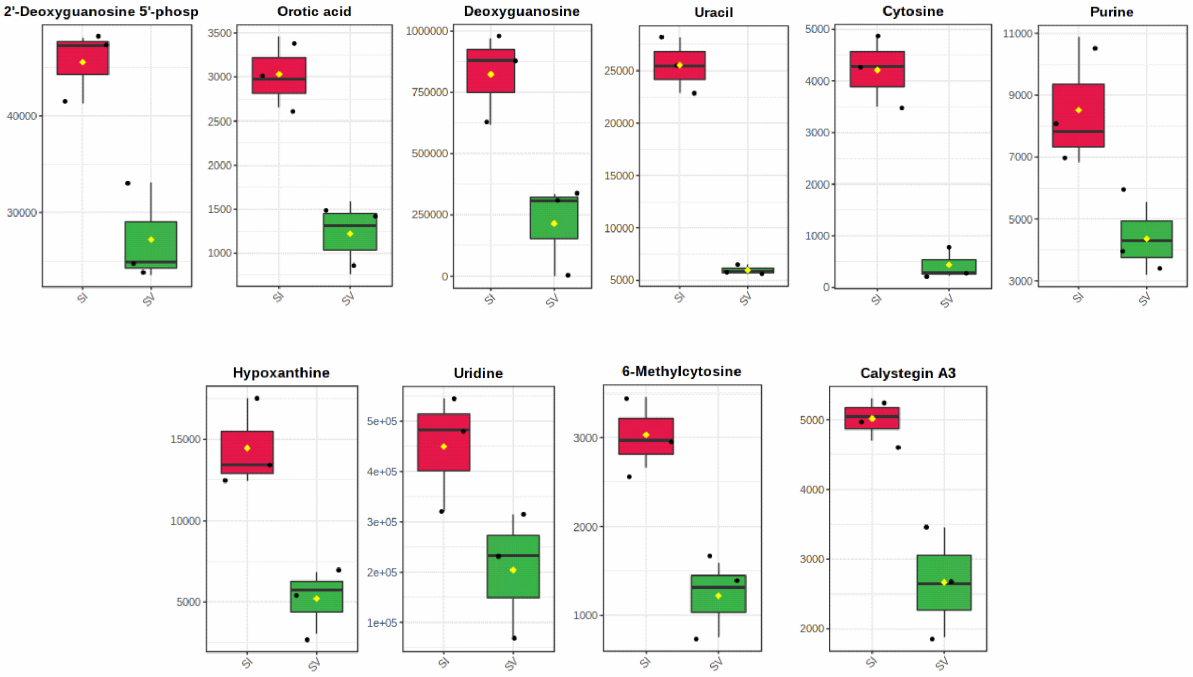

(B)

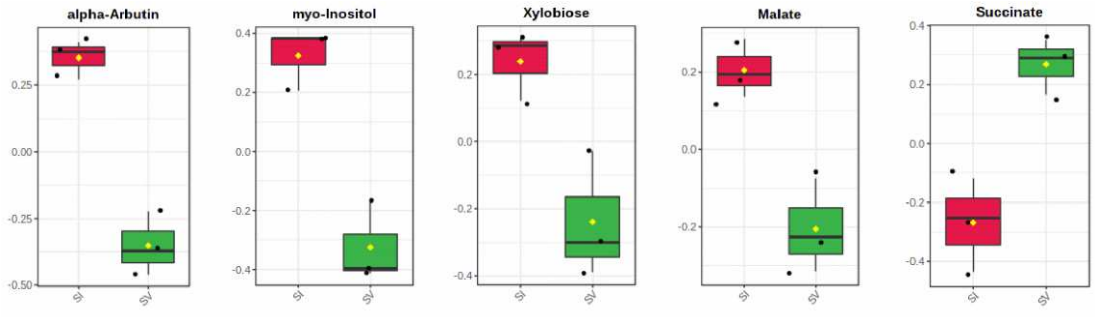

Source: own authorship.

Lipids metabolism heat map showed all metabolites with low abundance in the SV treatment. On the other hand, the SI treatment heat map showed four metabolites with up abundance in at least two replicates, and one metabolite reduced (Figure 9A). However, the resulting fatty acids were not homogeneous. A total of four metabolites were up and six metabolites down in the SV. The SI treatment showed half of the compounds with more significant intensity (Figure 9B).

Figure 9: Heat map displaying metabolites involved in the lipids metabolism (A) and fatty acids (B) found in the SI replicates (SI1, SI2, SI3) and SV (SV1, SV2, SV3) with different abundances. At the top, the dendrogram clustered treatments based on the similarity of the metabolites, whose red color represents SI treatment and green color represents SV treatment. Changes in abundance are shown by red color (increased) and blue (decreased).

(A)

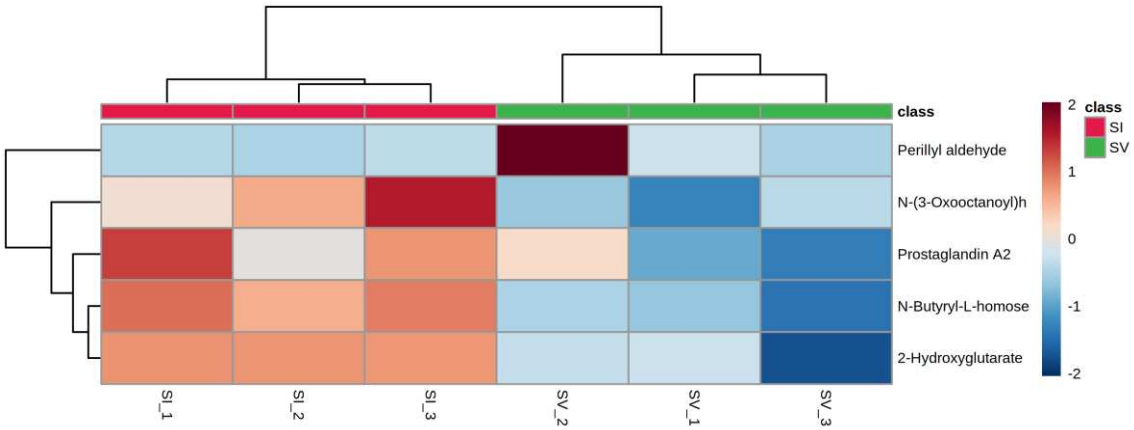

(B)

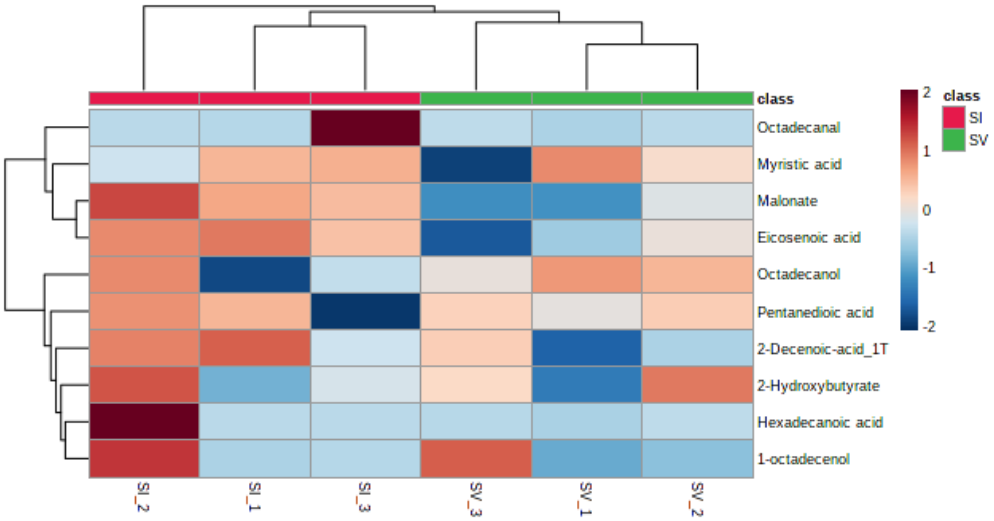

Source: own authorship.

In the fold change analysis, only two metabolites were considered up-accumulated in the SI/SV ratio to the lipids metabolism (Figure 10A). With similar results, fatty acids metabolism showed only two metabolites significantly abundant (Figure 10B).

Figure 10: Changes in the median of metabolites abundance in the SI (red) and SV (green) treatments to the lipids (A) and fatty acids metabolism (B). The distribution with inter-quartile and the replicates are shown.

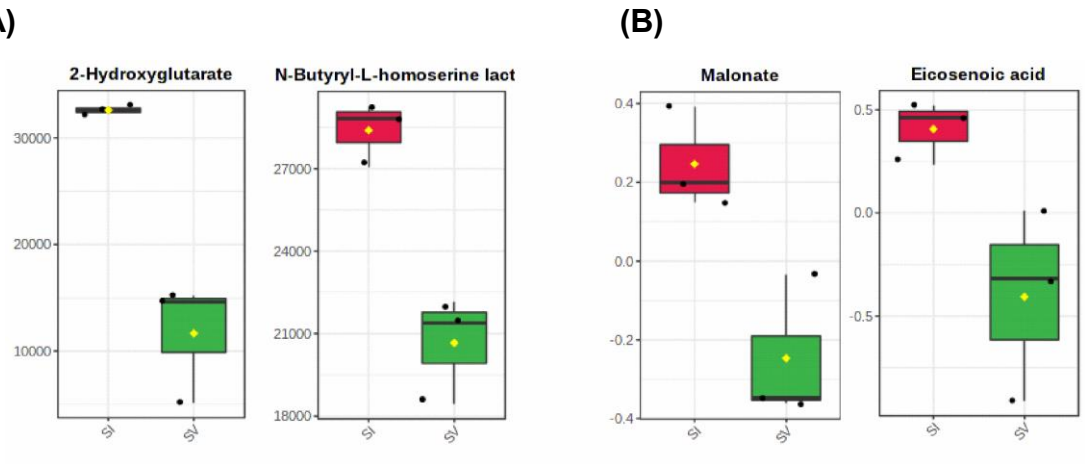

Source: own authorship.

The nicotinate, nicotinamide, pentose phosphate, and glutathione metabolic pathway were grouped in the same heat map (Figure 11). As a result, six metabolites were found with bigger abundance and two metabolites with less abundance in the SI treatment. In the SV treatment, all compounds showed a decrease in at least two replicates.

Figure 11: Heat map displaying metabolites involved in the Nicotinate, Nicotinamide, pentose phosphate, and glutathione metabolism found in the SI replicates (SI1, SI2, SI3) and SV (SV1, SV2, SV3) with different abundances. At the top, the dendrogram clustered treatments based on the similarity of the metabolites, whose red color represents SI treatment and green color represents SV treatment. Changes in abundance are shown by red color (increased) and blue (decreased).

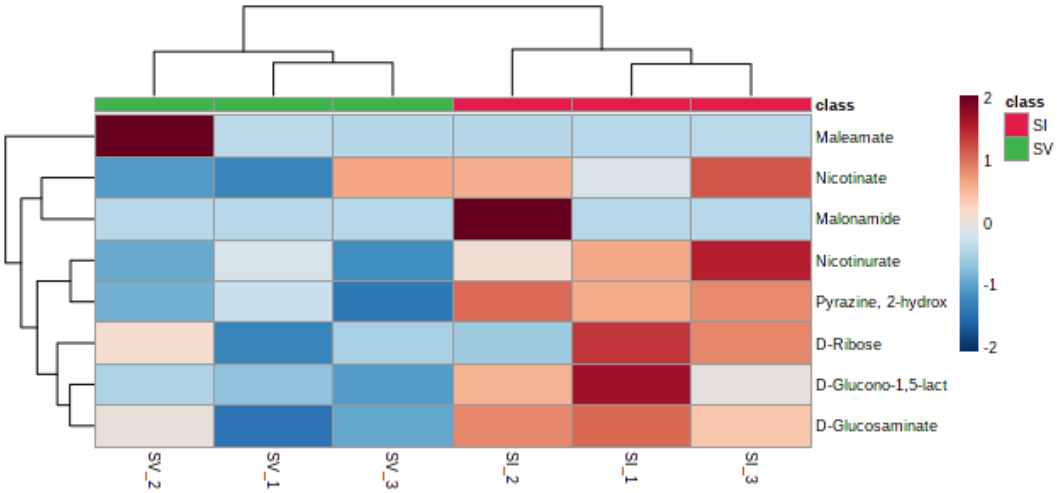

Source: own authorship.

In the nicotinate, nicotinamide, pentose phosphate, and glutathione metabolic pathway, the fold change showed three metabolites significantly increased (Figure 12).

Figure 12: Changes in the median of metabolites abundance in the SI (red) and SV (green) treatments to the metabolism of the nicotinate, nicotinamide, pentose phosphate, and glutathione metabolic pathway. The distribution with inter-quartile and the replicates are shown.

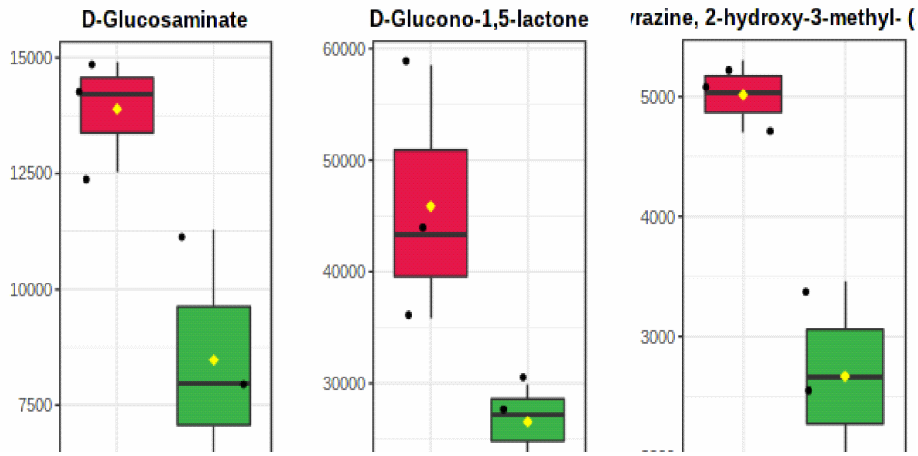

Source: own authorship.

Another pathways with at most two representative metabolites as transferases, oxidative phosphorylation, modify cysteine residues, glycerophospholipid, and glycerolipid metabolism were identified and grouped to the heat map analysis (Figure 13). As a result, 25 metabolites showed a bigger abundance in the SI treatment in at least two replicates. We highlight phosphoric acid, alfa-tocopherol acetate, 3-hydroxybutanoate, diethanolamine, L-selenomethionine, ethanolamine, D-glucosaminate, 3-aminopropane-1,2-diol, which was increased in all replicates in the SI treatment, and decreased in the SV treatment.

Figure 13: Heat map displaying metabolites involved in pathways with fewer than two representative compounds found in the SI replicates (SI1, SI2, SI3) and SV (SV1, SV2, SV3) with different abundances. At the top, the dendrogram clustered treatments based on the similarity of the metabolites, whose red color represents SI treatment and green color represents SV treatment. Changes in abundance are shown by red color (increased) and blue (decreased).

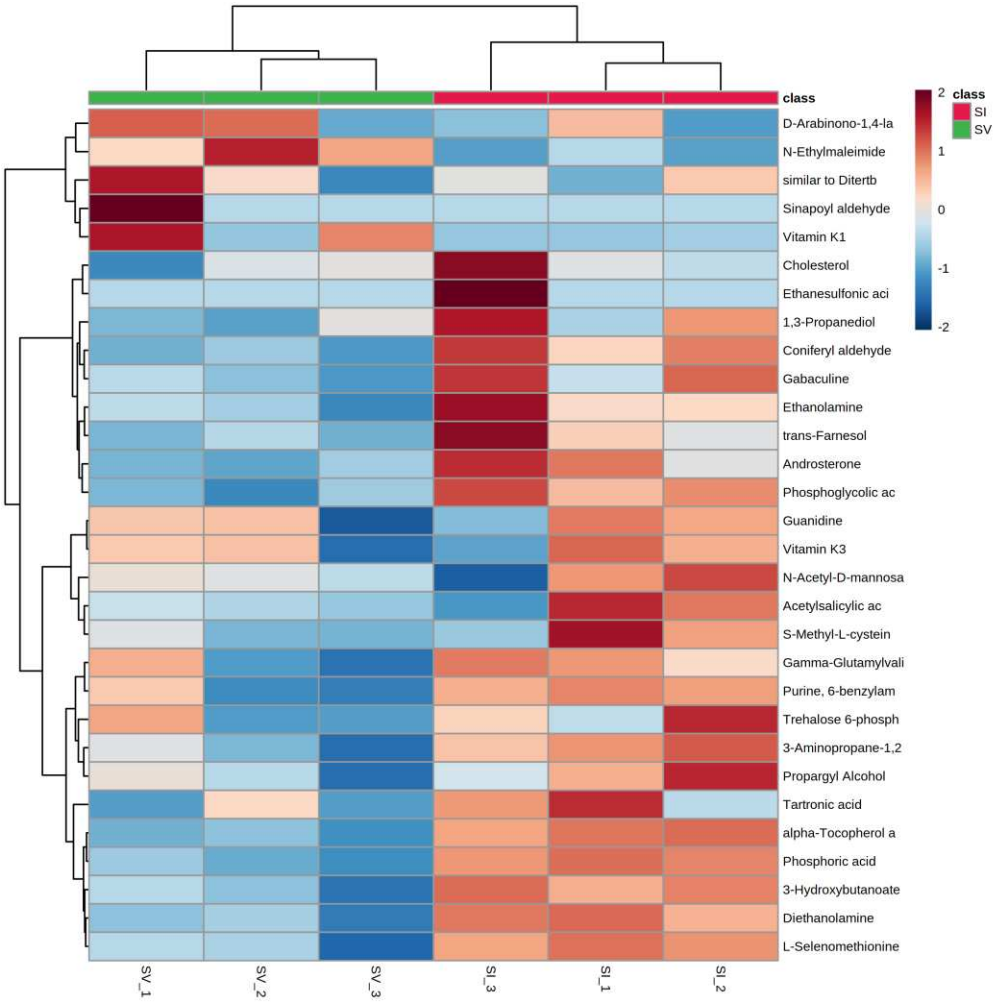

Source: own authorship.

The fold change for metabolites whose pathways were less representative was also calculated. As a result, we highlighted seven significantly increased metabolites and one decreased, shown in Figure 14.

Figure 14: Changes in the median of metabolites abundance in the SI (red) and SV (green) treatments to the metabolites fewer representatives (at most two metabolites in the same pathway). The distribution with inter-quartile and the replicates are shown.

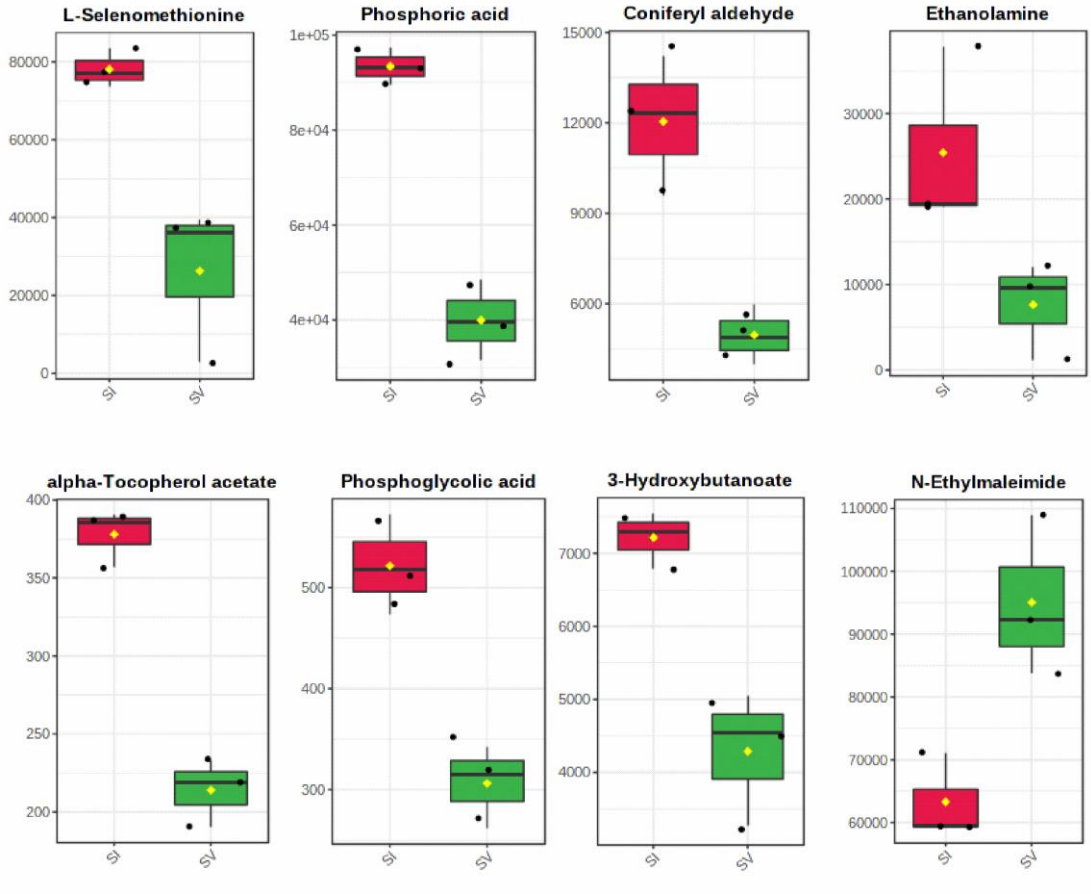

Source: own authorship.

4. DISCUSSION

In this study, we were able to get 323 metabolites, of which were identified and annotated 122 in the midgut of *A. sculptum* ticks unfed (C), fed only blood (S), blood + uninfected Vero cells (SV), and blood + infected Vero cells (SI) for 48 hours.

During PCA analysis, comparing all treatments, some replicates showed greater distance, demonstrating less homogeneity of the samples. These results suggest that the response of the ticks was variable, even standardizing the range of weight, age, and amount of blood made available during the experiment in the laboratory. In the biological system without a controlled environment, each tick may have characteristics that differ from the other. However, taking into account the analysis using the GC-MS platform, it is impossible to obtain a good extraction and yield of metabolites with just

an individual or an organ. For this, a set of midgut (ten) was used to achieve satisfactory yields and proceed with the analyzes.

Due to the large volume of data and numerous combinations of treatments, we chose SI and SV treatments for comparison. In the PCA analysis of the SI / SV set, the samples showed greater homogeneity. The standardization and quantification of infected and uninfected Vero cells were crucial for the reproducibility of the data.

During heat map analysis, the metabolites were organized according to their respective metabolic pathways. The main ones were: metabolism of amino acids, purine, pyrimidines, carbohydrates, TCA cycle, lipids, fatty acids, nicotinate, nicotinamide, pentose phosphate, which pathways showed more than three representatives metabolites.

4.1 Amino acid metabolism

Amino acids play an essential role in the metabolism of ticks. The primary source is obtained from the digestion of hemoglobin (predominantly) and serum albumin obtained through blood-feeding (SOJKA et al., 2016). Hemoglobin digestion occurs within the lysosome or in digestive vesicles present in the midgut. The free amino acids are distributed and incorporated into other tick tissues through the process of transcytosis and transport by hemolymph (SONENSHINE & ANDERSON, 2014).

The most abundant metabolites found in the infected treatment belong to the metabolic pathways of arginine and proline (1-pyrroline-2-carboxylate, spermine), and tryptophan (melatonin, picolinic acid, and 4-hydroxyphenylpyruvate). They were found in low abundance in the SV control group, suggesting that the presence of *R. amblyommatis* was able to positively regulate the availability of enzymes that previously participate in the pathway or negatively regulate enzymes that participate in posterior pathways.

According to DAHMANI et al. (2020), rickettsial pathogen uses arthropod tryptophan pathway metabolites to escape reactive oxygen species produced as a defense mechanism of host cells in response to an invasion by pathogens. Tryptophan can also be used and degraded in ketone bodies and acetyl-CoA. The latter is used at the beginning of the tick and rickettsia TCA cycle that has the necessary enzymes for conversion (DRISCOLL et al., 2017). In addition, arginine can be used for nitric oxide (NO) synthesis, limiting the development of bacteria and protozoa. In some arthropods and insects, the regulation of NO expression is associated with the immune response

of the organism (DIMOPOULOS et al., 1998; LUCKHARDT et al., 1998; SADEKUZZAMAN et al., 2018).

The amino acids arginine and proline can be converted into glutamate and participate in the TCA cycle through alpha-ketoglutarate. In addition, proline in some bacterial pathogens is exploited to protect against stress in the host's cellular environment (CHRISTGEN & BECKER, 2019).

The results found suggest that at 48 hours of feeding, the group of infected ticks used the metabolism of amino acids to fill the pathways for obtaining energy, whose final product is ATP. The metabolites related to amino acids tryptophan, arginine, and proline presented greater abundance in their pathways, contributing to the formation of intermediates of the TCA cycle and collaborating to participate in processes that assist in the survival and permanence of the bacteria inside the host.

4.2 Purine and Pyrimidine metabolism

Purines and pyrimidines are important constituents that play vital functions for cells, participating in the formation of ATP, cAMP, cGMP, nucleotides (cytosine, guanine, thiamine, adenine, and uracil), and precursors in the synthesis of DNA and RNA (CARTER et al., 2008).

During the infection of a host, the parasites need to colonize and replicate quickly, whose processes are dependent on the synthesis of DNA and RNA, using purines and pyrimidines. Nucleotides are also sources of energy and act as precursors and cofactors of various reactions (DEAN et al., 2014)

According to RENESTO et al. (2005), the de novo synthesis of purines and pyrimidines is not performed by rickettsiae. However, analyzing the bacterium's genome, several enzymes are encoded to recover of the adenine and guanine nucleotides, but those that participate in the initial steps in the conversion of adenine to guanine are not present, depending on availability in the host.

In this study, four metabolites identified in purine metabolism were up-regulated in SI treatment, which is essential in the synthesis of deoxyguanosine, hypoxanthine, xanthosine, and oxamate. In the metabolism of pyrimidines, six metabolites were abundant in the infected treatment, which determines the synthesis of uracil, cytosine, orotate, and uridine. This increase suggests that rickettsia could act in the synthesis of these components for greater availability in the cellular environment, being transported to its interior and used in the replication steps.

According to DEAN et al. (2014), the loss of biosynthetic pathways is common in protist parasites, which use specialized proteins to transport these components. Several proteins have already been identified and characterized to develop drugs capable of blocking the transport and capture of components made available by the host. In rickettsiae, nucleotide transport proteins (NtT) have been identified. However, further studies are needed to develop a drug capable of blocking them.

4.3 Carbohydrates metabolism and TCA cycle

The metabolites belonging to carbohydrate metabolism are used in several ways to obtain energy. In this study, no intermediary of the glycolytic pathway was identified with a statistical difference according to the treatments. This observation suggests that the glycolytic pathway has greater activation in the initial feeding moments, whose ticks can quickly convert carbohydrates from the host's blood into energy (REN et al., 2019), presenting lower concentrations, and consequently, more incredible greater difficulty of detection overtime of 48 hours feeding. In addition, the presence of myo-inositol (glucose isomer) reveals that its basic component can be used in other ways besides glycolysis, depending on the level of free energy capable of maintaining the system's homeostasis. According to Moreira (2017), in the transcriptomic data analysis, inositol metabolism enzymes are overexpressed in infected ticks with *R. amblyommatis*. In addition, excess ATP in the cell is able to inhibit the action of the phosphofructokinase enzyme and consequently reduce glycolysis. In advanced feeding stages (more than 48 hours), excess glucose can be converted into glycogen, stored as an energy source to be used in the post-feeding stage (ALASMARI & WALL, 2020).

In the TCA cycle, only three metabolites were identified, an abundance of which was more significant for the infected treatments. According to DRISCOLL (2017), Rickettsia species use the metabolites acquired by the host to fill their own TCA cycle. Thus, with the lower availability of intermediates in the pathway, the tick can alter the expression of enzymes involved in the degradation of amino acids so that the products of the catalysis reactions are incorporated into the pathways affected by the bacteria. Some amino acids can be converted into products belonging to the TCA cycle, such as converting arginine, glutamine, histidine, and proline to glutamate.

4.4 Lipids and fatty acids metabolism

Lipids also play an essential role in tick metabolism. In addition to serving as a source of energy, they are found in cell membranes, hormones, and egg development (ALASMARI & WALL, 2020; KLUCK et al., 2018). *Rickettsia* species depend on the precursors obtained by the host's metabolism to synthesize of fatty acids and glycerophospholipids (DRISCOLL et al., 2017). Enzymes involved in this classification showed high expression in the transcriptomes, suggesting that lipid could be a nutrient source for *A. sculptum* during feeding (MOREIRA, 2017).

Within 48 hours of feeding, several fatty acids and lipids showed greater abundance in the infected treatment, of which the following stood out significantly: malonate, eicosenoic acid, N-butyryl-L-homoserine lactone, and 2-hydroxyglutarate. The metabolites N- (3-oxioctanoyl) homoserine lactone and N-butyryl-L-homoserine lactone participate in the mechanism called quorum sensing, which is considered of extreme importance in the control of growth, replication, secretion of virulence factors, and extracellular polysaccharides of gram-negative bacteria, mediated by signal molecules in the form of acyl-homoserine lactones (ZIMMER, 2012). 2-hydroxyglutarate participates in the formation of butanoate fatty acid, which can be converted to acetyl-CoA through numerous metabolic reactions (based on the KEGG classification), the latter being used in the first stage of the TCA cycle.

Other metabolites involved in fatty acid metabolism were more abundant in the infected treatment, such as malonate, one of the first components in the fatty acid synthesis reaction, and eicosenoic acid, an essential metabolite in the formation of unsaturated fatty acids.

We can observe that compounds from different pathways are used to fill the TCA cycle that exists in *A. sculptum* ticks and *R. amblyommatis* bacteria, making the host provide other means of obtaining essential metabolites for its survival and energy production, even with the interference of the bacteria.

4.5 Nicotinate, nicotinamide, and pentose phosphate metabolism

Nicotinate (Nicotinic acids) and nicotinamide are known as vitamin B3 and precursors of the coenzymes nicotinamide - adenine dinucleotide (NAD+) and nicotinamide - adenine dinucleotide phosphate (NADP+), which play an important role in the glycolytic pathway, TCA cycle, fatty acid synthesis, pentose phosphate cycle, among others (DÖLLE et al., 2013; LOCKWOOD et al., 2016).

Nicotinate D-ribonucleotide, a fundamental component for the synthesis of NAD+ and NADPH+, can be obtained from the metabolism of tryptophan, alanine, aspartate, and glutamate, whose enzymes involved in the conversion reactions are absent in *Rickettsia* species and *Borrelia* spp. (LOCKWOOD et al., 2016). In this work, nicotinate and nicotinamide were identified in the infected treatment, suggesting that rickettsia could modify the availability of these components to make their capture and use favorably. In addition, the low availability of maleate in infected and non-infected groups indicates that in 48 hours of feeding, the fumarate formation pathway (TCA cycle) is disadvantaged in both, which must be obtained by other routes, such for example, from the metabolism of alanine, aspartate, and glutamate.

The pentose phosphate pathway is known as an alternative glucose oxidation route without the formation of ATP, generating NADPH and phosphate pentoses (ribulose, ribose, and xylulose). NADPH participates in fatty acid synthesis reactions and reacts to combat reactive oxygen species (FERNANDEZ-MARCOS & NÓBREGA-PEREIRA, 2016). Pentoses are used for the synthesis of nucleic acids (DNA and RNA) and other associated compounds. According to RENESTO et al. (2005), the *Rickettsia* genus has a deficiency in this pathway's enzymes, which are considered necessary in the synthesis of nucleotides (MIN et al., 2008), replication, transcription, and bacteria’s regulation (DRISCOLL et al., 2017).

With the tick feeding period has reached 48 hours, the pentose phosphate pathway in the infected treatment was favored over the glycolytic pathway, whose greater availability of D-Glucono-1,5-lactone and D-Glucosaminate support that observation. In addition, the maintenance, replication, and propagation processes of *R. amblyommatis* within the tick's midgut depend on these intermediates available in greater concentration, as found in this work.

The failure to identify metabolites of the main glucose pathway may be related to the biological moment, due to the large volume of food available in the midgut for processing, whose glucose available in the blood was rapidly metabolized, resulting a sufficient energy for the survival of ticks and maintenance of biological processes, thus ruling out possible limitations of the analysis in this pathway.

5. CONCLUSION

This study demonstrated that the developed untargeted metabolomics approach allowed detecting different metabolites in tick's midgut samples. However, several precautions must be taken to perform the feeding, dissection, extraction of metabolites, and statistical analysis of the data, whose experiment repeatability and error reduction depend on these factors.

We showed for the first time the metabolic profile of *A. sculptum* ticks fed and infected with *R. amblyommatis*, using artificial feeding for 48 hours and analyzing the metabolites extracted by gas chromatography coupled to the mass spectrometer (GC-MS).

During the identification of the metabolites, we had initially noted 323 compounds. Several were described as not identified or not available in the GOLM library used. With the separation of these, we arrived at a total of 122 identified metabolites distributed in several pathways, of which we emphasize the amino acids, purine and pyrimidine, carbohydrates and TCA cycle, lipids and fatty acids, nicotinate, nicotinamide, and pentose phosphate. With the increase in information sharing, databases, and libraries available, it is expected that this limitation in the identification of metabolites in the tick midgut will be lessened in the future.

The Metaboanalyst software was used to perform principal component analysis (PCA), Volcano Plot, Metabolite set enrichment analysis (MSEA), and heat maps. From these analyzes, we were able to: (a) list the metabolites found in fasting ticks, fed with blood, blood + uninfected and infected Vero cells; (b) separate which metabolites showed a statistically significant difference between infected and non-infected treatments; (c) to discuss the possible interference of rickettsia in the availability of these constituents, pointing out its metabolic deficiency in several pathways, and the need to obtain several intermediates in the tick's metabolism in order to favor their replication and maintenance in the midgut of this arthropod.

Future work will be able to determine which metabolites significantly found in greater availability in the infected treatment have a biological potential, to use drugs been able to block or decrease their transport into the bacteria, hindering the spread, limiting their permanence in these arthropods, and reducing transmission for other animals.

6. ACKNOWLEDGMENT

This work was supported by Fundação Arthur Bernardes (FUNARBE), Fundação de Amparo à Pesquisa do Estado de Minas Gerais (FAPEMIG), Conselho Nacional de Desenvolvimento Científico e Tecnológico (CNPq), and Coordenação de Aperfeiçoamento de Pessoal de Nível Superior (CAPES). C.M. is Productive Research grant recipient from Brazilian National Council for Scientific and Technological Development (CNPq).

7. REFERENCES

ALASMARI, S., WALL, R. Determining the total energy budget of the tick *Ixodes ricinus*. Exp Appl Acarol 80, 531–541, 2020.

AMMERMAN, N. C., BEIER-SEXTON, M., AZAD, A. F. Laboratory maintenance of *Rickettsia rickettsii*. Curr. Prot. Microbiol. 11, 1-27, 2008.

ANATRIELLO, E., RIBEIRO, J. M. C., MIRANDA-SANTOS, I. K. F., BRANDÃO, L. G., ANDERSON, J. M., VALENZUELA, J. G., MARUYAMA, S. R., SILVA, J. S., FERREIRA, B. R. An insight into the sialotranscriptome of the brown dog tick, *Rhipicephalus sanguineus*. BMC Genomics. 11,1-17, 2010.

BARROS-BATTESTI, D.M., ARZUA, M., BECHARA, G.H. Carrapatos de importância médico-veterinária da Região Neotropical: Um guia ilustrado para identificação de espécies. São Paulo: Vox/ICTTD-3/Butantan, 2006. 223 p.

BECHARA, G. H., SZABÓ, M. P. J., FERREIRA, B. R., GARCIA, M. V. 928 *Rhipicephalus sanguineus* tick in Brazil: feeding and reproductive aspects under 929 laboratorial conditions. Rev. Bras. Parasitol. Vet. 4, 61-66, 1995.

BIRNBOIM, H. C.; DOLY, J. A rapid alkaline extraction procedure for screening recombinant plasmid DNA. Nucleic Acids Research, 7 (6): 1513-1523, 1979.

CARTER N.S., YATES P., ARENDT C.S., BOITZ J.M., ULLMAN B. (2008) Purine and pyrimidine metabolism in Leishmania. In: Majumder H.K. (eds) Drug Targets in Kinetoplastid Parasites. Advances In Experimental Medicine And Biology, vol 625. Springer, New York, NY.

CARUSO, C. S. Clonagem, expressão e caracterização de proteínas recombinantes de *Xylella fastidiosa*. 2007. Tese de Doutorado. Universidade de São Paulo.

CHONG, J., SOUFAN, O., LI, C., CARAUS, I., LI, S., BOURQUE, G., et al. MetaboAnalyst 4.0: Towards more transparent and integrative metabolomics analysis. Nucleic Acids Research,46, W486–W494, 2018.

CHRISTGEN, S. L., BECKER, D. F. Role of proline in pathogen and host interactions. Antioxidants & redox signaling, 30(4), 683–709, 2019.

CUADROS-INOSTROZA, Á., CALDANA, C., REDESTIG, H., KUSANO, M., LISEC, J., PEÑA-CORTÉS, H., WILLMITZER, L., & HANNAH, M. A. TargetSearch - a Bioconductor package for the efficient preprocessing of GC-MS metabolite profiling data. BMC Bioinformatics, 10(1), 428, 2009.

DAHMANI, M., ANDERSON, J. F., SULTANA, H., NEELAKANTA, G. Rickettsial pathogen uses arthropod tryptophan pathway metabolites to evade reactive oxygen species in tick cells. Cellular Microbiology. 2020.

DEAN, P., MAJOR, P., NAKJANG, S., HIRT, R.P., EMBLEY, T.M. Transport proteins of parasitic protists and their role in nutrient salvage. Front. Plant Sci. 5:153, 2014.
DÖLLE, C., RACK, J.G., ZIEGLER, M. Nad and adp-ribose metabolism in mitochondria. Febs J.;280 (15):3530–41, 2013.

DELISLE, J., MENDELL, N.L., STULL-LANE, A., BLOCH, K.C., BOUYER, D.H., MONCAYO, A.C. Human infections by multiple spotted fever group Rickettsiae in Tennessee. Am J Trop Med Hyg; 94:1212–1217, 2016.

DIMOPOULOS, G., SEELEY, D., WOLF, A., KAFATOS, F.C. Malaria infection of the mosquito *Anopheles gambiae* activates immune-responsive genes during critical transition stages of the parasite life cycle. EMBO J;17:6115-6123, 1998.

DÖLLE, C., RACK, J. G., ZIEGLER, M. NAD and ADP□ribose metabolism in mitochondria. FEBS J, 280: 3530-3541, 2013.

DRISCOLL, T. P., VERHOEVE, V. I., GUILLOTTE, M. L., LEHMAN, S. S., RENNOLL, S. A., BEIER-SEXTON, M., RAHMAN, M. S., AZAD, A. F., GILLESPIE, J. J. Wholly Rickettsia! Reconstructed metabolic profile of the quintessential bacterial parasite of eukaryotic cells. MBio 8, 00859-17, 2017.

ESTRADA-PEÑA, A., GUGLIELMONE, A., MANGOLD, A. J. The distribution and ecological “preferences” of the tick *Amblyomma cajennense* (Acari: Ixodidae), an ectoparasite of humans and other mammals in the Americas. Annals of Tropic Medicine and Parasitology, v.98, p. 183-292, 2004.

FERNANDEZ-MARCOS, P. J, NÓBREGA-PEREIRA, S. NADPH: new oxygen for the ROS theory of aging. Oncotarget, 7(32), 50814–50815, 2016.

GALILI, T., O’CALLAGHAN, A., SIDI, J., & SIEVERT, C. Heatmaply: An R package for creating interactive cluster heatmaps for online publishing. Bioinformatics, 34(9), 1600–1602, 2018.

GUGLIELMONE, A. A., ROBBINS, R. G., APANASKEVICH, D. A., PETNEY, T. N., ESTRADA-PEÑA, A., HORAK, I. G., SHAO, R., BARKER, S. C. Zootaxa, The Argasidae, Ixodidae and Nuttalliellidae (Acari: Ixodida) of the world: a list of valid species names. Zootaxa 2528, 1–28, 2010.

HOXMEIER, J. C.; FLESHMAN, A. C.; BROECKLING, C. D.; PRENNI, J. E.; DOLAN, M. C.; GAGE, K. L.; EISEN, L. Metabolomics of the tick-Borrelia interaction during the nymphal tick blood meal. Scientific Reports, [S.L.], v. 7, n. 1, 2017.

KARPATHY, S. E.; SLATER, K. S.; GOLDSMITH, C. S.; NICHOLSON, W. L.; PADDOCK, C. D. *Rickettsia amblyommatis* sp. nov., a spotted fever group Rickettsia associated with multiple species of *Amblyomma* ticks in North, Central and South America. International Journal Of Systematic And Evolutionary Microbiology, [S.L.], v. 66, n. 12, p. 5236-5243, 2016.

KLUCK, G.E.G.; CARDOSO, L.S.; DE CICCO, N.N.T.; LIMA, M.S.; FOLLY, E.; ATELLA, G.C. A new lipid carrier protein in the cattle tick *Rhipicephalus microplus*. Ticks Tick-Borne Dis 9:850–859, 2018.

LABRUNA, M. B., WHITWORTH, T., BOUYER, D. H., MCBRIDE, J. W., PINTER, A., POPOV, V., WALKER, D. H. *Rickettsia* species infecting *Amblyomma cooperi* ticks from an area in the state of São Paulo, Brazil, where Brazilian spotted fever is endemic. J. Clin. Microbiol. 42, 90-98, 2004.

LISEC, J., SCHAUER, N., KOPKA, J., WILLMITZER, L., FERNIE, A. R. Gas chromatography mass spectrometry–based metabolite profiling in plants. Nat Protoc 1, 387–396, 2006.

LOCKWOOD, S., BRAYTON, K. A., BROSCHAT, S. L. Comparative genomics reveals multiple pathways to mutualism for tick-borne pathogens. BMC genomics, 17, 481, 2016.

LUCKHART, S., VODOVOTZ, Y., CUI, L., ROSENBERG, R. The mosquito *Anopheles stephensi* limits malaria parasite development with inducible synthesis of nitric oxide. Proc Natl Acad Sci USA;95:5700-5705, 1998.

MARTINS, T. F., BARBIERI, A. R. M., COSTA, F. B., TERASSINI, F. A., CAMARGO, L. M. A., PETERKA, C. R. L., et al. Geographical distribution of *Amblyomma cajennense* (sensu lato) ticks (Parasitiformes: Ixodidae) in Brazil, with description of the nymph of *A. cajennense* (sensu stricto). Parasites Vectors 9, 186, 2016.

MARTINS, L. A.; GALLETTI, M.; RIBEIRO, J. M.; FUJITA, A.; COSTA, F. B.; LABRUNA, M. B.; DAFFRE, S.; FOGAÇA, A. C. The Distinct Transcriptional Response of the Midgut of *Amblyomma sculptum* and *Amblyomma aureolatum* Ticks to *Rickettsia rickettsii* Correlates to Their Differences in Susceptibility to Infection. Frontiers in cellular and infection microbiology, *7*, 129, 2017.

MIN, C.; YANG, J.; KIM, S.; CHOI, M.; KIM, I.; CHO, N. Genome-based construction of the metabolic pathways of *Orientia tsutsugamushi* and comparative analysis within the Rickettsiales order. Comparative And Functional Genomics, [S.L.], v. 2008, p. 1-14, 2008.

MOREIRA, H. N. S. Anotação e montagem de transcriptomas de intestino médio e ovários do carrapato *Amblyomma sculptum*, antes e após a infecção por *Rickettsia amblyommii*, PhD thesis, Universidade Federal de Viçosa, Viçosa, 2017. Disponível em: https://locus.ufv.br//handle/123456789/9368 Acesso em: 10 fev.2021.

NARRA, Hema P.; SAHNI, Abha; ALSING, Jessica; SCHROEDER, Casey L. C.; GOLOVKO, George; NIA, Anna M.; FOFANOV, Yuriy; KHANIPOV, Kamil; SAHNI,

Sanjeev K. Comparative transcriptomic analysis of *Rickettsia conorii* during in vitro infection of human and tick host cells. Bmc Genomics, [S.L.], v. 21, n. 1, 25, 2020.

NAVA, S., BEATI, L., LABRUNA, M.B., CÁCERES, A.G., MANGOLD, A.J. and GUGLIELMONE, A.A. Reassessment of the taxonomic status of *Amblyomma cajennense* (Fabricius, 1787) with the description of three new species, *Amblyomma tonelliae* n. sp., *Amblyomma interandinum* n. sp. and *Amblyomma patinoi* n. sp., and reinstatement of *Amblyomma mixtum* Koch, 1844, and *Amblyomma sculptum* Berlese, 1888 (Ixodida: Ixodidae). Ticks Tick Borne Dis., 5(3): 252-276, 2014.

QUIROZ-CASTAÑEDA, R. E.; COBAXIN-CÁRDENAS, M.; CUERVO-SOTO, L. I. Exploring the diversity, infectivity and metabolomic landscape of Rickettsial infections for developing novel therapeutic intervention strategies. Cytokine, [S.L.], v. 112, p. 63-74, 2018.

R CORE TEAM. R: A language and environment for statistical computing (4.0.3). R Foundation for Statistical Computing. 2020. Disponível em: https://www.r-project.org/. Acesso: 12 fev. 2021.

REN, S., ZHANG, B., XUE, X., WANG, X., ZHAO, H., ZHANGI, X., WANG, M., XIAO, Q., WANG, H., LIU, J. Salivary gland proteome analysis of developing adult female *Haemaphysalis longicornis* ticks: molecular motor and TCA cycle-related proteins play an important role throughout development. Parasit Vectors. 12, 613, 2019.

RENESTO, P., OGATA, H., AUDIC, S., CLAVERIE, J. M., RAOULT, D. Some lessons from *Rickettsia* genomics. FEMS Microbiol. Rev. 29,99-117, 2005.

RIVAS, Juan J.; MOREIRA-SOTO, Andrés; ALVARADO, Gilberth; TAYLOR, Lizeth; CALDERÓN-ARGUEDAS, Olger; HUN, Laya; CORRALES-AGUILAR, Eugenia; MORALES, Juan Alberto; TROYO, Adriana. Pathogenic potential of a Costa Rican strain of 'Candidatus *Rickettsia amblyommii*' in guinea pigs (Cavia porcellus) and protective immunity against *Rickettsia rickettsii*. Ticks And Tick-Borne Diseases, [S.L.], v. 6, n. 6, p. 805-811, 2015.

ROESSNER-TUNALI, U., HEGEMANN, B., LYTOVCHENKO, A., CARRARI, F., BRUEDIGAM, C., GRANOT, D., FERNIE, A.R. Metabolic profiling of transgenic tomato plants overexpressing hexokinase reveals that the influence of hexose phosphorylation diminishes during fruit development. Plant Physiology, v. 133, n. 1, p. 84-99, 2003.

SADEKUZZAMAN, M., STANLEY, D., KIM, Y. Nitric Oxide Mediates Insect Cellular Immunity via Phospholipase A2 Activation. J Innate Immun; 10:70-81, 2018.

SÁNCHEZ-MONTES, S.; COLUNGA-SALAS, P.; LOZANO-SARDANETA, Y. N.; ZAZUETA-ISLAS, H. M.; BALLADOS-GONZÁLEZ, G. G.; SALCEDA-SÁNCHEZ, B.; HUERTA-JIMÉNEZ, H.; TORRES-CASTRO, M.; PANTI-MAY, J. A.; PENICHE-LARA,

G. The genus *Rickettsia* in Mexico: current knowledge and perspectives. Ticks And Tick-Borne Diseases, [S.L.], Elsevier BV. v. 12, n. 2, p. 101633, 2021.

SANTIBÁÑEZ, S.; PORTILLO, A.; PALOMAR, A.M.; OTEO, J.A.. Isolation of *Rickettsia amblyommatis* in HUVEC line. New Microbes And New Infections, [S.L.], v. 21, p. 117-121, 2018.

SOJKA, D., PYTELKOVÁ, J.., PERNER, J., HORN, M., KONVIČKOVÁ, J., SCHRENKOVÁ, J., MAREŠ, M., KOPÁČEK, P. Multienzyme degradation of host serum albumin in ticks. Ticks Tick Borne Dis.; 7(4):604-13, 2016.

SONENSHINE, D.E., ANDERSON, J.M. Mouthparts and digestive system: anatomy and molecular biology of feeding and digestion. In: Sonenshine DE, Roe RM, editors. *Biology of ticks.* Oxford: Oxford University Press; 2014. pp. 122–162.

USPENSKY, I. Argasid (Soft) Ticks (Acari: ixodida. Encyclopedia Of Entomology, [S.L.], p. 195-198, 2005.

VALIM, J. R. A., RANGEL, C. P., BAÊTA, B. A., RIBEIRO, C. C. D. U., CORDEIRO, M. D., TEIXEIRA, R. C., CEPEDA, P. B., FONSECA, A. D. H. Using plastic tips in artificial feeding of *Rhipicephalus sanguineus* sensu lato (Acari: Ixodidae) females. Rev. Bras. Parasitol. Vet., 26, 110-114, 2017.

VAN DEN DOOL, H., & KRATZ, P. D. A generalization of the retention index system including linear temperature programmed gas-liquid partition chromatography. JOURNAL OF CHROMATOGRAPHY, 11, 463–471, 1963.

VILLAR, M.; POPARA, M.; BONZÓN-KULICHENKO, E.; AYLLÓN, N.; VÁZQUEZ, J.; LAFUENTE, J. Characterization of the tick-pathogen interface by quantitative proteomics. Ticks And Tick-Borne Diseases, [S.L.], v. 3, n. 3, p. 154-158, 2012.

ZIMMER, K. R. (2012). Atividade antibiofilme e antibiótica da cera dos ovos e de metabólitos produzidos por bactérias associadas ao carrapato *Rhipicephalus* (*Boophilus*) *microplus.* PhD thesis, Universidade Federal do Rio Grande do Sul, Porto Alegre.

Disponível em: https://www.lume.ufrgs.br/bitstream/handle/10183/69694/000869251.pdf?sequence=1. Acesso: 01 maio 2021.

WALKER, A., BROWN, C., BELL, L., MCKELLAR, S. Artificial infection of the tick *Rhipicephalus appendiculatus* with *Theileria parva*. Res. Vet. Sci. 26, 264-265, 1979.

WIKEL, S. K. Acquired resistance to ticks. expression of resistance by C4-1068 deficient guinea-pigs. Am. J. Trop. Med. Hyg. 28, 586-590, 1979.

YUN, J. J., HEISLER, L. E., HWANG, I. I. L., WILKINS, O., LAU, S.K., HYRCZA, M.; JAYABALASINGHAM, B., JIN, J., MCLAURIN, J., TSAO, M., DER, S. D. Genomic DNA functions as a universal external standard in quantitative real-time PCR. Nucleic Acids Res. 34, e85, 2006.

Supplementary Table 1: Metabolites identified in the treatments SV and SI, whose name from the KEGG and the corrected peaks intensity (according to samples weight) was annotated.

			Samples					
Name	**Pathway**	**KEGG ID**	**SV1**	**SV2**	**SV3**	**SI1**	**SI2**	**SI3**
S-Methyl-L-cysteine	ABC transporters	C22040	38272.47421	31819.87981	31635.06697	54144.43422	45323.65071	33582.53752
1-Pyrroline-2-carboxylate	Amino acids metabolism	C03564	93550.84329	101960.3703	27997.04296	210470.1012	240719.0246	217828.1037
3-Hydroxyphenylacetate	Amino acids metabolism	C05593	82682.98674	76742.73185	79028.5267	91719.41122	83887.39466	83167.80355
3-Isopropylmalate	Amino acids metabolism	C04411	5203.864418	5147.799253	2830.057401	4109.475621	3325.264479	4273.7608
3-Sulfino-L-alanine	Amino acids metabolism	C00606	5171.933846	4238.265389	8631.935989	6305.427783	12259.27918	16115.50705
3,4-Dihydroxyphenylethyleneglycol	Amino acids metabolism	C05576	9051.907647	10998051	4607.757871	20648.57406	27345.34696	29996.36198
4-Hydroxyphenylpyruvate	Amino acids metabolism	C01179	1937.940069	2239.72714	1205.427031	3814.167433	5781.78232	5778.080946
4-Imidazoleacetate	Amino acids metabolism	C02835	5629.605371	5348.383953	8146.634197	15593.37626	14797.38211	6227.37608

Supplementary Table 1 (continued)

Creatinine	Amino acids metabolism	C00791	54158.34289	49497.32012	50977.56132	59813.24747	58308.23023	65360.61846
Dimethylglycine	Amino acids metabolism	C01026	27203.20943	29974.01332	22459.55818	58458.14167	43349.47104	35789.9045
Gentisate aldehyde	Amino acids metabolism	C05585	18980.67791	14651.61605	14582.53609	17552.89788	26050.74413	17036.83492
Glutarate	Amino acids metabolism	C00489	58217.61913	88830.59932	28796.3124	134001.8399	187619688	135764.4384
Hippurate	Amino acids metabolism	C01586	32678.07434	35200.5847	22063.83719	60871.20515	32442.17321	45311.50523
Histidinol	Amino acids metabolism	C00860	16142.13198	15503.49196	15269.61211	17424.10304	18336.91949	18315598
Homovanillate	Amino acids metabolism	C05582	9818.241362	10193.27595	10093.92938	14860.16559	15451.85584	17400.63665
Indolepyruvate	Amino acids metabolism	C00331	269484.1985	242026.9612	253811.9673	288453.5419	287538.9995	271088.6767
L-Alanine	Amino acids metabolism	C00041	68017.02964	77394.83515	35026.96121	184907.0837	220910884	271865.3934
L-Homoserine	Amino acids metabolism	C00263	5852.300639	6266.850739	3589.319882	5092.916283	7260.175722	5309.686221
L-Kynurenine	Amino acids metabolism	C00328	18980.67791	14651.61605	14582.53609	17552.89788	26050.74413	17036.83492

Supplementary Table 1 (continued)

L-Leucine	Amino acids metabolism	C00123	58217.61913	88830.59932	28796.3124	134001.8399	187619688	135764.4384
L-Phenylalanine	Amino acids metabolism	C00079	710.6598985	786.909209	14582.53609	1413.983441	1449.704142	1602.546612
L-Proline	Amino acids metabolism	C00148	8315.867038	7523.956472	6643.764133	8537.25851	11937.42155	12716.6894
L-Serine	Amino acids metabolism	C00065	1779.924677	4304.856261	4089.406853	3213.431463	6241.707011	4265.575261
LL-2,6-Diaminoheptanedioate	Amino acids metabolism	C00666	7741.935484	5790.969628	5166.115846	7509.659614	8286.713287	12629.37699
Melatonin	Amino acids metabolism	C01598	1139.675782	1090.628553	721.8646721	2033.118675	2783.754707	3247.839927
N-Acetyl-L-glutamate	Amino acids metabolism	C00624	1893.728508	3738.021764	1408.940685	3961.361546	2361.484669	3488.858572
N-Acetylhistamine	Amino acids metabolism	C05135	8315.867038	7523.956472	6643.764133	8537.25851	11937.42155	12716.6894
N-Acetylmethionine	Amino acids metabolism	C02712	54158.34289	49497.32012	50977.56132	59813.24747	58308.23023	65360.61846
N-Acetylputrescine	Amino acids metabolism	C02714	270807.2703	249611.8239	228911.9847	295353.2659	306819.0784	284998.6357
N6-Acetyl-L-lysine	Amino acids metabolism	C02727	20101.52284	21938.44405	16710.7323	29522.5391	31584.18505	27176.89859

Supplementary Table 1 (continued)

Phenylglycine	Amino acids metabolism	C18623	10275.09415	9172.486601	8813.706732	11424.10304	10658.05989	12745.79354
Picolinic acid	Amino acids metabolism	C10164	5556.738169	6800.3898	16604.62689	12064.39742	16245.29317	19708.04911
Quinazoline, 4-hydroxy-	Amino acids metabolism		68910.26691	69806.72405	29579.05723	79853.72585	73809.39573	47390.63211
Serotonin	Amino acids metabolism	C00780	270807.2703	249611.8239	228911.9847	295353.2659	306819.0784	284998.6357
Spermidine	Amino acids metabolism	C00315	270807.2703	249611.8239	228911.9847	295353.2659	306819.0784	284998.6357
Spermine	Amino acids metabolism	C00750	86705.42001	149585.0252	46349.79997	216982.5207	267816.9267	242752.1601
trans-3-Hydroxy-L-proline	Amino acids metabolism	C05147	49205.82938	49125.38574	40022.61263	48402.02392	60308.40954	61376.98954
N-Acetyl-D-mannosamine	Amino sugar and nucleotide sugar metabolism	C00645	32893.40102	31605.48969	27945.72969	42099.35603	48359.33297	11672.57844
D-Arabinono-1,4-lactone	Ascorbate and aldarate metabolism	C00652	2052.562633	2018.840344	1260.219169	1804.967801	1212.121212	1340.609368
similar to Ditertbutylphenol (1TMS)	Bacterial metabolite		68651.5474	59407.9909	50205.25309	52678.93284	60632.06025	57879.03593

Supplementary Table 1 (continued)

Acetylsalicylic acid	Bile secretion	C01405	3911.904372	3420.496995	2936.162811	9011.039558	7537.206383	1585.26603
alpha-Arbutin	Carbohydrate metabolism	C06186	1589.15998	1312.327432	761.8716298	2656.853726	2972.924511	3464.301955
D-Fructose 6-phosphate	Carbohydrate metabolism	C00085	13677.74685	13994.64025	15066.96817	14662.37351	14497.04142	16281.94634
L-Rhamnose	Carbohydrate metabolism	C00507	365028.6556	376181.5819	319142.4596	407694.5722	464884.3464	490853.1151
myo-Inositol	Carbohydrate metabolism	C00137	7493.040773	8611.33669	4390.328753	15467.34131	15804.1958	15317.87176
Sequoyitol	Carbohydrate metabolism	C03365	1395.939086	2071.625792	1653.331014	2816.00736	3818.361126	4967.712597
Xylobiose	Carbohydrate metabolism	C01630	1973.964303	1759.78561	1413.289268	3125.114995	3239.196701	3209.640746
Tartronic acid	Catalytic oxidation of glycerol	C02287	14175.53627	20834.82215	14134.63211	27264.02944	17625.06724	23543.42883
Guanidine	Degradation of guanine	C17349	68910.26691	69806.72405	29579.05723	79853.72585	73809.39573	47390.63211
Gamma-Glutamylleucine_4TMS	Dipeptides		418.3723596	297.2226734	364.4112019	515.1793928	552.2682446	482.946794
Gamma-Glutamylvaline_2TMS	Dipeptides		72874.57017	53301.93276	48574.5347	74810.48758	68104.7158	77113.23329

Supplementary Table 1 (continued)

Allantoin	Excreta, nitrogen elimination	C01551	576.3877518	448.2702615	562.7065577	431.4627415	482.3381746	782.1737153
2-Decenoic-acid_1TMS	Fatty acid biosynthesis		4368.757164	3967.029397	4240.73752	7016.559338	6270.39627	6101.864484
Hexadecanoic acid	Fatty acid biosynthesis	C00249	85686.91665	90181.09469	73858.06227	104264.9494	104431594	124507.5034
Malonate	Fatty acid biosynthesis	C00383	5047.486491	4545.233068	3271.003653	6793.00828	7294.244217	7552.523874
Myristic acid	Fatty acid biosynthesis	C06424	13713.77108	6065.453955	1240.21569	9946.642134	5337.098799	11877.21692
Pentanedioic acid	Fatty acid degradation	C00489	72452.10414	68183.36852	59738.21534	99043.23827	112201.9007	19658.02638
1-octadecenol	Fatty acid degradation		34688.06288	25462.07569	26748.99983	32911.68353	35890.26358	38087.31241
Octadecanal	Fatty acid degradation		16142.13198	15503.49196	15269.61211	17424.10304	18336.91949	18315598
Octadecanol	Fatty acid degradation		5144.915671	3664.122137	3209.253783	4013.799448	4441.45598	5077.762619
Eicosapentaenoic acid, 5,8,11,14,17-(Z,Z,Z,Z,Z)-, n- (1TMS)	Fatty acids Biosynthesis (unsaturated)	C06428	542.8197151	447.4581777	442.6856845	827.0469181	1922.180384	924.9658936

Supplementary Table 1 (continued)

2-Hydroxybutyrate	Fatty acids metabolism	C05984	49205.82938	49125.38574	40022.61263	48402.02392	60308.40954	61376.98954
Eicosenoic acid	Fatty acids metabolism	C16526	962.8295399	1050.836446	299.1824665	2530.818767	2188.452573	2035.470668
Dehydroascorbic acid	Glutathione metabolism	C05422	8097.265433	6455.254182	6339.363368	13234.59062	8063.474987	7880.854934
Pyrazine, 2-hydroxy-3-methyl- (1TMS)	Glutathione metabolism		3460.782708	2653.889881	1888.154462	4698.25207	5309.306079	5037.744429
Malonamide	Glutathione metabolism		68017.02964	77394.83515	35026.96121	184907.0837	220910884	271865.3934
Purine, 6-benzylamino-, 9-beta-D-glucopyranosyl- (4TMS)	Glycerolipid metabolism		4401.506468	2039.142439	1852.496086	5167.433303	4904.070289	4739.427012
1,3-Propanediol	Glycerolipid metabolism	C02457	5171.933846	4238.265389	8631.935989	6485.74057	12259.27918	16115.50705
Ethanolamine	Glycerophospholipid metabolism	C00189	12111.51138	9663.797304	1154.983475	19033.11868	19443.24906	37781.71896
Diethanolamine	Glycerophospholipid metabolism	C06772	21400.03275	22152.83417	18434.51035	29289.78841	27059.35091	28833.10596
Androsterone	Hormone biosynthesis	C00523	55104.79777	54386.06464	56352.40911	63659.61362	58695.53523	65999.0905

Supplementary Table 1 (continued)

Cholesterol	Insect hormone biosynthesis	C00187	31514.65531	34490.82345	34688.6415	34597.97608	33830.91268	39742.61028
trans-Farnesol	Insect hormone biosynthesis	C01126	16667.75831	22058.63245	16023.65629	32514.25943	26933.8354	54160.98226
3-Hydroxybutanoate	Ketone body biosynthesis	C01089	5047.486491	4545.233068	3271.003653	6793.00828	7294.244217	7552.523874
2-Aminoadipic-acid_2TMS	Lipids		20101.52284	21938.44405	16710.7323	29522.5391	31584.18505	27176.89859
N-(3-Oxooctanoyl)homoserine lactone	Lipids	C11841	2922.056656	3441.611174	3642.372587	4117.75529	4672.763134	5906.321055
N-Butyryl-L-homoserine lactone	Lipids	C11837	21400.03275	22152.83417	18434.51035	29289.78841	27059.35091	28833.10596
Perillyl aldehyde	Lipids	C02576	9267.234321	88221.53646	7362.149939	7906.163753	7438.587054	8471.123238
Prostaglandin A2	Lipids	C05953	168412.4775	216617.6709	153071.8386	284218.9512	207489.6898	249184.1746
2-Hydroxyglutarate	Lipids	C02630	15213.68921	14626.44145	5140.024352	32982.5207	32559.61987	32235.56162
Acacetin	Lipids	C01470	934.1738988	874.6142602	1413.289268	1545.538178	1169.983862	1344.247385
N-Ethylmaleimide	Modify cysteine residues	C02441	83748.15785	109034.4324	92335.18873	71161.91352	59471.04178	59241.4734
Maleamate	Nicotinate and nicotinamide metabolism	C01596	9267.234321	88221.53646	7362.149939	7906.163753	7438.587054	8471.123238

Supplementary Table 1 (continued)

Nicotinate	Nicotinate and nicotinamide metabolism	C00253	5556.738169	6800.3898	16604.62689	12064.39742	16245.29317	19708.04911
Nicotinurate	Nicotinate and nicotinamide metabolism	C05380	10275.09415	9172.486601	8813.706732	11424.10304	10658.05989	12745.79354
Phosphoglycolic acid	Organic acids and derivatives	C00988	315.2120517	261.4909859	341.7985737	473.7810488	518.199749	572.9877217
Ethanesulfonic acid, 2-cyclohexylamino- (2TMS)	Organosulfonic acids		16142.13198	15503.49196	15269.61211	17424.10304	18336.91949	18315598
Phosphoric acid	Oxidative phosphorylation	C00009	48658.09727	39538.7364	31626.3698	97496.78013	93241.88632	89503.41064
D-Glucono-1,5-lactone	Pentose phosphate pathway	C00198	27203.20943	29974.01332	22459.55818	58458.14167	43349.47104	35789.9045
D-Glucosaminate	Pentose phosphate pathway	C03752	6174.062551	11289.58909	7963.124022	14926.40294	14214.63152	12542.97408
D-Ribose	Pentose phosphate pathway	C00121	47556.08318	89368.1988	70337.44999	126717.5713	68220.36937	110934.9704
Coniferyl aldehyde	Phenylpropanoid biosynthesis	C02666	4903.389553	5989.118077	4003.304923	9579.576817	12321.1404	14228.28558

Supplementary Table 1 (continued)

Sinapoyl aldehyde	Phenylpropanoid biosynthesis	C05610	28282299	28990.57983	24626.02192	35413.98344	36851.35377	40226.46658
2'-Deoxyguanosine 5'-phosphate	Purine metabolism	C00362	24945.96365	33183.36852	23551.92207	47298.06808	41277.56859	48068.21282
Deoxyguanosine	Purine metabolism	C00330	307901.5883	337307.9422	337.4499913	619461.8215	879865.5191	969819.9181
Hypoxanthine	Purine metabolism	C00262	5711.478631	6860.484002	3079.666029	12431.46274	13406.84956	17557.0714
Oxamate	Purine metabolism	C01444	68017.02964	77394.83515	35026.96121	184907.0837	220910884	271865.3934
Purine	Purine metabolism	C15587	5562.469298	4305.668345	3204.905201	6835.326587	10892.9532	7831.741701
Xanthosine	Purine metabolism	C01762	34688.06288	25462.07569	26748.99983	32911.68353	35890.26358	38087.31241
Calystegin A3	pyridine alkaloid biosynthesis	C10850	3460.782708	2653.889881	1888.154462	4698.25207	5309.306079	5037.744429
Scopolamine	pyridine alkaloid biosynthesis	C01851	5195.677092	7696.930323	6646.373282	9495.860166	9098.081406	7500.682128
Senecionine	pyridine alkaloid biosynthesis	C06176	5195.677092	7696.930323	6646.373282	9495.860166	9098.081406	7500.682128

Supplementary Table 1 (continued)

3-Ureidopropionate	Pyrimidine metabolism	C02642	168412.4775	216617.6709	153071.8386	284218.9512	207489.6898	249184.1746
5-Methylcytosine	Pyrimidine metabolism	C02376	5107.253971	4672.730226	3891.981214	5256.669733	5726.19688	6794.906776
6-Methylcytosine	Pyrimidine metabolism	C02376	1589.15998	1312.327432	761.8716298	2656.853726	2972.924511	3464.301955
7-Methylcytosine	Pyrimidine metabolism	C02376	8574.58654	5494.559038	5913.202296	7887.764489	7358.795051	7406.093679
Barbiturate	Pyrimidine metabolism	C00813	1641.558867	1573.006334	1684.640807	2067.157314	2073.695535	2643.929059
Cytosine	Pyrimidine metabolism	C00380	230.0638611	291.5380867	787.0934075	3495.860166	4281.871974	4850.386539
Orotic acid	Pyrimidine metabolism	C00295	1589.15998	1312.327432	761.8716298	2656.853726	2972.924511	3464.301955
Uracil	Pyrimidine metabolism	C00106	5819.551335	6472.307942	5561.836841	22870.28519	28213.19706	25465.21146
Uridine	Pyrimidine metabolism	C00299	232054.2001	66079.25938	314290.3114	545829.8068	320815.8508	482280.1273
L-Selenomethionine	Selenocompound metabolism	C05335	39658.5885	36261.16615	3005.740129	83593.37626	77006.45508	73511.59618

Supplementary Table 1 (continued)

Trehalose 6-phosphate	Starch and sucrose metabolism	C00689	3892.25479	2497.96979	2507.39259	3069.917203	4553.5234	3576.170987
3-Aminopropane-1,2-diol	Sugar glider food	C06057	270807.2703	249611.8239	228911.9847	295353.2659	306819.0784	284998.6357
cis-Aconitate	TCA cycle	C00417	13607.33584	13719.34384	8146.634197	15593.37626	14797.38211	15112.32378
Malate	TCA cycle	C00711	5047.486491	4545.233068	3271.003653	6793.00828	7294.244217	7552.523874
Succinate	TCA cycle	C00042	5203.864418	5147.799253	2830.057401	4109.475621	3325.264479	4273.7608
Gabaculine	Transferases	C12110	8315.867038	7523.956472	6643.764133	8537.25851	11937.42155	12716.6894
Vitamin K3	Vitamin digestion and absorption	C05377	40582.93761	41230.30697	24598.19099	46632.93468	42450.24207	28962.25557
alpha-Tocopherol acetate	Vitamin digestion and absorption	C13202	218.6016047	233.0680526	190.4679075	385.4645814	390.8911601	357.4351978
Vitamin K1	Vitamin digestion and absorption	C02059	12331.75045	425.5319149	8531.918595	571.2971481	1049.847588	520.2364711
Propargyl Alcohol (1TMS)			12846.73326	12319.31135	11030.61402	13514.25943	14593.86767	12570.25921

Source: own authorship.

1. COMENTÁRIO FINAL

A partir dos resultados encontrados no Capítulo 1 e 2 deste trabalho, construímos um modelo metabólico, levando em consideração a influência da riquétsia no intestino médio dos carrapatos em nível de expressão e metabolismo (Figure 1S).

Figura 1S: Representação final dos resultados obtidos de expressão gênica e perfil metabólico das vias alteradas pela presença da bactéria *R. amblyommatis* no intestino médio de carrapatos *A. sculptum.* Blocos em azul representam metabólitos sintetizados pelo carrapato. Blocos em cinza representam metabólitos sintetizados pelo carrapato e pela bactéria. Letras com destaque vermelho são enzimas também presentes em riquétsias.

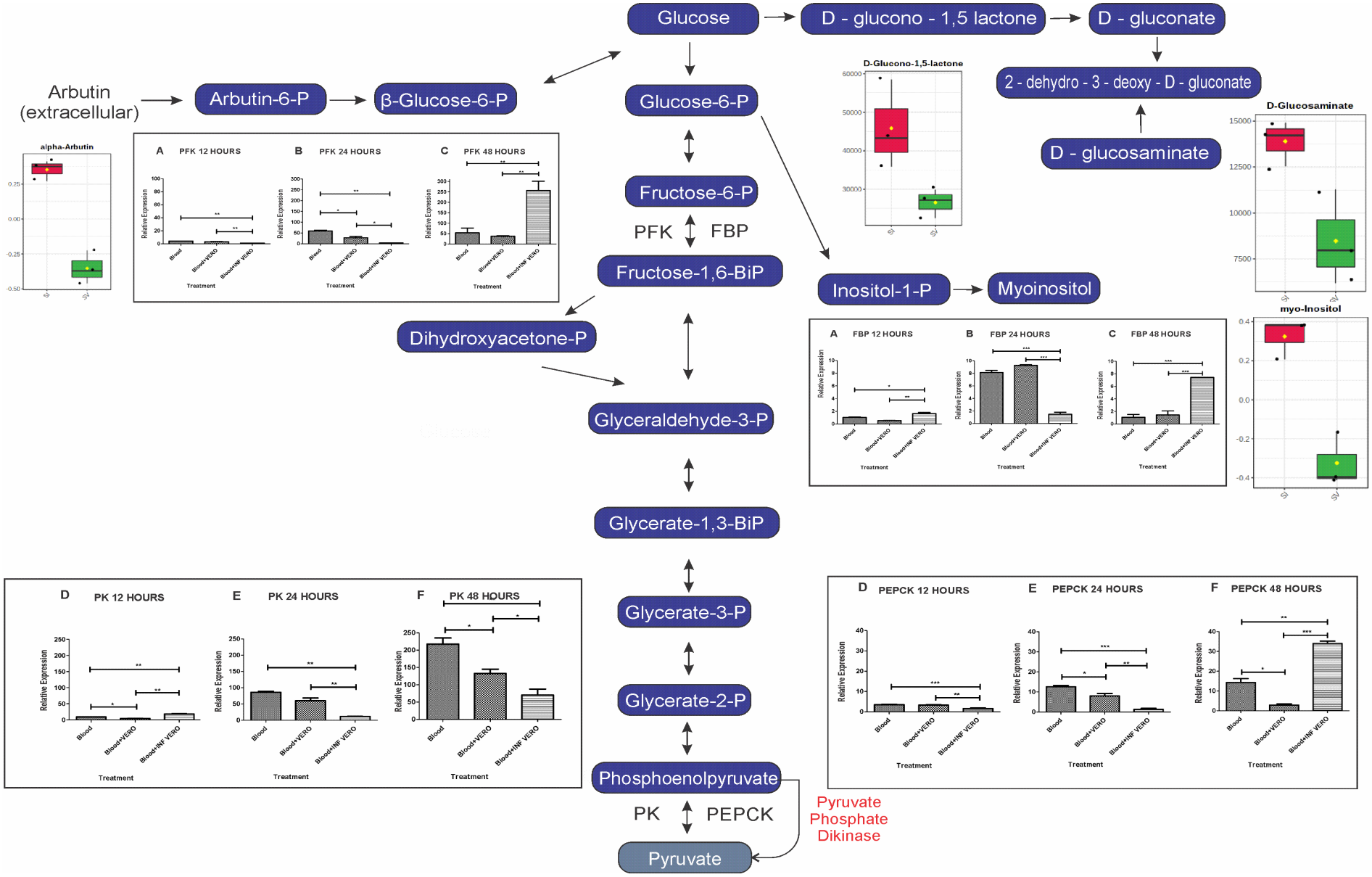

Fonte: autoria própria.

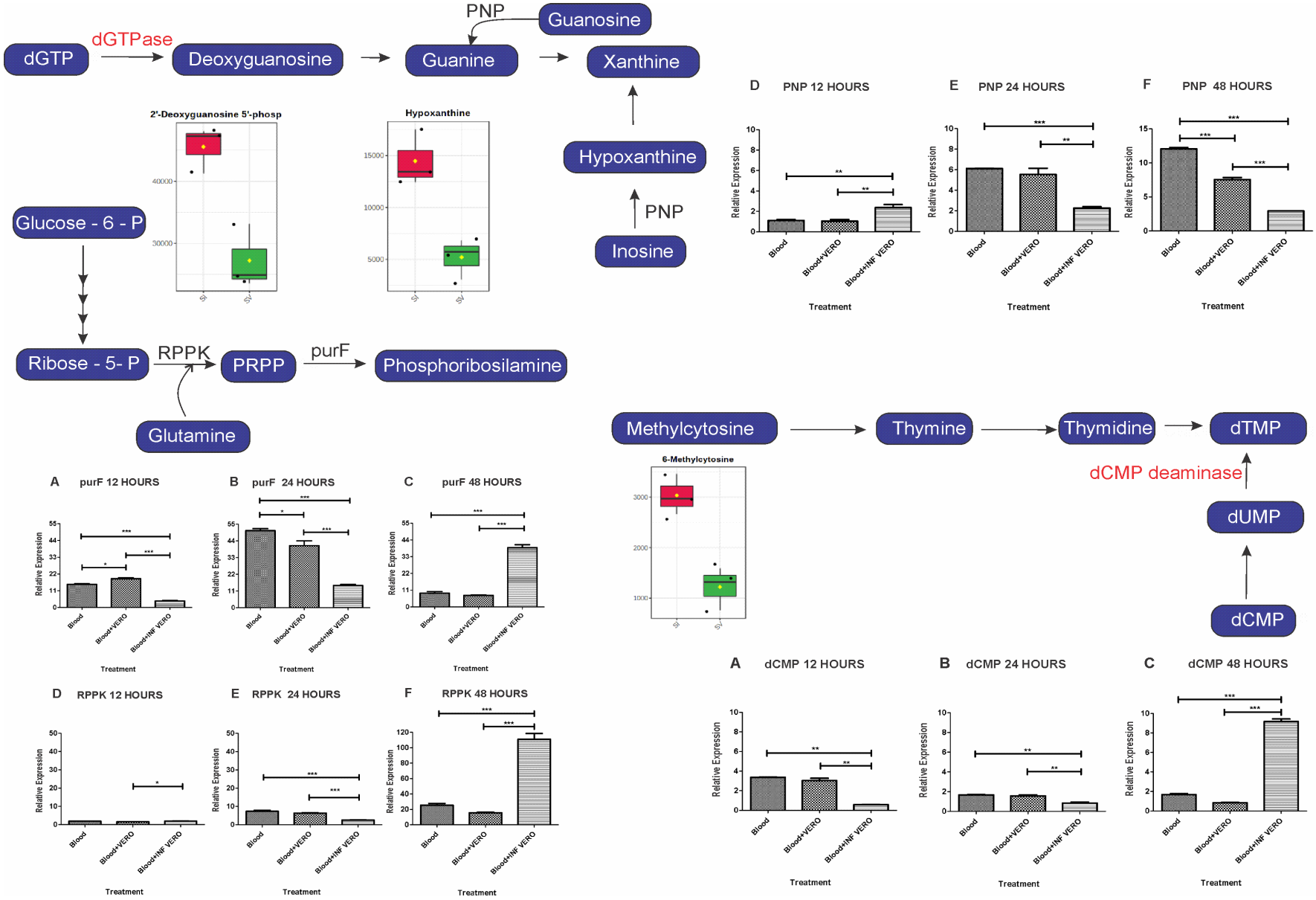

Fonte: autoria própria.

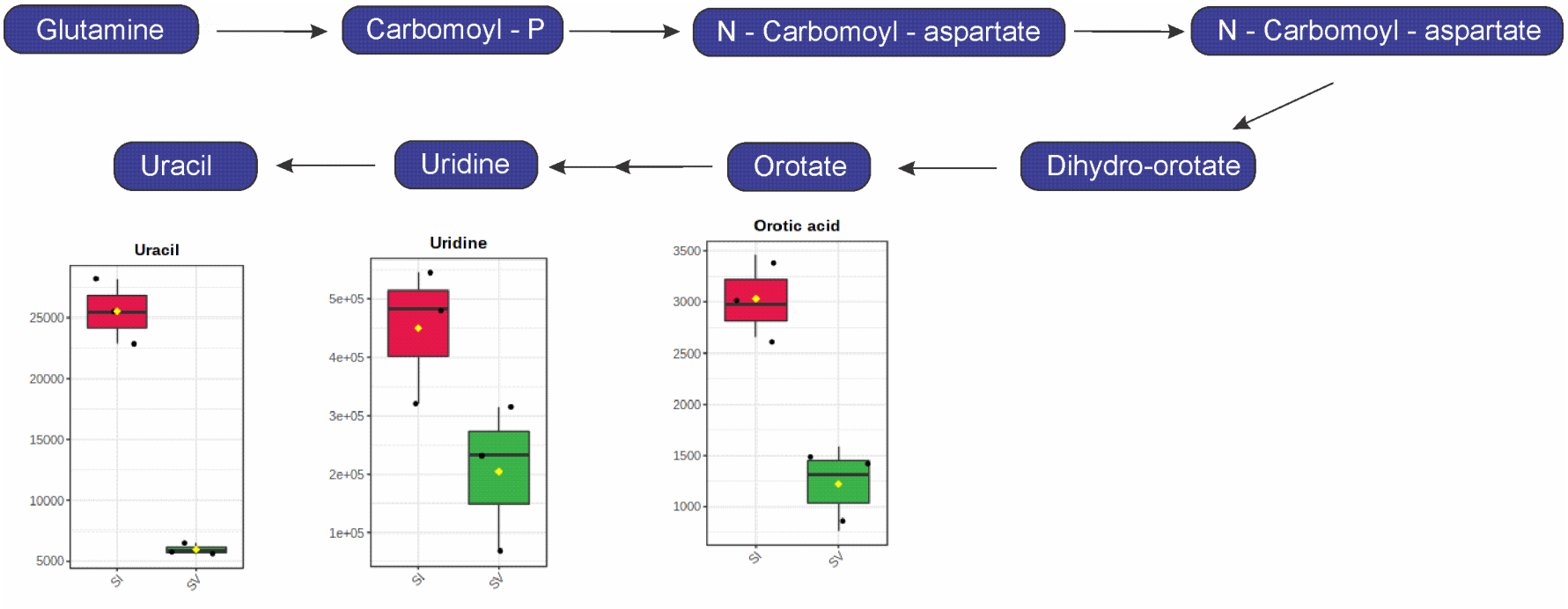

Fonte: autoria própria.

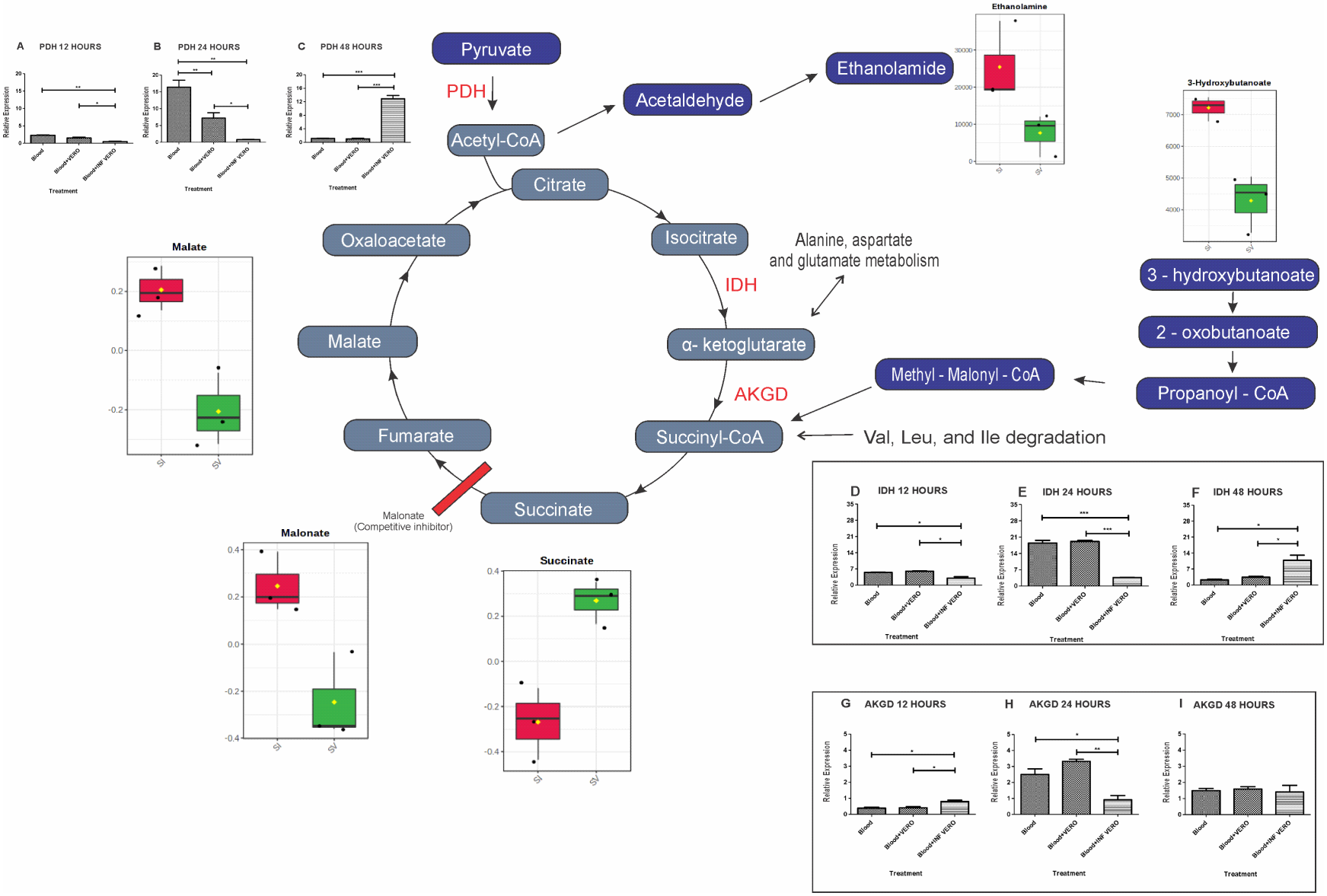

Fonte: autoria própria.

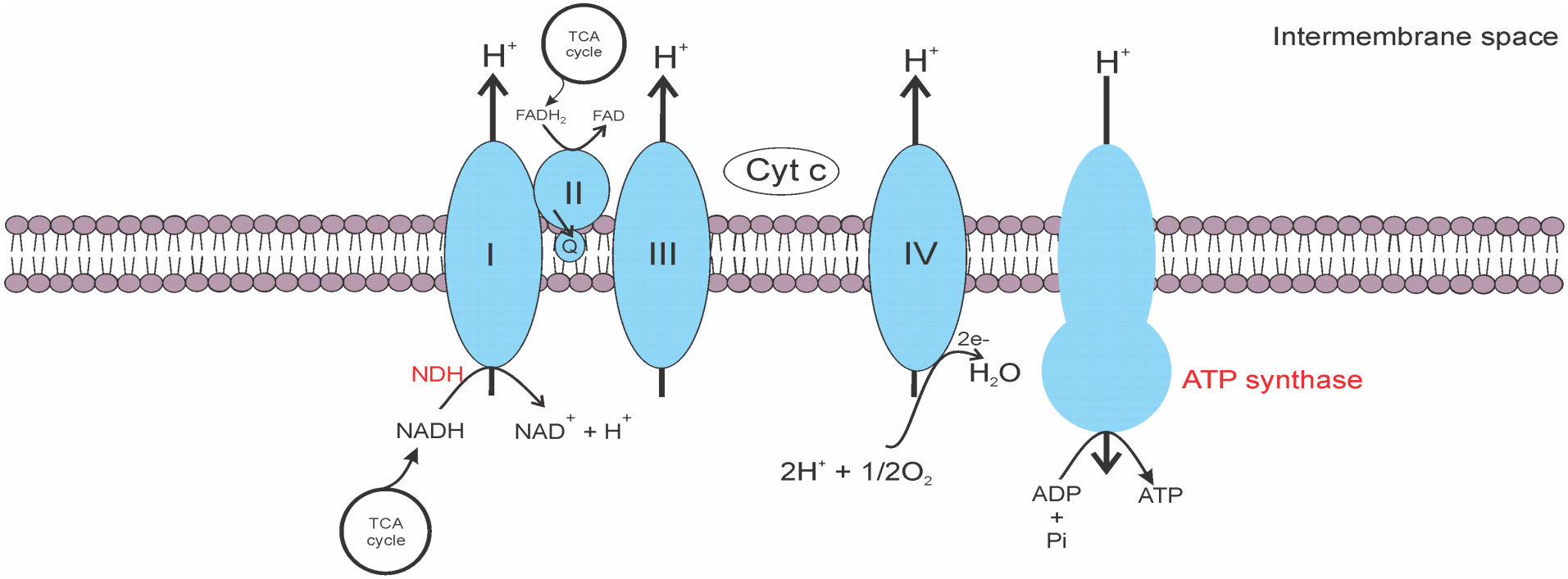

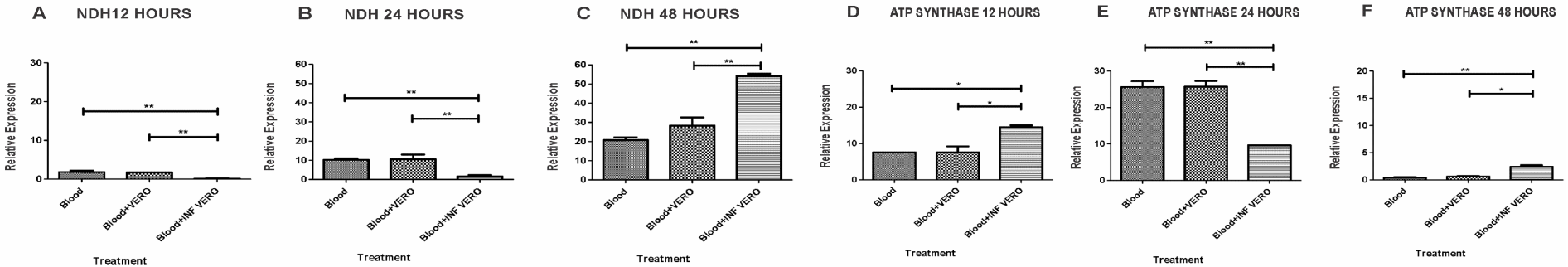

Fonte: autoria própria.

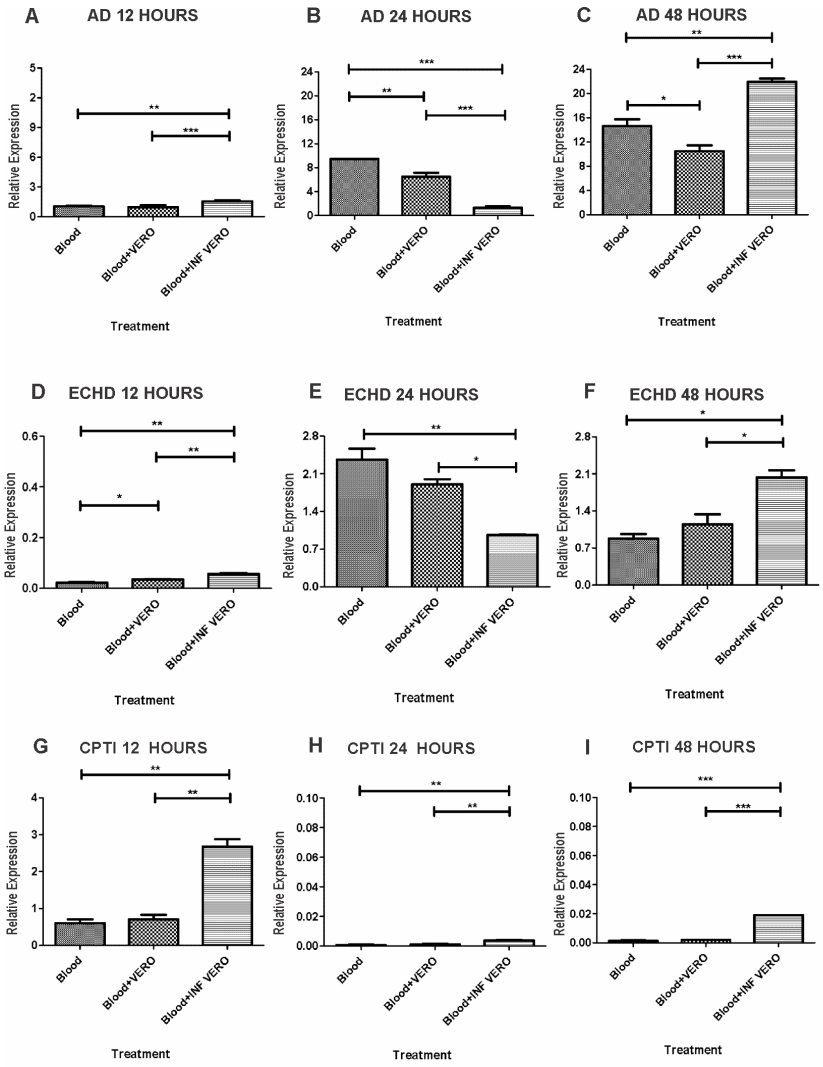

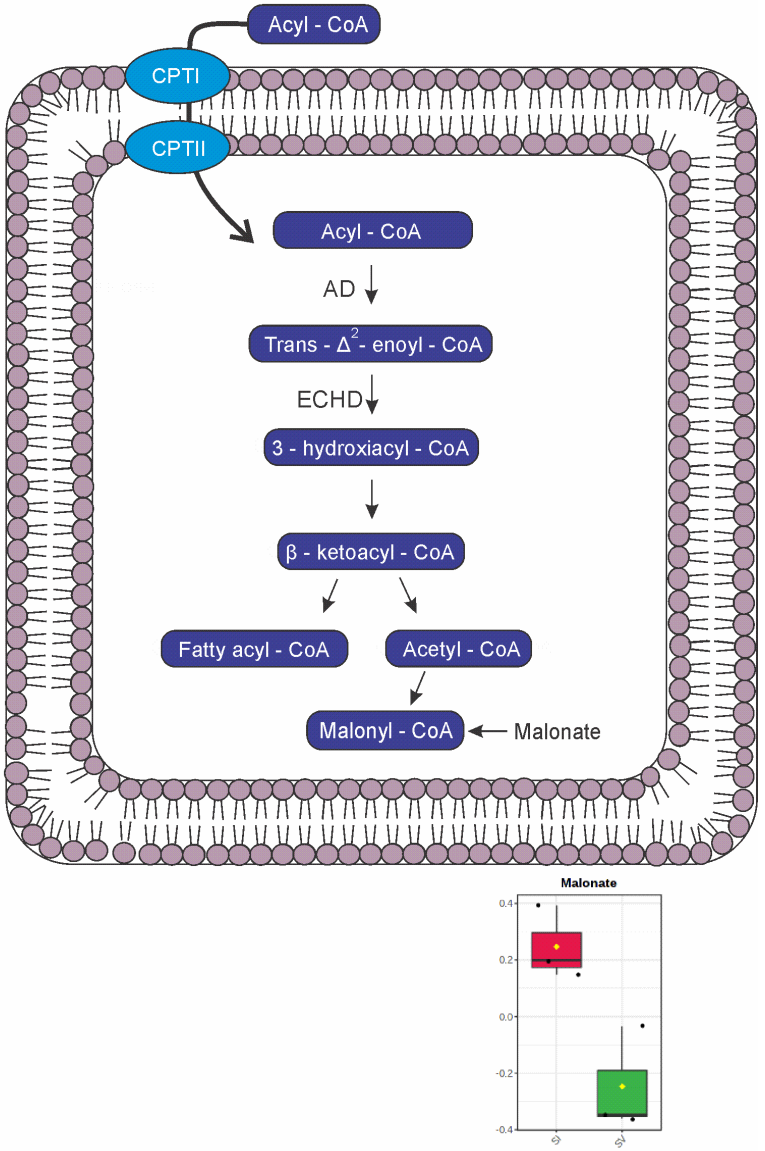

Fonte: autoria própria.

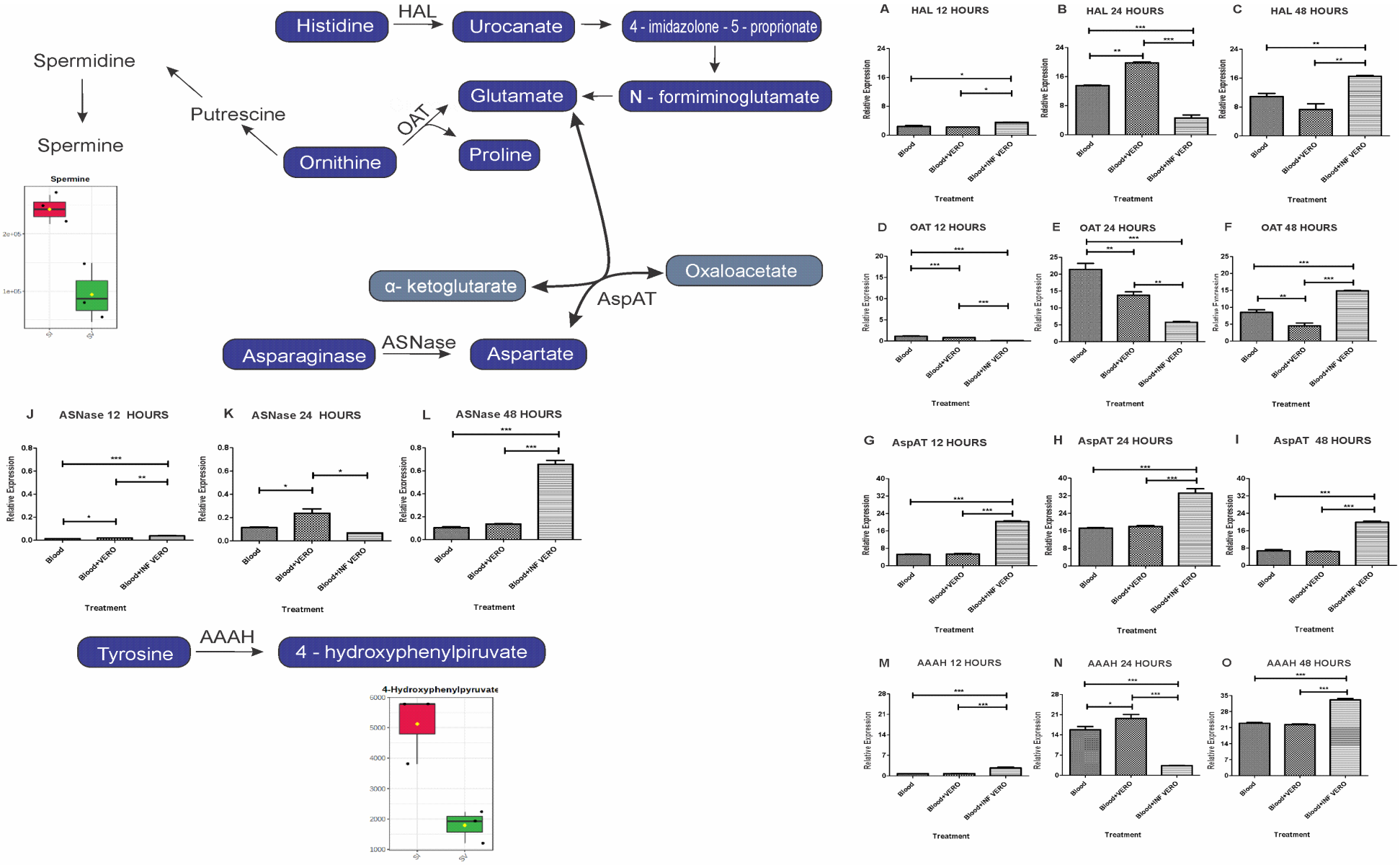

Fonte: autoria própria.

2. CONCLUSÕES GERAIS

Neste trabalho dividido em dois capítulos, conclui-se que:

- O número de cópias de *R. amblyommatis* no intestino médio de carrapatos *A. sculptum* variou significativamente no tempo de 48 horas de alimentação corroborando com a observação de que quanto mais sangue infectado o carrapato ingere, maior a probabilidade de infecção e sobrevivência da mesma no órgão estudado.

- A presença da riquétsia pode alterar a capacidade do carrapato ganhar peso durante a alimentação, dificultando o desenvolvimento do mesmo. Além disso, a correção de Spearman's demonstrou que o tempo de exposição dos carrapatos à alimentação com a bactéria afetou negativamente o ganho de peso.

- Durante a análise da expressão de enzimas envolvidas no metabolismo de carboidratos, gliconeogênese, ciclo TCA, lipídeos, aminoácidos e nucleotídeos, a expressão esteve aumentada nos tratamentos controle (S e SV) em 12 e 24 horas de alimentação devido à possível indisponibilidade de intermediários essenciais para os processos biológicos do carrapato, obtidos pelo sangue utilizado. Em contraste, na presença da bactéria a expressão das enzimas manteve-se baixa durante 12 e 24 horas, sugerindo que o carrapato pode possuir mecanismos de defesa para impedir o desenvolvimento e sobrevivência de um organismo externo, diminuindo assim a disponibilidade dos seus metabólitos. Esse mecanismo, pode não ser suportado por longos períodos, cujo aumento na expressão das enzimas em 48 horas de alimentação demonstra a necessidade de produzir intermediários mesmo na presença da bactéria. Além disso, algumas enzimas apresentaram maior expressão nos tempos iniciais de infecção dos carrapatos, sugerindo que a bactéria pode ser capaz de modular mecanismos a nível molecular.

- Os resultados apresentados na análise de expressão gênica auxiliam na compreensão do fenótipo apresentado pelo carrapato infectado, cuja dificuldade no ganho de peso após 48 horas de alimentação está relacionada com as modificações a nível de expressão apresentadas neste trabalho.

- Durante a abordagem utilizando GC-MS para a análise de metabólitos e posterior identificação e anotação utilizando *TargetSearch* e *Metaboanalyst,* diversas vias metabólicas tiveram seu intermediários com abundâncias distintas comparando-se os modelos infectados e não infectados, as quais foram discutidas levando em consideração sua importância no metabolismo dos carrapatos e das riquétsias.
- Os dados obtidos poderão auxiliar em análises futuras, a fim de traçar estratégias capazes de controlar a propagação e sobrevivência das riquétsias em artrópodes, utilizando como alvo os metabólitos e enzimas que apresentaram diferenças significativas na comparação dos tratamentos infectados e não infectados.
- Faz-se necessária a construção de um modelo metabólico mais detalhado, levando em consideração a influência da riquétsia no intestino dos carrapatos em nível de expressão e metabolismo.